Human inflammasomes are novel sensors of lipids

Doctoral thesis

to obtain a doctorate (PhD)

from the Faculty of Medicine

of the University of Bonn

Matilde Bartolomei Viegas de Vasconcelos

from Rome, Italy

2026

Written with authorization of

the Faculty of Medicine of the University of Bonn

First reviewer: Prof. Dr. Eicke Latz

Second reviewer: Prof. Dr. Sammy Bedoui

Day of oral examination: 11.03.2026

From the Institute of Innate Immunity

Porque hoje é sábado.

Per la mamma e para o pai.

Table of Contents

List of abbreviations

aa	amino acids
ACK	Ammonium-Chloride-Potassium
AIM2	absent in melanoma 2
ALR	AIM2-like receptor
alum	aluminum salt
ASC	apoptosis-associated speck-like protein containing a CARD
AUC	area under the curve
BCA	bicinchoninic acid
BM	bone marrow
BMDM	bone marrow-derived macrophage
BSA	bovine serum albumin
CARD	caspase activation and recruitment domain
CARPA	complement-associated pseudoallergy
CAPS	cryopyrin-associated periodic syndromes
CCL	C-C motif chemokine ligand
CETSA	cellular thermal shift assay
cGAS	cyclic GMP-AMP synthase
CHX	cycloheximide
CLR	C-type lectin-like receptor
CRID3	cytokine release inhibitory drug-3
COVID-19	coronavirus disease 2019
CytoD	cytochalasin D
CXCL	C-X-C motif chemokine ligand
DAMP	damage-associated molecular pattern
DC	dendritic cell
ddC	2′,3′-dideoxycytidine
DMEM	Dulbecco’s Modified Eagle’s Medium
DMSO	dimethylsulfoxide

DNA	deoxyribonucleic acid
DOPE	dioleoylphosphatidylethanolamine
DOSPA	2,3-dioleyloxy-N-[2-(sperminecarboxamido)ethyl]-N,N-dimethyl-1 propanaminium
DPBS	Dulbecco's Phosphate Buffered Saline
ds	double-stranded
DSPC	distearoylphosphatidylcholine
EDTA	ethylenediaminetetraacetic acid
ELISA	Enzyme-Linked Immunosorbent Assay
EMA	European Medicines Agency
FACS	Fluorescence-Activated Cell Sorting
FC	fold change
FcR	Fc receptor
FCS	fetal calf serum
FDA	Food and Drug Administration
FDR	false discovery rate
Fig.	figure
FISNA	fish-specific NACHT-associated
GLA	glucopyranosyl lipid adjuvant
GM-CSF	granulocyte-macrophage colony-stimulating factor
GSDMD	gasdermin D
h	hours
HAMPs	homeostasis-altering molecular processes
HBSS	Hanks' Balanced Salt Solution
HEK	Human Embryonic Kidney 293T
HEPES	4-(2-hydroxyethyl)-1-piperazineethanesulfonic acid
HET	House for Experimental Therapy
hlink	human linker
hmut	human mutation
HRP	horseradish peroxidase

HTRF	homogenous time-resolved fluorescence
hum	human
IBD	inflammatory bowel disease
IFN	interferon
III	Institute of Innate Immunity
IL	interleukin
IL-1RA	IL-1 receptor antagonist
i.m.	intramuscularly
iMacs	immortalized macrophages
IRF	IFN regulatory factor
ISG	interferon stimulated gene
IVT	in vitro transcription
KO	knockout
LDH	lactate dehydrogenase
LF	lipofectamine
LN	lymph node
LNP	lipid nanoparticle
LPS	lipopolysaccharide
LRR	leucine-rich repeat
mac	macaque
MACS	Magnetic-Activated Cell Sorting
MDA	melanoma differentiation-associated gene
min	minutes
mou	mouse
mRNA	messenger RNA
MSU	monosodium urate
mtDNA	mitochondrial DNA
MxA	Myxovirus Resistance protein A
NACHT	nucleotide-binding oligomerization domain
NF-κB	nuclear factor kappa-light-chain-enhancer of activated B cells

NINJ1	Ninjurin-1
NK	natural killer
NLR	NOD-like receptor
NLRC	NLR family CARD domain-containing
NLRP	NLR family PYD domain-containing
NOD	nucleotide-binding oligomerization domain
PAMP	pathogen-associated molecular pattern
PBMC	peripheral blood mononuclear cell
PCR	polymerase chain reaction
PEG	polyethylene glycol
PI3K	phosphoinositide 3-kinase
PI4P	phosphatidylinositol-4-phosphate
PISA	proteome integral solubility alteration
PMA	phorbol-12-myristate 13-acetate
poly(dA:dT)	poly(deoxyadenylic-deoxythymidylic) acid
PRR	pattern recognition receptor
PYD	pyrin domain
RIG	retinoic acid-inducible gene
RIPA	radioimmunoprecipitation assay
RLR	RIG-I-like receptor
RNA	ribonucleic acid
ROS	reactive oxygen species
RPMI	Roswell Park Memorial Institute
RT	room temperature
sec	seconds
SARS-CoV-2	severe acute respiratory syndrome coronavirus 2
SD	standard deviation
SE	squalene oil-in-water emulsion
siRNA	short interfering RNA
SLE	systemic lupus erythematosus

SPF	specific pathogen-free
Suppl.	Supplementary
TIFF	tagged image file format
TLR	toll-like receptor
TNF	tumor necrosis factor
VEGF-A	Vascular Endothelial Growth Factor A
VLP	virus-like particle
WES	capillary western blotting technique
WT	wild-type

1. Introduction

1.1 The immune system and inflammation

The immune system is our body's defense network, which monitors, detects and protects us from harmful microorganism invaders, such as viruses, bacteria, fungi, and parasites. This system is constantly monitoring the body, and distinguishing between "self" (*i.e.*, our own cells) and "non-self" (*i.e.*, foreign organisms) (Janeway, 1989). The "self" components are supposed to be recognized as such, and thus not be fought against. On the other hand, once a foreign invader is detected, the immune system rapidly and efficiently mounts an appropriate response, including spatial containment and pathogen elimination (Marshall et al., 2018). The immune system also contributes to the resolution of sterile inflammation, resulting for example from trauma, ischemia-reperfusion or chemically-induced injury in the absence of any microorganism (G. Y. Chen & Nuñez, 2010).

The immune system is a complex and coordinated network, organized at the levels of molecular receptors and effectors (such as antibodies), specialized immune cells (described below), barrier organs (*e.g.*, skin, gut, lung), and lymphoid organs (*e.g.*, bone marrow (BM), thymus, lymph nodes (LNs), spleen, tonsils). It is divided into two interconnected and closely co-operating branches: the innate and the adaptive immune system (Janeway CA Jr, 2001). The innate immune system is fast, operating as "the first line of defense", which can act within minutes to hours from the recognition of the non-self. This system includes physical and chemical barriers (such as the skin, stomach acid, and mucous membranes in the respiratory tract) as well as diverse specialized immune cells (neutrophils, monocytes, macrophages, dendritic cells (DCs), and natural killer (NK) cells). Its aim is to detect and contain an infection as early as possible. It is evolutionarily old, found in diverse animals (such as insects), and active from birth onwards. However, it is not specific: the innate immune mechanisms do not recognize and attack one individual invasive species, but instead react to common molecular signals shared by many pathogens, collectively known as pathogen-associated molecular patterns (PAMPs). Sensors and receptors that are activated by PAMPs are known as pattern

recognition receptors (PRRs) and are expressed by innate immune cells (Janeway & Medzhitov, 2002).

The adaptive immune system is evolutionarily more recent, the organization similar to that found in the human is only shared with other vertebrates (Cooper, 2010). The adaptive immune response is slower on first exposure, taking from several days to 1-2 weeks to develop. Yet, it then provides highly specific and long-lasting protection. The main drivers are B and T lymphocytes, which recognize specific pathogen-derived antigens with the help of their somatically recombined B and T cell receptors (Janeway CA Jr, 2001). B cells produce antibodies (essentially the soluble version of their B cell receptors), which mainly recognize the antigens and bind to the pathogens, marking them for destruction by other immune cells or the innate complement system. Moreover, antibodies can also mark virus-infected or tumor cells for destruction, block viruses from entering cells, and neutralize toxins (Schroeder & Cavacini, 2010). After infection (or vaccination), some B cells become long-lived memory cells – so that upon pathogen re-exposure, the body is able to respond faster and more strongly (Janeway CA Jr, 2001). This development of immunological memory to the specific pathogens, allows the adaptive immune response, in the future, to remember past infections with the same microorganism. Vaccines take advantage of this memory formation and use it preventively to protect the body from infectious diseases in the future (Janeway CA Jr, 2001). While the primary role of B cells is antibody production, T lymphocytes exhibit a very broad range of phenotypic and functional diversity: While helper T cells coordinate immune responses, for example by secreting cytokines that govern polarization and activity of other host cell types, cytotoxic T cells directly kill infected or tumor cells (Janeway CA Jr, 2001).

In contrast, if cells strongly react against the “self”, the host’s own antigens, which are not supposed to be attacked, they get eliminated to provide the so-called immune tolerance. In innate immunity, receptors are germline-encoded, which enriches reactivity against foreign microorganisms. Thus, immune tolerance is inbuilt: either the host doesn’t produce ligands for the receptors (such as for toll-like receptor (TLR) 4, or nucleotide-binding oligomerization domain (NOD)-like receptor (NLR) family caspase activation and recruitment domain (CARD) domain-containing 4 (NLRC4)), or self-ligands (such as deoxyribonucleic acid (DNA) and

ribonucleic acid (RNA)) are cleared or shielded from the receptors (*e.g.*, absent in melanoma 2 (AIM2), cyclic GMP-AMP synthase (cGAS), TLR7-9). In adaptive immunity, tolerance is enforced during lymphocyte development in the thymus (for T cells) and the BM (for B cells), chiefly through negative selection of self-reactive lymphocytes, or in the periphery, through regulatory T cell induction for example. If these tolerance control mechanisms fail, and the immune system initiates a reaction against the host's own body, this leads to autoimmune diseases (Janeway CA Jr, 2001; Medzhitov, 2008).

Taken together, the immune system is a complex, but fine-tuned structure, coordinating multiple cell types and soluble mediators, all linked by molecular signaling pathways. All of these interactions have to be controlled to avoid damaging the host's body, but strong enough to rapidly and effectively fight invaders and abnormal malignant cells.

1.2 Innate immunity and the inflammasomes

Various immune cells, including monocytes and macrophages, express a large group of innate immune receptors, the PRRs. These receptors recognize conserved microbial structures, the before-mentioned PAMPs, but also endogenous damage-associated molecular patterns (DAMPs) released from stressed or damaged cells, and homeostasis-altering molecular processes (HAMPs) (Garg et al., 2015; Janeway, 1989; Liston & Masters, 2017). Upon sensing of these signals, PRR activation induces intracellular signaling cascades, which contribute to pathogen elimination and initiation of diverse immune responses.

PRRs include five different protein families: TLRs, NLRs, retinoic acid-inducible gene-I (RIG-I)-like receptors (RLRs), C-type lectin-like receptors (CLRs), and AIM2-like receptors (ALRs) (Takeuchi & Akira, 2010). While TLRs and CLRs are transmembrane proteins in the plasma or endosomal membranes that screen the extracellular compartment for microorganisms, NLRs, RLRs and ALRs are intracellular proteins monitoring the cytosolic compartment. Thus, the diversity of PRR-driven responses derives from their different subcellular localizations, ligand specificity and downstream effector engagement. For many of the receptors, it has

been identified what exactly they sense and potentially bind to (Takeuchi & Akira, 2010). DNA, for example, can activate TLR9 (CpG-rich DNA) (Hemmi et al., 2000), cGAS (Ablasser et al., 2013; Civril et al., 2013; Sun et al., 2013), or AIM2 (double-stranded (ds)DNA) (Fernandes-Alnemri et al., 2009; Hornung et al., 2009); while RNA activates diverse TLRs (3 (Alexopoulou et al., 2001), 7 and 8 (Diebold et al., 2004; Heil et al., 2004)), RIG-I, or the RLR melanoma differentiation-associated gene 5 (MDA5) (Kato et al., 2006; Rehwinkel & Gack, 2020). Several bacteria-derived PAMPs can be recognized: Extracellular lipopolysaccharide (LPS), a component of the outer membrane of gram-negative bacteria, is sensed by TLR4 (Poltorak et al., 1998; Qureshi et al., 1999), while intracellular LPS is recognized by human caspases-4 and -5 (Shi et al., 2014). Flagellin, a protein that makes up the flagella, used by many bacteria for movement, activates TLR5 (Gewirtz et al., 2001; Hayashi et al., 2001), and intracellularly NLRC4 (Miao et al., 2006). Bacterial lipopeptides and lipoproteins can bind to TLR2, in complex with TLR1 or TLR6 (Kirschning & Schumann, 2002; Takeda et al., 2002; Takeuchi et al., 2002). Some NLRs can also sense bacterial components, for example NOD 1 and 2 proteins are activated by bacterial peptidoglycans (Girardin, Boneca, Carneiro, et al., 2003; Girardin, Boneca, Viala, et al., 2003). However, not all PRR ligands have been identified yet. For one of the most studied members within the NLR family, the NLR family pyrin domain (PYD) domain-containing 3 (NLRP3), the exact activation mechanism is still not completely understood (Akbal et al., 2022).

Upon PRR activation, multiple downstream signaling pathways can be initiated. TLRs, CLRs, and RLRs can engage two groups of transcription factors (Janeway CA Jr, 2001): the classical nuclear factor kappa-light-chain-enhancer of activated B cells (NF-κB) branch, which induces a strong pro-inflammatory transcriptional response (Tak & Firestein, 2001); or interferon (IFN) regulatory factors (IRFs), which lead to a type I IFN cascade, often associated with antiviral immunity (Honda & Taniguchi, 2006).

Activation of several NLRs (such as NLRP1, 3, 10) and of the ALR family member AIM2 drives formation of inflammasomes (Broz & Dixit, 2016) and subsequent inflammatory pyroptotic cell death and release of the cytokines interleukin (IL)-1β and -18. Upon detecting pathogens and sterile cell damage and stress, these diverse sensors form macromolecular

complexes with the adaptor apoptosis-associated speck-like protein containing a CARD (ASC) and the cysteine protease caspase-1 (Ming et al., 2015), the so-called inflammasomes. Most sensors, such as NLRP3 and AIM2, have an N-terminal PYD, which interacts with the N-terminal PYD of ASC upon sensing of inflammasome-activating signals. In this process, all cellular ASC molecules polymerize (Cai et al., 2014; Lu et al., 2014) and (irreversibly) form one large ASC speck complex (Richards et al., 2001). In turn, one ASC speck then recruits multiple pro-caspase-1 molecules: the other domain of ASC, the C-terminal CARD, interacts with the CARD of pro-caspase-1 (Srinivasula et al., 2002). Finally, pro-caspase-1 undergoes autoproteolysis and activation (Elliott et al., 2009). This activated inflammatory caspase then cleaves gasdermin D (GSDMD), allowing the released N-terminal domain of GSDMD to oligomerize and form pores in the plasma membrane, which lead to the leakage of the cytosolic contents and a form of cell death called pyroptosis (Ding et al., 2016; W. He et al., 2015; Shi et al., 2015). In addition to GSDMD, caspase-1 also cleaves the pro-forms of the cytokines IL-1β (Black et al., 1989; Kostura et al., 1989) and -18 (Ghayur et al., 1997). Through the GSDMD pores and downstream Ninjurin-1 (NINJ1), which oligomerizes in the plasma membrane to drive the final membrane rupture step (Degen et al., 2023; Kayagaki et al., 2021), the cleaved, mature inflammatory IL-1β and -18 are secreted to the extracellular space (Garlanda et al., 2013), where they can then bind to the IL-1 and -18 receptors on responder cells. This initializes or amplifies inflammation and the immune response, supporting recruitment and activation of other immune cells and, in some cases, initiation of tissue repair processes (Akbal et al., 2022).

Interestingly, NLRP3 is not directly activated by a simple pathogen-derived product. Instead, it first requires the so-called priming stimulus – which, usually through TLR activation, leads to NF-κB activation and the consequent increase in *NLRP3* and *IL1B* transcription – and then an activation stimulus, which triggers the inflammasome formation. Examples of priming stimuli include LPS, which activates TLR4, or the synthetic triacylated lipopeptide Pam3CSK4, an agonist for TLR2/TLR1. Regarding the activation stimuli, while AIM2 is known to bind to dsDNA, NLRP3 does not seem to be activated by one specific direct ligand. Diverse events have been linked to NLRP3 activation, such as K^+ efflux (as for example induced by nigericin, a microbial toxin, which acts as an ionophore, causing K^+ efflux from cells) (Muñoz-

Planillo et al., 2013; Pétrilli et al., 2007; Tapia-Abellán et al., 2021; Vyleta et al., 2012), but also mitochondrial dysfunction (Gong et al., 2018) and subsequent release of mitochondrial DNA (mtDNA) (Shimada et al., 2012) and/or production of reactive oxygen species (ROS) (Heid et al., 2013; Mishra et al., 2021), and lysosomal damage (Dostert et al., 2008; Halle et al., 2008; Hornung et al., 2008). These processes are involved in the canonical NLRP3 activation pathway. NLRP3 can, however, be also activated through a non-canonical pathway, whereby intracellular LPS binds to human caspases-4 and -5 (and the mouse homolog caspase-11), leading to activation of these inflammatory caspases and GSDMD cleavage and oligomerization. These GSDMD-consisting pores mediate K^+ efflux, which activates NLRP3 (Downs et al., 2020; Kayagaki et al., 2015; Rühl & Broz, 2015; Shi et al., 2014). In addition, in DCs, caspases-4/5/11 have been shown to be activated by cytoplasmic oxidized phospholipids, released by dying cells and internalized by DCs with the help of CD14, leading to NLRP3 inflammasome activation with robust IL-1β secretion, but no pyroptosis (little GSDMD cleavage and minimal lactate dehydrogenase (LDH) release). In this state, DCs are defined as hyperactive, while remaining viable and capable of antigen presentation (Zanoni et al., 2016). Finally, there is a third, alternative NLRP3 activation pathway specific to human monocytes, in which extracellular LPS administered overnight induces NLRP3 activation in a TLR4- and caspase-8-dependent manner, and in a slightly unconventional fashion, as no ASC speck formation and also no pyroptosis are observed (Gaidt et al., 2016).

Gain-of-function mutations, but also aging and metabolic dysfunction, can lead to pathogenic chronic inflammasome activation. This can contribute to a broad spectrum of inflammatory diseases, such as cryopyrin-associated periodic syndromes (CAPS), gout, cardiovascular diseases (such as atherosclerosis), neurodegenerative diseases (such as Alzheimer's), inflammatory bowel disease (IBD), rheumatoid arthritis, and systemic lupus erythematosus (SLE) (Broderick et al., 2015). Hence, members of this innate immune receptor family represent possible targets for pharmacological intervention (Mangan et al., 2018). For a better understanding of disease pathogenesis and productive drug development, however, a clearer characterization of the activation signals and mechanisms of NLRP3, but also other NLR family members, is of absolute need.

1.3 Vaccination

In the face of danger and disease, our body is equipped to protect us with the help of the innate and adaptive immune systems. However, this is not always enough, and medical interventions are needed to improve human health and wellbeing. Moreover, many infections that are efficiently cleared by the adaptive immune mechanisms can, nevertheless, still lead to secondary effects or sequelae, which are sometimes more harmful than the pathogen itself (*e.g.*, Group A streptococcus, Campylobacter jejuni, measles virus). Thus, avoiding an infection altogether is always a more beneficial scenario than acquiring the disease and subsequently recovering from it. One of the most powerful and effective tools in medicine are vaccines, which help us to prevent infectious diseases.

The idea behind vaccination is to safely expose the body to a harmless form or part of a germ (virus or bacterium). This way, the immune system learns to recognize it by expanding and maturing lymphocyte clones responsive to the pathogen-associated antigens, and if later the actual pathogen appears, it can respond quickly and strongly. This often prevents the illness altogether, or at least decreases its severity and long-term complications.

The first vaccine was developed by Edward Jenner against smallpox in 1796, starting from an interesting observation and an experiment that nowadays would not be ethically accepted, but that laid the foundation for vaccination. Cowpox, unlike smallpox, is a mild disease in humans – but, interestingly, milkmaids who had caught it, seemed to be protected from the deadly smallpox. Thus, Jenner deliberately exposed a boy first to cowpox and then to smallpox – and the boy did not get sick. Smallpox vaccination, in more advanced forms than that first used by Jenner, became widespread over time and, in 1980, smallpox was finally declared eradicated worldwide (Plotkin, 2014).

Today, vaccines still protect us from many other diseases, such as chickenpox, influenza, human papillomavirus, measles, hepatitis B, polio and tetanus – some of which have even been almost eliminated in many parts of the world (*e.g.*, polio) (Kayser & Ramzan, 2021). Their relevance is thus not only still undebatable, but potentially even increasing, considering that we live in a globalized world, where infections can spread across natural and administrative borders within a very short period of time. Importantly, vaccines do not just

protect individuals, but whole communities. Some vulnerable people cannot be safely or productively vaccinated, such as some newborns and young children, older adults, or people with certain medical conditions and weakened immune systems. Yet, vaccines help to protect them as well, as they create herd immunity by reducing the spread of infections (Fine et al., 2011). Moreover, they also help stabilize the healthcare system and the economy, by reducing extreme hospitalizations and the accompanying social and economic trouble (Pierre et al., 2023; Rodrigues & Plotkin, 2020).

Vaccines consist of two essential immunologically active components.

The first is the antigen, *i.e.*, what the immune system is supposed to learn to recognize and then fight. It can be the whole virus/bacterium, just inactivated (*e.g.*, some flu vaccines) or live attenuated (weakened; *e.g.*, measles), or just a specific part of the pathogen, like a surface protein (*e.g.*, hepatitis B). Instead of administering the antigen as a protein, genetic material (messenger RNA (mRNA) or DNA) encoding the vaccination-targeted antigen can be delivered. In this scenario, the cells make the protein themselves, using the endogenous protein translation machinery. Lastly, the vaccine can also comprise a viral vector: a harmless virus acting as a 'delivery vehicle' that carries the genetic instructions to make the protein from the virus of interest (Kyriakidis et al., 2021).

The second vaccine component is the adjuvant. It is an immune booster, a substance that generally enhances the immune response (not specific to the antigen of interest) (O'Hagan & Fox, 2015). During vaccination, it is important to induce a strong innate immune response, since it is indispensable for generating a long-lasting adaptive immune response, comprising strong activation of T and B cells and antibody production, important for better protection. Adjuvants are necessary, because the antigen alone is frequently not sufficiently immunogenic to elicit a durable memory response at a scale that protects the host from future challenge. Common adjuvants stimulate local innate immune cells, such as DCs and monocytes/macrophages, by recruiting them to the injection site and/or activating their PRRs. Because of the effect of adjuvanticity, usually less antigen or fewer vaccine doses are needed (Reed et al., 2013). The most widely used traditional adjuvant is aluminum salt (alum): it releases the antigen slowly, keeping it longer at the injection site providing more time for immune recognition, and stimulates local inflammation (T. Zhao et al., 2023). Alum has been

shown to activate the NLRP3 inflammasome – however, while one study states that NLRP3 is dispensable for adjuvant activity (Franchi & Núñez, 2008), another one declares that alum's adjuvant effect is mediated by NLRP3 (H. Li et al., 2008). Otherwise, oil-in-water emulsions or TLR agonists (PAMPs, nucleic acids, lipids) are used (Pulendran et al., 2021; Reed et al., 2013). Another adjuvant which is being tested in clinical trials in humans at the moment, glucopyranosyl lipid adjuvant (GLA), a synthetic TLR4 agonist, which synergizes with the squalene oil-in-water emulsion (SE), creating GLA-SE, has been shown to induce strong $CD4^+$ T and B cell responses, which required NLRP3, ASC and IL-1R signaling. These were responsible, for example, for infiltration of innate cells into the draining LNs, production of IFN-γ, and proliferation of antigen-specific $CD4^+$ T cells (Seydoux et al., 2018). By stimulating the immune system, adjuvants contribute to the immunogenicity of a vaccine (*i.e.*, the optimal antigen-specific immune response) – however, they also have an impact on the vaccine's reactogenicity, since they are often responsible for the short-term local reactions and systemic effects, such as redness, swelling and pain at the injection site as well as mild fever and muscle aches. Thus, effective and safe vaccines have to find a balance between immuno- and reactogenicity: stimulate the immune system at a suitable level, without causing excessive inflammation.

1.4 Lipid nanoparticle (LNP)-mRNA vaccines

Not too long ago, starting in 2020, we have lived through a worldwide outbreak of a very harmful coronavirus disease 2019 (COVID-19) pandemic, caused by the severe acute respiratory syndrome coronavirus 2 (SARS-CoV-2). Luckily, COVID-19 vaccines against SARS-CoV-2 emerged in record time, and already in December 2020, the first person received an approved vaccine outside of a clinical trial (Watson et al., 2022), more precisely the Pfizer-BioNTech COVID-19 vaccine (Polack et al., 2020; Walsh et al., 2020). Mass vaccination followed, with rapidly increasing numbers of diverse approved vaccines.

A novelty was the form of the two most common COVID-19 vaccines: the Pfizer-BioNTech (BNT162b2, Comirnaty) and Moderna (mRNA-1273, Spikevax) vaccines (Jackson et al., 2020). They were the first mRNA-LNP vaccines approved by the Food and Drug

Administration (FDA) and the European Medicines Agency (EMA). Beforehand, only one other RNA-LNP based drug had been approved in 2018 (the amyloidosis short interfering RNA (siRNA) gene therapy, Onpattro) (Zhang et al., 2020).

In the last years, RNA therapeutics have been investigated and developed to enable protein expression (from mRNA template), inhibit gene expression (*e.g.*, mRNA silencing by siRNAs), or for gene editing (CRISPR/Cas9 system) (Sparmann & Vogel, 2023). On the other hand, nanotechnology has also seen a steady development, enabling the design of nanostructures that allow encapsulation, protection and delivery of antigens. There have been recent advances in nanomaterial-based vaccines, aiming to target infectious diseases (such as COVID-19), but also cancer, and inflammatory/autoimmune and allergic diseases.

The two COVID-19 mRNA-LNP vaccines consist of nucleoside-modified mRNA encoding the antigen, the SARS-CoV-2 spike protein, encapsulated in LNPs.

At the onset of mRNA therapeutics, the first tested mRNAs consisted of unmodified mRNA synthesized by in vitro transcription (IVT), which was highly inflammatory, as it could be recognized by diverse innate sensors. Uridine-containing RNA can be recognized by TLR7 and TLR8, and undesirable dsRNA byproducts of IVT by TLR3, RIG-I or MDA5. This recognition induces expression of type I IFNs, which amplify IFN production by increasing the expression of RNA sensors and decrease the efficiency of antigen synthesis (due to IFN-dependent stress response targeting protein translation), thus lowering immunogenicity. In the COVID-19 vaccines, nucleoside-modified mRNA was used. Replacing uridine with a derivative, N1-methyl-pseudouridine, creates N1-methyl-pseudouridine-modified RNA, which is poorly recognized by innate immune sensors (Andries et al., 2015), thereby increasing translation of the spike protein. The invention of immunosilenced nucleoside-modified mRNA was awarded the Nobel Prize in Physiology or Medicine in 2023 (to Katalin Karikó and Drew Weissman).

mRNA is not very stable, and on its own would be quickly degraded. Thus, mRNA in vaccines is delivered in LNPs, spheres composed of lipids, which protect mRNA from being degraded and, by fusing with the cell membrane, enable the mRNA payload to reach the inside of cells

(X. Hou et al., 2021), which subsequently allows translation of the encoded protein. Usually, LNPs contain four different lipids (X. Hou et al., 2021):

- ionizable lipid: helps package mRNA and promotes its escape from the endosomes inside the cell;
- phospholipid (helper lipid): stabilizes the structure;
- cholesterol: adds stability and fluidity;
- polyethylene glycol (PEG)ylated-lipid (shielding lipid): helps control particle size and behavior in the body, increasing vaccine stability and supporting prolonged circulation.

While it was customary to use permanently charged cationic lipids, for example in liposomes, ionizable cationic lipids have recently been developed. Both COVID-19 vaccines use ionizable cationic lipids: SM-102 in the Moderna vaccine (Jackson et al., 2020), ALC-0315 in the Pfizer vaccine (Polack et al., 2020; Walsh et al., 2020). These lipids allow complexing of the negatively charged mRNA molecules, enabling their encapsulation. Moreover, after cellular uptake of the LNPs through micropinocytosis or endocytosis, LNPs are trapped in endosomes, where the pH-dependent ionizable lipids then facilitate the disruption of the endosomal membrane – a process defined as endosomal escape – to allow the consequent release of vaccine mRNA into the cytosol (X. Hou et al., 2021). Maturing endosomes become more acidic, and the low pH leads to protonation of the ionizable lipids and thus a change in the LNP structure, which promotes the disruption of the endosomal membrane. Once released into the cytosol, the ionizable lipids are re-neutralized, losing the positive charge, which abolishes their binding to the mRNA, allowing its translation with the cellular machinery (X. Hou et al., 2021).

Depending on the LNP formulation (*e.g.*, its size and surface properties) and the route of administration, the mRNA-LNP vaccine disseminates in the body (Verbeke et al., 2022). The COVID-19 vaccines were administered intramuscularly (i.m.), and already a few hours later the antigen was produced at the site of injection as well as in the draining LNs (C. Li et al., 2022). The main cells efficiently taking up the LNP and translating the released mRNA are monocytes, macrophages and DCs – neutrophils, in contrast, efficiently internalize LNPs, but produce the antigen only poorly (Liang et al., 2017). While small LNPs can reach the LNs

minutes after injection, larger LNPs have to be internalized by the immune cells, which then migrate into the lymphatics and finally to the LNs over the course of hours (Verbeke et al., 2022). Thus, LNPs impact the biological distribution and the lymphatic transport of the vaccines. In the case of COVID-19 vaccines, spike mRNA/protein was detectable in the draining LNs for up to 60 days after the second dose, and, at lower levels, even in other tissues (*e.g.*, in the spleen) and in the plasma and serum, suggesting that the mRNA/protein can spread systemically after administration (Verbeke et al., 2022).

At the injection site, local inflammation characterized by secretion of cytokines and chemokines recruits more immune cells which take up the LNPs (*i.e.*, monocytes, DCs, neutrophils) from the blood (Liang et al., 2017; Ndeupen et al., 2021). In the blood itself, cell frequencies can also change upon vaccination – as seen, for example, in healthy volunteers with strongly augmented numbers of inflammatory monocytes after the second dose of the Pfizer COVID-19 vaccine (Arunachalam et al., 2021). So, after the uptake of the LNP-mRNA, monocytes and DCs express the spike protein, and become highly activated, expressing high levels of co-stimulatory molecules CD80 and CD86 and secreting cytokines (such as IL-1β, IL-6) and chemokines (such as C-X-C motif chemokine ligand (CXCL) 10 and 2, and C-C motif chemokine ligand (CCL) 2) (Arunachalam et al., 2021; C. Li et al., 2022; Tahtinen et al., 2022). In the LNs, they then present the antigen-derived peptides on their cell surface to T cells, supporting lymphocyte activation. In turn, T follicular helper cells then direct B cells in germinal center reactions, driving affinity maturation, resulting in high-affinity antibody production (Verbeke et al., 2022).

Some of the advantages of this mRNA-LNP platform are its strong immunogenicity in the elderly (population that, in the case of other vaccines, sometimes requires stronger adjuvants or higher vaccine doses to reach sufficient protection (Y. Hou et al., 2024)) and the lack of a requirement for an additional adjuvant (Anderson et al., 2020; Polack et al., 2020). Moreover, the genetic sequence of the antigen needs to be known, but it can then be quite quickly and flexibly exchanged between different viruses or variants, in a “plug-and-play” design (Al Fayez et al., 2023; Lee et al., 2021; Usdan et al., 2024). Even though there is no additional adjuvant in the COVID-19 vaccines and the mRNA component is nucleoside-modified with

the aim to be non-inflammatory and increase synthesis of the spike protein, the vaccines still elicited strong innate immune responses with a systemic release of pro-inflammatory cytokines, and even some local and systemic adverse events in patients. Examples were pain, redness, swelling at the injection site, and fatigue, headaches, chills and fever (Chapin-Bardales et al., 2021; Rosenblum et al., 2022). These events were mostly mild to moderate, both in severity and duration. Just in few cases, stronger adverse events were reported, including myocarditis, thrombotic thrombocytopenia, allergic reactions (such as anaphylaxis) and autoimmune reactions (Chapin-Bardales et al., 2021; Rosenblum et al., 2022). PEG lipids were shown to be the cause for anaphylaxis and complement-associated pseudoallergy (CARPA), due to pre-existing anti-PEG IgE or IgM antibodies, respectively (Chapin-Bardales et al., 2021; Lee et al., 2023; Rosenblum et al., 2022; Szebeni et al., 2022). Autoimmune reactions, on the other hand, were probably triggered by the recognition of mRNA-LNPs as self-antigens, leading to expansion of autoreactive T and B cells (Lee et al., 2023).
Interestingly, most of these dose-limiting, systemic inflammatory reactions were not predicted from mice models and preclinical studies. Remarkably, mice seem to be more tolerant to RNA vaccines (Tahtinen et al., 2022), with a more limited release of cytokines for example.

1.5 Immunogenicity and reactogenicity of lipid-mRNA-based vaccines

Many questions regarding both the immunogenicity and reactogenicity of the mRNA vaccines, in humans and mice, remain open. Why do these vaccines not require an adjuvant? What are the mechanisms, at the molecular level, behind the local inflammation and innate responses? What are the main drivers of the reported side effects? Why do mice tolerate higher doses and are more protected from toxicity? What is the precise contribution of the nucleoside-modified mRNA vs. the LNP component to the general immune response? Which pathways contribute to the protective immunogenicity, and which to the (dispensable) reactogenicity? Can these two branches even be disentangled? Clinical studies suggest that there are no or weak associations between the reactogenicity/severity of adverse events and the magnitude of antibody or T cell responses (Coggins et al., 2022; Held et al., 2021; Jorda et al., 2023; Lim et al., 2021; Sáez-Peñataro et al., 2024). If this means that strong protective

immunity could be mechanistically dissociated from adverse reactions, this opens attractive opportunities for future vaccine development. Nonetheless, these data need to be confirmed and mechanistically corroborated. Better understanding is of utter importance for tailored development of both the mRNA payloads and the LNP carriers for the future design of vaccines with greater and more durable effectiveness and fewer and milder adverse events.

An important hypothesis is that LNPs do not only function as delivery agents, but are also highly inflammatory and have intrinsic adjuvant activity, possibly also contributing to the reported side effects (Alameh et al., 2021; Liang et al., 2017; Ndeupen et al., 2021; Tahtinen et al., 2022). As a result, the interest in and research on LNPs have significantly increased in the last years.

Interestingly, empty LNPs, without any mRNA, have been shown to induce a strong immune response, leading to secretion of a variety of cytokines and chemokines (Tahtinen et al., 2022). On the one hand, this immune activation can be desirable for vaccine-mediated immunogenicity, but on the other hand, if excessive, it could lead to strong adverse effects. For mRNA-based therapies of autoimmune/inflammatory diseases (*e.g.*, LNP-based therapeutics delivering silencing siRNAs), this immune activation is also not desired.

Although studying single components of LNPs is challenging, as they are not soluble, separate entities but instead form large complexes, and analysis of single components cannot entirely predict the behavior of the complete LNP, various components of LNPs have been linked to immune responses. Accumulation of cholesterol is linked to many different inflammatory pathways (Anand, 2020), and PEGylated lipids have been linked to allergic reactions (Ju et al., 2022; Szebeni et al., 2022). Cationic lipids can be strongly pro-inflammatory (Lonez et al., 2014; Tanaka et al., 2008), and empty LNPs without the ionizable lipid may induce an impaired adaptive immune response (Alameh et al., 2021).

Already back in 2008 and 2014, the first articles were published showing that cationic liposomes or LNPs activate TLRs (2 or 4) and NLRP3, acting through MyD88- and TRIF-dependent pathways and inducing NF-κB-dependent gene expression in human and mouse cells, such as DCs and macrophages (Lonez et al., 2014; Tanaka et al., 2008). Since the COVID-19 pandemic, many more studies have used the Pfizer COVID-19 vaccine or other

LNPs and liposomes (empty or with (un)modified mRNA), in humans, mice, and non-human primates like macaques, both *in vivo* and *in vitro*. While some studies focus on the effect of the LNP vaccines on the adaptive immune response, showing how they promote robust antibody production and antigen-specific T cell responses, other reports try to understand the inflammatory role and mechanism of LNPs in the innate immune system and characterize them as adjuvants.

Firstly, in mice and macaques, a strong innate immune cell infiltration (from the blood) (Liang et al., 2017; Ndeupen et al., 2021) as well as activation (high expression of CD80 and CD86) (C. Li et al., 2022; Liang et al., 2017; Rizzo et al., 2024) have been observed at the injection site and in the draining LNs. After the booster dose of the Pfizer vaccine, also higher fractions of classical inflammatory monocytes and in general IFN-conditioned myeloid cells, enriched in IFN-response transcription factors, were found in the blood of healthy volunteers (Arunachalam et al., 2021). The innate immune cells show very robust classical innate antiviral/IFN transcriptional signatures – for example, both in humans (Jiang et al., 2023) and macaques (Liang et al., 2017), Myxovirus Resistance protein A (MxA), an IFN-stimulated antiviral protein, was found highly expressed. In mice, transcriptional upregulation of inflammatory cell death pathways (such as necroptosis and pyroptosis) has been reported (Ndeupen et al., 2021). Several studies show activation of inflammasomes. In injected mice and macaques (Liang et al., 2017; Ndeupen et al., 2021), significant upregulation of genes associated with inflammasomes (e.g. *Nlrp3*, *Il1b*) was observed. Also in humans, activation of NLRP3 and Caspase-1 has been shown (Rizzo et al., 2024; Tahtinen et al., 2022). Tahtinen et al. (2022) show how the resulting release of mature IL-1β, which binds to IL-1 receptor and initiates a MyD88-dependent signaling cascade, amplifying the inflammatory response through the secretion of many other downstream cytokines (*e.g.*, tumor necrosis factor (TNF), IL-6, IL-10, IL-12p70, IFN-γ). Very high secretion of several cytokines and chemokines in general has been shown in numerous papers, in all the mentioned experimental models. IL-6 has been reported to be essential for the consequent adaptive immune response (Alameh et al., 2021; Tahtinen et al., 2022), consistent with its role of a B cell stimulator. In addition to cytokines produced by myeloid cells, IFN-γ induction in natural killer cells has been reported after the first dose of the Pfizer vaccine, and in $CD8^+$ T cells

after the second dose in i.m. injected mice (C. Li et al., 2022). Both in mice (C. Li et al., 2022) and humans (Arunachalam et al., 2021), IFN-γ levels in the plasma were much higher after the second dose. The mouse study also shows how IFN-γ is required to activate the innate immune cells. For type I IFN (IFN-α) and IL-1β, differences between species have been observed. Upon the Pfizer vaccine administration *in vivo* (Arunachalam et al., 2021) or *in vitro* (Jiang et al., 2023) in humans, IFN-α could not be detected, while it was found in vaccinated mice (C. Li et al., 2022). On the contrary, high levels of IL-1β are released in humans, but only much lower levels are seen in mice, that, in contrast to humans, strongly upregulate IL-1 receptor antagonist (IL-1RA) both *in vitro* and in serum *in vivo* (Tahtinen et al., 2022). This substantial IL-1RA secretion in mice explains why these animals show less inflammation (downstream cytokine secretion), adaptive immune activation (T cell responses), and adverse side effects compared to humans. In evidence of the anti-inflammatory role of IL-1RA in mice, IL-1RA knockout (KO) animals respond to the mRNA vaccines in a manner more similar to humans. The study reports these findings as the explanation for why mice are more tolerant to and protected from high-doses' toxicity, and suggests that IL-1RA KO mice could be a more predictive preclinical model for human reactogenicity to specific vaccines. In general, and consistent with immune memory development mechanisms, stronger immune responses of myeloid and T cells have been observed after second vaccine doses (*e.g.*, higher innate immune cell frequency, higher IFN-γ levels, more pronounced IFN signature) in both mice and humans (Arunachalam et al., 2021; C. Li et al., 2022), which fits the observation that more human volunteers report (mild) side effects after the second vaccine dose than after the first dose (Arunachalam et al., 2021; Chapin-Bardales et al., 2021; Rosenblum et al., 2022).

This opens up the question whether the innate immune system can also be durably "primed" by mRNA vaccines. Is there a crosstalk between lymphocytes and myeloid cells, with lymphocytes instructing the innate immune system to reignite? Or is trained immunity in myeloid cells a factor in this vaccination regimen, involving epigenetic changes in these cells, increasing their responsiveness to subsequent vaccines (Mantovani & Netea, 2020)?

Even "upstream" of this question, the issue remains of how, after the first vaccine dose, the mRNA-LNP vaccines elicit the innate immune response. Are the LNPs directly sensed by

PRRs, such as inflammasome-forming sensors? If so, what exactly is being sensed: the entire LNP, individual lipids (*e.g.*, ionizable lipids), modified/metabolized lipid products (such as oxidized phospholipids (Weismann & Binder, 2012; Zanoni et al., 2016))? Are they sensed directly or indirectly, for example due to membrane disturbances, as shown for virus-like particles (VLPs) and cationic liposomes that activated DCs in a membrane fusion-dependent manner (Holm et al., 2012)?

Both in humans and mice, it has been reported that monocytes are the main cell type to produce cytokines and chemokines in the context of mRNA vaccine administration (Arunachalam et al., 2021; Tahtinen et al., 2022). Regarding the vaccine components, in macaques, mRNA has been shown to be important for activation of myeloid cells (CD80/CD86 expression) and type I IFN signaling (Liang et al., 2017). In contrast, in the same species, the LNP and not the mRNA seems to be responsible for the immune cell recruitment to the site of injection (Liang et al., 2017). The ionizable lipid of the LNP appears to be very important in driving immune activation: If specific ionizable lipids are removed or replaced with other cationic/ionizable lipids, less leukocyte infiltration and lower inflammation (Ndeupen et al., 2021), cytokine secretion (Tahtinen et al., 2022), and antibody titers (Alameh et al., 2021) have been observed in different species. One study tested six different mRNA-LNP formulations in mice for their capability of activating NLRP3, stating that this capability depends on the ionizable and cationic lipids, and cholesterol (Forster III et al., 2022). The formulations that activated NLRP3 the strongest had high concentrations of ionizable and cationic lipids, and low of cholesterol, while the LNP size and surface charge did not have an impact. Regarding signaling pathways, IL-6 seems to play an important role for the later adaptive immune responses, both in humans and mice (Alameh et al., 2021; Tahtinen et al., 2022). The same holds true for IFN-γ, reported in different studies (Arunachalam et al., 2021; C. Li et al., 2022). In contrast to these well-established cytokine signaling pathways, the roles of other immune mechanisms are less clear. Older studies show how specific liposomes activate TLR4 in human and mouse DCs, which leads to the production of inflammatory cytokines and maturation of DCs (Tanaka et al., 2008), and how certain cationic LNPs activate TLR2, inducing robust cytokine secretion (Lonez et al., 2014). A study administering the Pfizer COVID-19 vaccine to mice, however, shows how the vaccine's immunogenicity is

independent of many TLRs (2, 3, 4, 5, 7) (C. Li et al., 2022). The Tanaka et al. (2008) liposome paper shows that TLR4 activation engages the MyD88-pathway (Tanaka et al., 2008), and the Tahtinen et al. (2022) study shows that mRNA vaccine-encapsulated liposomes lead to a MyD88-dependent signaling cascade producing inflammatory cytokines (such as IL-6) responsible for the vaccine's immunogenicity in humans (Tahtinen et al., 2022). Yet, a study injecting different LNPs in mice, shows how these LNPs promote an IL-6-dependent robust adaptive immune response, which does not require LNP sensing by receptors signaling through MyD88 (Alameh et al., 2021). The Lonez et al. (2014) paper reports that certain LNPs activate NLRP3, which leads to IL-1β secretion (Lonez et al., 2014); the Tahtinen et al. (2022) study shows how both liposomal and LNP-based vaccines induce NLRP3 activation and IL-1β secretion in humans, which is the first step for the IL-1R1- and MyD88-dependent signaling cascade inducing an innate inflammatory response responsible for immunogenicity (Tahtinen et al., 2022). On the other hand, one study investigating the Pfizer vaccine-immunized mice excludes the role of NLRP3, ASC, and GSDMD in the vaccine's immunogenicity (antigen-specific antibody production and T cell responses) (C. Li et al., 2022). The same paper also excludes the role of STING in mice – instead, it states that MDA5-driven type I IFN is required for strong $CD8^+$ T cell responses to the vaccines (C. Li et al., 2022). In contrast, a work focusing on VLPs observe that these induce the production of IFN-β and other interferon stimulated gene (ISG) products in human and mouse DCs, dependent on STING but not on TLR and MAVS pathways (Holm et al., 2012). Moreover, the Alameh et al. (2021) paper, which excluded LNP sensing by receptors signaling through MyD88 also excluded signaling through MAVS (Alameh et al., 2021).

However, it is important to mention that many mouse studies are performed by deleting individual genes – yet, many sensors (especially nucleic acid sensors) are redundant and LNPs likely hit several innate pathways at once rather than acting through a single receptor. Thus, potentially, individual gene deletions might not be the right strategy, leading to overly simplistic conclusions regarding the dependence of the vaccination outcome on the different PRRs (C. Li et al., 2022; Ndeupen et al., 2021).

Taken together, it is clear that more research is needed on the immune mechanisms driven by LNP administration. A better understanding of these processes could lead to better control of the LNP: improve its immunogenicity and reduce its reactogenicity – for example by adjusting the composition and characteristics of LNPs (size, surface charge, lipids) (Lee et al., 2023). Improving the LNP formulation, together with the already much improved design of mRNA, and possibly the route of vaccine administration, could help to develop better vaccine candidates with enhanced efficacy, safety, and tolerability.

1.6 Aims of thesis

The aim of my PhD thesis was to investigate a potential new role of inflammasomes in sensing of the lipids used for delivery of nucleic acids into the cells, either in the form of transfection reagents or LNP-based vaccines. Following an initial serendipitous finding that the transfection reagent lipofectamine (LF) 2000 alone produced a pro-inflammatory response in mouse macrophages and human monocytes, leading to NLRP3 and AIM2 activation, we quickly got interested in a potential inflammasome response to LNP-based mRNA vaccines. To systematically characterize the impacts of LNPs and transfection reagents on inflammasome signaling, we addressed the following points:

- Which transfection reagents are sensed by the inflammasome and what are the inflammasome-forming sensors initiating this response?;
- Are LNP-mRNA vaccines sensed by the inflammasome in the human system?;
- What signaling modules are activated by LNP-mRNA vaccines in human cells and how do they contribute to the immune response?;
- Are the innate immune responses to LNP-mRNA vaccines similar in the mouse and human systems?.

2. Material and Methods

2.1 Material

2.1.1 Experimental models

Table 1: Cell lines.

Name	**Source**
Human Embryonic Kidney 293T (HEK) cells	III Bonn (CL 23)
HEK cells inducible NLRP3, fluorescent ASC	III Bonn (AG F. Schmidt)
HEK cells inducible AIM2, fluorescent ASC	III Bonn (AG F. Schmidt)
HEK cells mitochondrial reporter	III Bonn (CL 117)
THP-1 monocytes, fluorescent ASC	III Bonn (CL 190)
Immortalized macrophages (iMacs), wild-type (WT)	III Bonn (CL 105)
Immortalized macrophages (iMacs), AIM2$^{-/-}$	III Bonn (CL 104)
Immortalized macrophages (iMacs), NLRP3$^{-/-}$	III Bonn (CL 19)
Immortalized macrophages (iMacs), mouse NRLP3, fluorescent ASC	III Bonn (CL 119)
NLRP3$^{-/-}$ iMacs (BALB/c background)	III Bonn (CL 800)
NLRP3$^{-/-}$ iMacs, human (hum) NLRP3	III Bonn (CL 801)
NLRP3$^{-/-}$ iMacs, mouse (mou) NLRP3	III Bonn (CL 802)
NLRP3$^{-/-}$ iMacs	III Bonn (CL 979)
NLRP3$^{-/-}$ iMacs, hum NLRP3	III Bonn (CL 980)
NLRP3$^{-/-}$ iMacs, mou NLRP3	III Bonn (CL 981)
NLRP3$^{-/-}$ iMacs, macaque (mac) NLRP3	III Bonn (CL 982)
NLRP3$^{-/-}$ iMacs, rat NLRP3	III Bonn (CL 983)
NLRP3$^{-/-}$ iMacs	III Bonn (CL 993)
NLRP3$^{-/-}$ iMacs, hum NLRP3	III Bonn (CL 994)
NLRP3$^{-/-}$ iMacs, mou NLRP3	III Bonn (CL 995)
NLRP3$^{-/-}$ iMacs, mouse NLRP3 with human linker	III Bonn (CL 996)

(mou N3_hlink)	
NLRP3$^{-/-}$ iMacs, mouse NLRP3 with human mutation (mou N3_hmut)	III Bonn (CL 997)
NLRP3$^{-/-}$ U937s monocytes	III Bonn (CL 986)
NLRP3$^{-/-}$ U937s monocytes, hum NLRP3	III Bonn (CL 987)
NLRP3$^{-/-}$ U937s monocytes, mou NLRP3	III Bonn (CL 988)

Table 2: Mice.

Strain	**Source**
C57BL/6J WT	Charles River
C57BL/6J AIM2$^{-/-}$	III Bonn
C57BL/6J NLRP3$^{-/-}$	III Bonn

2.1.2 Tissue culture reagents, media, chemicals, buffers, inhibitors and activators, antibodies, commercial assays

Table 3: Tissue culture reagents.

Name	**Company**
Dulbecco's Modified Eagle's Medium (DMEM), with 4.5 g/L glucose, 2 mM L-glutamine, phenol red	Gibco
Roswell Park Memorial Institute (RPMI) 1640 (1x) with L-glutamine	Gibco
Opti-MEM	Gibco
Fetal calf serum (FCS)	Thermo Fisher Scientific
Penicillin-Streptomycin (10,000 U/mL)	Thermo Fisher Scientific
GlutaMAX	Gibco
4-(2-hydroxyethyl)-1-piperazineethanesulfonic acid (HEPES)	Gibco

Sodium Pyruvate	Gibco
L929	III Bonn
Dulbecco's Phosphate Buffered Saline (DPBS) (1x)	Gibco
Hanks' Balanced Salt Solution (HBSS)	Gibco
TrypLE Express (1x) Enzyme	Thermo Fisher Scientific
Ethylenediaminetetraacetic acid (EDTA) (0.5 M, pH 8.0)	Life Technologies

Table 4: Media.

Name	**Composition**
Complete DMEM	DMEM supplemented with 10 % FCS, 1 % Penicillin-Streptomycin
Complete DMEM (BMDM differentiation)	DMEM supplemented with 10 % FCS, 1 % Penicillin-Streptomycin, 15-20% L929
Complete RPMI (primary cells)	RPMI supplemented with 10 % FCS, 1 % Penicillin-Streptomycin
Complete RPMI (tissue culture, U937 cells)	RPMI supplemented with 10 % FCS, 1 % Penicillin-Streptomycin, 1 % Glutamax, 1 % HEPES, 1 % sodium pyruvate
Freezing medium	90 % FCS + 10 % Dimethylsulfoxide (DMSO)

Table 5: Chemicals.

Name	**Company**
DMSO, cell culture grade	PanReac AppliChem
Ethanol absolute (molecular biology grade)	Thermo Fisher Scientific
Chloroform	Merck
Glycogen (molecular biology grade)	Thermo Fisher Scientific
RNaseZap Rnase Decontamination Solution	Invitrogen

TRIzol	Qiagen
UltraPure Dnase/Rnase-Free Distilled Water	Invitrogen
Bovine serum albumin (BSA)	Thermo Fisher Scientific
Poly-L-lysine (0.1 % aqueous solution)	Sigma
16 % Formaldehyde Solution, methanol-free	Thermo Fisher Scientific
Goat serum	Life Technologies
Triton X-100	Carl Roth
DRAQ5	eBioscience
cOmplete EDTA-free protease inhibitor cocktail (50x)	Roche Diagnostics
PhosSTOP easypack phosphatase inhibitor cocktail (10x)	Roche
Fc receptor (FcR) blocking reagent, human	Miltenyi Biotec
FcR blocking reagent, mouse	Miltenyi Biotec
UltraComp eBeads compensation beads	Invitrogen
Ficoll Paque PLUS	GE Healthcare
CD14 MicroBeads UltraPure, human	Miltenyi Biotec
Liberase TL	Roche
Dnase I	Sigma Aldrich
Ammonium-Chloride-Potassium (ACK) lysing buffer	Gibco
Doxycycline	Sigma Aldrich
Phorbol-12-Myristate 13-Acetate (PMA)	Sigma Aldrich

Table 6: Buffers.

Name	**Composition**
Isolation buffer (human monocytes and DCs)	DPBS + 2 % FCS + 1 mM EDTA
Magnetic-Activated Cell	DPBS + 0.5 % BSA + 2 mM EDTA

Sorting (MACS) buffer (human macrophages)	
Digestion buffer (mouse splenocytes)	HBSS + Liberase TL (50 µg/mL) + Dnase I (10 µg/mL)
Fluorescence-Activated Cell Sorting (FACS) buffer	DPBS + 2 % FCS
Radioimmunoprecipitation assay (RIPA) lysis buffer (2x)	2.4 g Tris base, 8.8 g NaCl, 2 mL EDTA (500 mM), 10 mL Triton X-100, 5 g sodium deoxycholate, 1 g SDS, 100 mL glycerol; dissolved in 450 mL H_2O
Complete RIPA	5 mL RIPA lysis buffer (2x), 3.6 mL H_2O, 400 µL cOmplete EDTA-free protease inhibitor cocktail (50x)
Permeabilization and blocking buffer	1x PBS, 10 % goat serum, 1 % FCS, 0.5 % Triton X-100

Table 7: Low-molecular-weight inhibitors and activators of biological processes.

Name	**Company**
Recombinant human IFN-γ	ImmunoTools
Recombinant mouse IFN-γ	ImmunoTools
Recombinant human granulocyte-macrophage colony-stimulating factor (GM-CSF)	Immunotool
Recombinant mouse GM-CSF	Peprotech
Lipopolysaccharide (LPS), tlrl-b5lps	Invivogen
Pam3CSK4	Invivogen
Nigericin	Thermo Fisher Scientific
R837	Invivogen
Monosodium urate (MSU) crystals	Invivogen
Thapsigargin	Enzo Life Sciences
Poly(deoxyadenylic-deoxythymidylic) acid (poly(dA:dT))	Sigma

Lipofectamine (LF) 2000	Thermo Fisher Scientific
LF3000	Thermo Fisher Scientific
LF MessengerMAX	Thermo Fisher Scientific
LF RNAiMAX	Thermo Fisher Scientific
LF CRISPRMAX Cas9	Thermo Fisher Scientific
LF LTX Plus	Thermo Fisher Scientific
DOTAP	Roche
GeneJuice	Merck
FuGeneHD Transfection Reagent	Promega
2,3-dioleyloxy-N-[2-(sperminecarboxamido)ethyl]-N,N-dimethyl-1-propanaminium (DOSPA)	Avanti Lipids
Dioleoylphosphatidylethanolamine (DOPE)	Avanti Lipids
SM-102	Cayman Chemical
Pfizer COVID-19 vaccine	Pfizer/BioNTech
Moderna COVID-19 vaccine	Moderna
AstraZeneca COVID-19 vaccine	Oxford/AstraZeneca
Novavax COVID-19 vaccine	Novavax
Cytokine release inhibitory drug-3 (CRID3) (MCC950, PF-456773)	Pfizer
VX-765	Selleckchem
Cytochalasin D (CytoD)	Sigma-Aldrich
Wortmannin	Cayman Chemical
PitStop2	Merck
Chloroquine	Sigma-Aldrich
CA-074Me	Enzo Life Sciences
2′,3′-dideoxycytidine (ddC)	abcam
Cycloheximide (CHX)	Sigma-Aldrich

Table 8: Antibodies.

Name	Company
ASC, human; TMS-1	BioLegend
Alexa Fluor 488 F(ab) 2 fragment of goat anti-mouse IgG (H+L)	Invitrogen
Gasdermin D (full-length and cleaved), human; E9S1X	Cell Signaling Technology
Caspase-1 (full-length and cleaved), human; BALLY-1	AdipoGen Life Sciences
IL-1β (cleaved), human; 83186S	Cell Signaling Technology
NLRP3, human/mouse; D4D8T	Cell Signaling Technology
AIM2, human; D5X7K	Cell Signaling Technology
AIM2, mouse; 63660	Cell Signaling Technology
Anti-Rabbit Detection Module for Jess/Wes; DM-001	Biotechne
Human CD41a FITC; HIP8 (1:50 dil)	eBioscience
Human CD14 APC; 61D3 (1:200 dil)	eBioscience
Human CD45 PE; 2D1 (1:200 dil)	eBioscience
Mouse CD41a APC; MWReg30 (1:50 dil)	BioLegend
Mouse CD45 PE-Cy7; 30-F11 (1:200 dil)	BioLegend
Mouse CD19 PerCP; 6D5 (1:200 dil)	BioLegend
Mouse CD3e PE; REA606 (1:200 dil)	Miltenyi
Mouse CD11b AF488; 53-0112-82 (1:200 dil)	eBioscience
Mouse Ly6C eFluor450; HK1.4 (1:200 dil)	Invitrogen

Table 9: Commercial assays.

Name	Company
EasySep Human Monocyte Isolation Kit	Stemcell
EasySep Human Pan-DC Pre-Enrichment Kit	Stemcell

12-230 kDa Jess or Wes Separation Module, 25 capillary cartridges	ProteinSimple
CellTiter-Blue™ cell viability assay	Promega
CyQUANT™ LDH Cytotoxicity Assay	Thermo Fisher Scientific
Human IL-1β kit (homogenous time-resolved fluorescence (HTRF))	Cisbio
Mouse IL-1β kit (HTRF)	Cisbio
Mouse IL-1ra/IL-1F3 Enzyme-Linked Immunosorbent Assay (ELISA) Kit – Quantikine	R&D Systems
ProcartaPlex Mix&Match Human 33-plex	Luminex
ProcartaPlex Custom Mouse 22-plex	Luminex
Pierce bicinchoninic acid (BCA) Protein-Assay	Thermo Fisher Scientific

2.1.3 Laboratory plastics and equipment, software

Table 10: Laboratory plastics.

Product	**Company**
20, 200, 1000 µL filtered and unfiltered tips	Mettler-Toledo/Rainin
5, 10, 25 mL serological pipettes	Greiner Bio-One
15, 50 mL centrifuge tubes, conical bottom	Greiner Bio-One
0.5, 1.5, 2 mL Eppendorf-type tubes	Eppendorf
1.5 mL Eppendorf Safe-Lock Tubes (PCR clean)	Eppendorf
5 mL polystyrene flow cytometry tubes	Sarstedt
100, 250, 500 mL vacuum filter bottles	Corning
T-25, T-75, T-175 cm^2 tissue culture flasks, tissue culture-treated, with filter	Greiner Bio-One
10-, 15-cm tissue culture dishes, tissue culture-treated	Greiner Bio-One
6-, 12-, 24-, 48-well plates, tissue culture-treated	Sarstedt/Greiner Bio-One
96-well plates, flat-bottom, tissue culture-treated	Sarstedt/Greiner Bio-One

(for seeding and stimulation)	
96-well plates, U-bottom, tissue culture-treated (for supernatant collection)	Sarstedt/Greiner Bio-One
96-well plates, V-bottom, tissue culture-treated (for flow cytometry)	Sarstedt/Greiner Bio-One
PhenoPlate 96-well microplates, flat-bottom, tissue culture-treated, black (for microscopy)	Revvity
Polymerase chain reaction (PCR) Plate, 96-well	Thermo Fisher Scientific
384-well microplates, white, polystyrol (for HTRF)	Greiner Bio-One
384-well plates, clear, polystyrene (for LDH)	ThermoFisher
Viewseal Sealer, Clear	Greiner Bio-One
Cell scrapers	Labomedic
Liquid reservoirs, 50 mL	VWR
Liquid reservoirs, 12-channel	Carl Roth
Cryo.s vials, 2 mL	Greiner Bio-One
Mr. Frosty freezing containers	Thermo Fisher Scientific
Needles, 20-25G (for mouse work)	B. Braun
Syringes, 5mL (for mouse work)	BD Bioscences
40, 70, 100 µm cell strainer (for mouse work)	Greiner Bio-One
Safety-Multifly needle, 20G x 3/4", 200 mm	Sarstedt
S-Monovette K3 EDTA, 9 mL, (LxØ): 92 x 16 mm	Sarstedt
MACS LS Columns	Miltenyi Biotec
30 µm pre-separation filter	Miltenyi Biotec
Needles (Butterfly-needle), 20G, 21G (for blood collection from humans and mice)	B. Braun

Table 11: Laboratory equipment.

Device	Company
0.1-2 µL, 2-20 µL, 20-200 µL, 100-1000 µL pipettes	Mettler-Toledo/Rainin
2-20 µL, 20-200 µL 12-channel pipette	Mettler-Toledo/Rainin
PIPETBOY Acu2 Pipette Controller	Integra
Centrifuges	Eppendorf
IKA Vortex 3 mixer	Sigma/Merck
Vi-CELL BLU Cell Counter	Beckman Coulter
Thermomixer	Eppendorf
EasyEights EasySep Magnet	Stemcell
MidiMACS separator	Miltenyi Biotec
Flow cytometer BD Canto	BD Bioscience
NanoDrop One Spectrophotometer	Thermo Fisher Scientific
SpectraMax i3 Multi-Mode Microplate Reader	Molecular Devices
Simple Western	Protein Simple
MAGPIX system	Luminex
FLEXMAP 3D system	Luminex
Wide-field fluorescent microscope Zeiss Observer.Z1	Carl Zeiss Jena
Incubator for tissue culture	Sanyo Biomedical
4 °C fridge	Liebherr
-20 °C freezer	Liebherr
-80 °C freezer	Thermo Fisher Scientific
-150 °C freezer	Sanyo Biomedical

Table 12: Software.

Name	Version	Source
Affinity Designer	1.10.8	Affinity
Cell Profiler (for quantification of nuclei, ASC specks, and granularity)	2.2.0	(Carpenter et al., 2006)
Compass for Simple Western	4.0.0	Protein Simple
Fiji (ImageJ)	2.0.0	Java
FlowJo	v10.10	FlowJo, LLC
GraphPad Prism 10	10.5.0	GraphPad Software, LLC
Mendeley	2.135.0	Mendeley Ltd.
Microsoft Excel	16.101.1	Microsoft
SoftMax Pro	6.3.0	Molecular Devices
ZEN Pro	2.3	Zeiss

2.2 Methods

2.2.1 Isolation of primary human cells

2.2.1.1 Isolation of human peripheral blood mononuclear cells (PBMCs), monocytes and DCs

Primary human PBMCs, monocytes and DCs were isolated from fresh whole blood collected from healthy volunteers, who provided informed consent in accordance with the Declaration of Helsinki.

Peripheral venous blood was collected in S-Monovettes K3 ethylenediaminetetraacetic acid (EDTA), diluted 2:1 with pre-warmed Dulbecco's Phosphate Buffered Saline (DPBS), and slowly layered over Ficoll Paque PLUS for density gradient centrifugation (20 minutes (min), 700 x g, acceleration 1, no brake, room temperature (RT)). Upon collection of the PBMC interphase, cells were washed with DPBS, and either used directly for PBMC experiments or further processed for monocyte or DC isolation. Herefor, PBMCs were resuspended in cold isolation buffer (Table 6). For monocyte and DC isolation, PBMCs were negatively selected with the EasySep Human Monocyte Isolation Kit or the EasySep Human Pan-DC Pre-Enrichment Kit, respectively, both following the manufacturer's protocols, followed by magnetic separation using the EasyEights EasySep Magnet.

The purity of the isolated monocytes was assessed by flow cytometry (Method 2.2.3).

Finally, cells were resuspended in complete Roswell Park Memorial Institute (RPMI) medium, and cell concentration was adjusted to $1x10^6$ cells/mL (for PBMCs and monocytes), $0.75x10^6$ cells/mL (for imaging experiments of monocytes), or $0.5x10^6$ cells/mL (for DCs). Cells were either left untreated or supplemented with recombinant human IFN-γ (final concentration: 10 ng/mL), seeded at 100 µL/96-well (F-bottom plate), and stimulated on the next day.

2.2.1.2 Generation of CD14-depleted PBMCs and human macrophages

Blood from healthy donors (buffy coats) was obtained from the Blood Bank of the University Hospital according to protocols accepted by the institutional review board at the University of Bonn (Local Ethics Votes Lfd. Nr. 075/14).

Human PBMCs were obtained from the blood concentrates by diluting them 1:1 with pre-warmed DPBS, followed by density gradient centrifugation in Ficoll Paque PLUS. Upon

washing the PBMC layer with DPBS, cells were resuspended in Magnetic-Activated Cell Sorting (MACS) buffer (Table 6). For monocyte isolation, PBMCs were positively selected by co-incubation with human CD14 UltraPure MicroBeads and magnetic separation using LS columns topped with 30 µm pre-separation filters and mounted on a MidiMACS separator, according to the manufacturer's instructions.

The resulting flowthrough, containing $CD14^-$ blood cells, was then used as CD14-depleted PBMCs. These cells were resuspended in complete RPMI medium, adjusted to a concentration of $1x10^6$ cells/mL, supplemented with recombinant human IFN-γ (final concentration: 10 ng/mL), seeded at 100 µL/96-well (F-bottom plate), and stimulated on the next day.

The collected $CD14^+$ cells were also resuspended in complete RPMI medium, but at a density of $2x10^6$ cells/mL, and supplemented with recombinant human granulocyte-macrophage colony-stimulating factor (GM-CSF; final concentration: 55.5 ng/mL). Cells were then seeded at $10x10^6$ cells/6-well and incubated for the following three days to allow differentiation of monocytes into macrophages. Then, macrophages were harvested and adjusted to a concentration of $1x10^6$ cells/mL in fresh complete RPMI medium complemented with GM-CSF (final concentration: 13.9 ng/mL) and with our without recombinant human IFN-γ (final concentration: 10 ng/mL). Cells were then seeded at 100 µL/96-well (F-bottom plate) and stimulated on the next day.

2.2.2 Isolation of primary mouse cells

2.2.2.1 Mice

C57BL/6J wild-type (WT), NLRP3- and AIM2-KO mice were obtained from Charles River Laboratories or from other groups at the Institute of Innate Immunity (III) (Bonn) and housed in the House for Experimental Therapy (HET) facility at the University Hospital of Bonn under standard specific pathogen-free (SPF) conditions. When possible, mice were sex- and age-matched and sacrificed between 6-24-weeks of age.

2.2.2.2 Isolation of mouse PBMCs

Mice were euthanized by CO_2 inhalation to allow cardiac blood collection from the still-beating heart. Intracardiac puncture was performed using 21G needles and syringes pre-coated with sodium citrate, and blood was collected into EDTA-containing 1.5 mL Eppendorf tubes. Blood from three to four mice (total volume: 2-3 mL) was pooled in a 15 mL falcon tube and diluted with 5-6 mL of DPBS. The diluted blood was then carefully layered over 4.5 mL Ficoll Paque PLUS in a new 15 mL tube. Upon centrifugation (20 min, 850 x g, acceleration 1, no brake, RT), the PBMC layer was collected, filtered through a 40 µm nylon mesh, and diluted to 15 mL with DPBS. Then, cells were pelleted by centrifugation (10 min, 550 x g, RT) and resuspended in complete RPMI medium. Finally, PBMCs were adjusted to a concentration of $1x10^6$ cells/mL, supplemented or not with recombinant mouse GM-CSF (final concentration: 1 ng/mL) or IFN-γ (final concentration: 10 ng/mL), seeded at 100 µL/96-well (F-bottom plate), and stimulated on the next day.

The composition of the isolated PBMCs was assessed by flow cytometry (Method 2.2.3).

2.2.2.3 BM extraction and generation of BM-derived macrophages (BMDMs)

Following euthanasia, legs from the different mice were dissected to obtain clean femurs and tibias, which were briefly washed in DPBS and disinfected in 70 % ethanol. BM was then flushed out from the bones using a syringe filled with approximately 10 mL ice-cold DPBS and filtered through a 70 µm cell strainer. Upon centrifugation (5 min, 340 x g), cells were either cryopreserved at -150 °C in fetal calf serum (FCS) supplemented with 10 % Dimethylsulfoxide (DMSO), or resuspended in complete Dulbecco's Modified Eagle's Medium (DMEM) supplemented with 15-20 % L929-conditioned medium. Cells obtained from one leg were seeded into three 10 cm tissue-culture dishes and left differentiating into BMDMs for 6 days in the incubator (37 °C, 5 % CO_2). Subsequently, adherent BMDMs were once washed with 10 mL DPBS and then detached using 10 mL cold DPBS and a cell scraper. After centrifugation (5 min, 340 x g), cells were resuspended in complete DMEM, adjusted to a final concentration of 0.75×10^6 cells/mL, supplemented or not with recombinant

mouse GM-CSF (final concentration: 1 ng/mL) or IFN-γ (final concentration: 10 ng/mL), seeded at 100 µL/96-well (F-bottom plate), and stimulated on the next day.

2.2.2.4 Isolation of splenocytes

Following euthanasia, spleens were collected and briefly washed in 6-wells with DPBS, before being transferred to 6-well plates containing pre-warmed digestion buffer (Table 6). Spleens were then shredded into small pieces with the help of tweezers and incubated for 30 min (37 °C, 5 % CO_2) to allow for digestion. Subsequently, the digested cell suspension was transferred into a 50 mL falcon tube through a 100 µm cell strainer, which was rinsed with 5 mL DPBS. Upon centrifugation (5 min, 500 x g, 4 °C), each spleen cell pellet was resuspended in 1 mL of Ammonium-Chloride-Potassium (ACK) lysing buffer and incubated for 5 min at RT. Upon addition of 5 mL DPBS, the cell suspension was transferred into a new 50 mL falcon tube through a 40 µm cell strainer, which was again gently rinsed with 5 mL DPBS. The cell suspension was then transferred into a 15 mL falcon tube and centrifuged (5 min, 500 x g, 4 °C). Upon washing the cells three times with 10 mL DPBS, splenocytes were resuspended in complete RPMI, adjusted to a final concentration of 1 x 10^6 cells/mL, supplemented or not with recombinant mouse GM-CSF (final concentration: 1 ng/mL) or IFN-γ (final concentration: 10 ng/mL), seeded at 100 µL/96-well (F-bottom plate), and stimulated on the next day.

2.2.3 Flow cytometry

To evaluate the purity of isolated human monocytes or the composition of isolated mouse PBMCs, flow cytometry analyses were performed using a BD Fluorescence-Activated Cell Sorting (FACS) Canto. Herefor, cells were transferred to 96-well V-bottom plates and washed with FACS buffer (Table 6). Upon incubation with the human or mouse Fc receptor (FcR) blocking reagent (20 min, 4 °C) and a FACS-buffer-wash, cells were stained with fluorochrome-conjugated monoclonal antibodies (30 min, 4 °C, dark). Finally, after three washes with FACS buffer, cells were directly analyzed by flow cytometry.

For assessment of the human monocyte purity, cells were stained with antibodies against CD14 (monocyte marker), CD45 (leukocyte marker) and CD41a (platelet marker). For characterization of the composition of mouse PBMCs, cells were stained with fluorescently labeled antibodies against CD41a (to assess platelet contamination) and CD45 (leukocyte marker). To help detangle the presence of the different leukocytes, cells were additionally stained with CD19 (B cell marker), CD3 (T cell marker), CD11b and Ly6C (monocyte markers).
Finally, flow cytometry data were analyzed using FlowJo v.10.10.

2.2.4 Cell culture

2.2.4.1 Cell culture

All cell lines used in this study (Table 1) were maintained under standard culture conditions (37 °C, 5 % CO_2). Human Embryonic Kidney 293T (HEK) cells and mouse immortalized macrophages (iMacs) were cultured in complete DMEM (Table 4) in tissue-culture treated T-25, T-75, T-175 cm^2 flasks. When approximately 70-80 % confluent, cells were passaged by washing with DPBS, detaching from the flask's surface with TrypLE Express Enzyme, and subsequent neutralization with complete DMEM.
THP-1 and U937 monocytes were cultured in non-tissue culture-treated flasks in complete RPMI (Table 4) and maintained at cell densities between 0.15-0.8 x 10^6 cells/mL.
Experiments were performed using cultures up to 15-passages-old.
Cell counting was performed with the automated Vi-CELL BLU Cell Counter, according to the manufacturer's instructions.

2.2.4.2 Cell seeding

HEK cells expressing a doxycycline-inducible inflammasome (NLRP3 or AIM2) and a fluorescently tagged ASC protein, were used for stimulation experiments with an ASC speck formation microscopy readout. Therefore, HEK cells were adjusted to a concentration of 0.4 x 10^6 cells/mL, and either left untreated (HEK^{ASC} and None) or supplemented with doxycycline (final concentration: 1 µg/mL; HEK^{ASC} and NLRP3/AIM2). Cells were seeded at

100 µL/96-well in a black PhenoPlate pre-coated with poly-L-lysine (Method 2.2.7.1). After a 3 hours (h)-rest, the medium was exchanged for fresh complete DMEM and cells were stimulated.

ASC speck formation readout was also assessed in THP-1 monocytes expressing a fluorescently tagged ASC protein. Cells were adjusted to a concentration of 0.5 x 10^6 cells/mL, seeded at 100 µL/96-well in a black, pre-coated PhenoPlate, and directly stimulated.

For the mtDNA depletion experiments in HEK cells expressing AIM2 and ASC, cells were adjusted to a concentration of 0.025 x 10^6 cells/mL in complete DMEM supplemented with 1 mM sodium pyruvate and seeded at 100 µL/96-well in a black, pre-coated PhenoPlate. Then, 2′,3′-dideoxycytidine (ddC; final concentration: 80 µg/mL) was added and cells were incubated for 72 h (Próchnicki et al., 2023). Afterwards, the medium was exchanged for fresh complete DMEM supplemented with doxycycline (final concentration: 1 µg/mL) and incubated for 3 h. Finally, the medium was replaced with complete DMEM and cells were stimulated.

For the mitochondrial granularity microscopy readout, HEK cells expressing a fluorescent mitochondrial reporter (mCherry targeted to the mitochondrial matrix via cytochrome c oxidase subunit 8 mitochondrial targeting sequence) were used as an indicator of mitochondrial integrity, measured by calculating mitochondrial granularity. Cells were adjusted to a concentration of 0.4 x 10^6 cells/mL, seeded at 100 µL/96-well in a black, pre-coated PhenoPlate, and rested for 3 h. After a fresh DMEM medium exchange, cells were stimulated.

iMacs expressing mouse NLRP3 and a fluorescent ASC were also used for microscopy readouts. Thus, these cells were also seeded at 100 µL/96-well in a black, pre-coated PhenoPlate, after adjusting the concentration to 0.4 x 10^6 cells/mL. After a 3 h-rest, medium was exchanged to fresh complete DMEM and cells were stimulated.

The WT, AIM2-KO and NLRP3-KO mouse iMacs were used for cytokine secretion assays. Cells were adjusted at a concentration of 0.4 x 10^6 cells/mL the evening before, seeded at 100 µL/96-well (F-bottom plate) and rested overnight, before stimulation in the next morning. NLRP3-KO mouse iMacs expressing either mCitrine alone (NLRP3$^{-/-}$ iMacs and None) or a mCitrine-tagged NLRP3 were either adjusted to a concentration of 0.3 x 10^6 cells/mL the evening before, seeded at 100 µL/96-well (F-bottom plate) and left resting overnight, or adjusted to a concentration of 0.75 x 10^6 cells/mL and seeded at 100 µL/96-well (F-bottom plate) in the morning immediately prior to stimulation.

U937 monocytes expressing either mCitrine only (NLRP3$^{-/-}$ U937 macrophages and None) or a mCitrine-tagged NLRP3 were used as macrophages for cytokine secretion assays. First, cells were differentiated overnight at a concentration of 0.25 x 10^6 cells/mL in the presence of 50 ng/mL phorbol-12-myristate 13-acetate (PMA). On the next day, cells were harvested using TrypLE Express Enzyme, adjusted to a concentration of 1 x 10^6 cells/mL in complete RPMI without PMA, and seeded at 100 µL/96-well. Upon overnight resting, cells were stimulated the next day.

2.2.4.3 Cell freezing and thawing

Frozen cell stocks were prepared from early-passage cultures by resuspending 5-10 x 10^6 cells in 1 mL of freezing medium and aliquoting into pre-labeled cryovials. These were then placed in a Mr. Frosty freezing container and stored at -80 °C overnight. The next day, cells were transferred to -150 °C for long-term storage.

For thawing of cell lines, cryovials were thawed and cells were immediately transferred to a 15 mL falcon tube containing pre-warmed complete medium. Upon centrifugation, cells were resuspended in complete medium and transferred to culture flasks.

2.2.5 Stimulation assays

2.2.5.1 Stimulation

For inflammasome activation assays, cells were first primed with the TLR4 agonist LPS for 3-4 h at different concentrations as follows:

- primary human PBMCs, monocytes, macrophages: 2 ng/mL (Hawwari et al., 2024; Rodríguez-Alcázar et al., 2019);
- primary human DCs: 1 µg/mL (Dos Reis et al., 2019);
- U937 macrophages: 40 ng/mL;
- primary mouse cells and iMacs: 200 ng/mL (Hornung & Latz, 2010).

Instead, THP-1 monocytes were primed with the TLR1/2 agonist Pam3CSK4 for 3-4 h at a concentration of 1 µg/mL. In contrast, HEK cells do not require any priming step.

After priming, the medium was replaced with fresh complete medium, and cells were treated with potential inhibitors and activators, in a final volume of 100 µL/96-well.
Cells were either left untreated or pre-treated with inhibitors for 10-30 min. The most commonly used inhibitors include NLRP3 inhibitor cytokine release inhibitory drug-3 (CRID3; 5 µM) (Coll & O'Neill, 2011), and caspase-1 inhibitor VX-765 (50 µM) (Wannamaker et al., 2007). Alternatively, other inhibitors were used: cytochalasin D (CytoD; 1 µg/mL), Wortmannin (100 nM), Chloroquine (10 µM), CA-074Me (50 µM), cycloheximide (CHX; 50 µg/mL).

Subsequently, different inflammasome activators were prepared in Opti-MEM as 10 x concentrated working solutions and added to the cells:

- nigericin for NLRP3 (final concentration: 10 µM);
- monosodium urate (MSU) crystals for NLRP3 (final concentration: 250 µg/mL);
- R837 for NLRP3 (final concentration: 10-40 µg/mL);
- poly(deoxyadenylic-deoxythymidylic) acid (poly(dA:dT)) for AIM2 (model dsDNA transfection complexes, final concentration of 200 ng/well of dsDNA, complexed with 0.5 µL/well of LF2000);
- thapsigargin for AIM2 (final concentration: 20 µM).

The following agents were also investigated in this work for their inflammasome-inducing potential:

- LPS transfection complexes (final concentration of 5 ng/mL of LPS, complexed with 5 µg/mL of LF2000, added as 10 x concentrated working solution);
- the following transfection reagents: LF2000, LF3000, LF MessengerMAX, LF RNAiMAX, LF CRISPRMAX Cas9, LF LTX PLUS, DOTAP, GeneJuice, FuGene (final concentration: 5 µg/mL, added as 10 x concentrated working solution);
- the following lipids: 2,3-dioleyloxy-N-[2-(sperminecarboxamido)ethyl]-N,N-dimethyl-1-propanaminium (DOSPA), dioleoylphosphatidylethanolamine (DOPE), SM-102 (lipid transfection complexes, final concentration of 5 µg/mL of DOSPA/DOPE or 10 µg/mL of SM-102, complexed with 5 µg/mL of LF3000, added as 10 x concentrated working solution);
- the LNP-mRNA COVID-19 vaccines manufactured by BioNTech/Pfizer or Moderna (final: 50 µg/mL, added as 2 x concentrated working solution);
- the COVID-19 vaccines manufactured by AstraZeneca (final: 2.5 x 10^8 infectious units (iu)/mL, added as 2 x concentrated working solution) or Novavax (final: 5 µg/mL, added as 2 x concentrated working solution).

Immediately after addition of inflammasome activators, the plates were centrifuged (15 min, 500 x g, RT), and incubated either for 90 min, 5 h, or overnight (20-24 h; 37 °C, 5 % CO_2), as specified in the in the figure legend.

2.2.5.2 Overview of readouts

After the stimulation, 50 µL/well of cell-free supernatant were collected for analysis of cytokine secretion (by homogenous time-resolved fluorescence (HTRF) or Enzyme-Linked Immunosorbent Assay (ELISA) (Method 2.2.6.1), capillary western blotting technique (WES) (Method 2.2.6.5), or Luminex (Method 2.2.6.2)) or LDH (Method 2.2.6.3) secretion. The supernatants were either analyzed immediately after harvesting, stored at 4 °C for up to 24 h, or at -20 °C for longer time periods.

In contrast, the cells were either used for cell viability assays (Method 2.2.6.4), cell lysis (Method 2.2.5.3) or microscopy (Method 2.2.7).

To test inflammasome activation, multiple readouts were assessed:

- percentage of specking cells, *i.e.*, ASC speck formation per cell (the number of cells in a field of view is approximated by counting cell nuclei);
- GSDMD cleavage (detection of cleaved GSDMD in the lysates);
- caspase-1 cleavage (detection of cleaved Caspase-1 in the supernatants);
- IL-1β cleavage or release (detection of cleaved IL-1β in the supernatants);
- LDH release (in the supernatants).

2.2.5.3 Cell lysis

For cell lysis experiments, cells were seeded in 6-well plates (0.5-2 x 10^6 cells/well, 2 mL/well), left untreated or treated with IFN-γ or GM-CSF overnight, and lysed on the next day.

Before being lysed, cells were placed on ice and washed with ice-cold DPBS. Lysis was then performed using a cell scraper, in 30-100 µL/well of complete radioimmunoprecipitation assay (RIPA) buffer (Table 6). Lysates were incubated on ice for 10 min, and subsequently harvested into 1.5 mL Eppendorf tubes.

After a centrifugation step (10 min, 20000 x g, 4 °C), the supernatants containing nuclei-free cell fractions were transferred to fresh 1.5 mL tubes and stored at -80 °C until further processing.

Next, the protein concentration in the samples was measured via the bicinchoninic acid (BCA) assay, following the manufacturer's instructions. Following a 30-min incubation at 37 °C, absorbance was measured with the SpectraMax i3x plate reader, and protein concentrations of the unknown samples were interpolated from the values of the bovine serum albumin (BSA) standard curves.

2.2.6 Various readouts

2.2.6.1 Cytokine measurement: HTRF or ELISA

To quantify extracellular levels of human or mouse IL-1β, the supernatants of stimulated cells were subjected to HTRF immunoassays in white, small-volume 384-well microplates, according to the manufacturer's instructions. After a 3-h (for human IL-1β) or 6-h (for mouse IL-1β) incubation at RT or a 16-h incubation at 4 °C (both in the dark), the donor and the acceptor fluorescence signals were measured on a SpectraMax i3x plate reader.

To quantify the extracellular levels of mouse IL-1RA, the supernatants of the stimulated cells were subjected to an ELISA in a pre-coated 96-well plate, following the manufacturer's instructions, and the colorimetric signals were measured on a SpectraMax i3x plate reader. Then, the final cytokine concentrations (ng/mL) of the samples were interpolated from the values of the standard curves. When necessary (Fig. 8G), background corrected IL-1β was determined by subtracting, for each cell subline, the values of the different conditions by the value of the unstimulated sample (None), the negative control, for which the IL-1β concentration was thus set to 0 ng/mL.

2.2.6.2 Multiplex measurement

For multiplexed measurement of diverse cytokines, chemokines and growth factors in the supernatants, either a ProcartaPlex Mix&Match Human 33-plex or a ProcartaPlex Custom Mouse 22-plex was applied, according to the manufacturer's instructions. Levels were measured using the Luminex MAGPIX (for the human assay) or the Luminex FLEXMAP 3D (for the mouse assay) system.

2.2.6.3 Cell viability measurement: LDH secretion

The extracellular LDH concentrations present in the supernatants of the stimulated cells were always measured directly after supernatant collection using the CyQUANT LDH cytotoxicity assay, according to the manufacturer's instructions. Following a 30-min incubation at 37 °C, colorimetric detection was performed with the SpectraMax i3x plate reader. The percentual extracellular presence (%) of LDH was determined by subtracting the values of the different

conditions by the value of the unstimulated sample (None), which was thus determined as a negative control for percentual absence of LDH with 0 %.

2.2.6.4 Cell viability measurement: CellTiter Blue (CTB) assay

To evaluate cell viability, upon collection of half the volume of supernatants, the remaining cells were incubated with the CellTiter Blue (CTB) cell viability assay reagent, for 1-2 h at 37 °C and 5 % CO_2, following the manufacturer's instructions. Measurements were performed with the SpectraMax i3 plate reader, and the percentual cell viability (%) was determined by dividing the values of the different conditions by the value of the unstimulated sample (None), which was thus determined as a positive control for percentual cell viability with 100 %.

2.2.6.5 Protein level measurements: Simple Western assay

Both supernatants and cell lysates were also analyzed by Simple Western assays using the WES module, following the manufacturer's instructions.

For the inflammasome assays, supernatants were analyzed for cleaved caspase-1 and IL-1β, while cell lysates for cleaved GSDMD levels. Otherwise, cell lysates from primary human or mouse cells, or from cell lines, were examined for NLRP3 or AIM2 expression.

Cell lysates were prepared as described in Method 2.2.5.3, whereas supernatants were directly used in the Simple Western assay. For cell lysates, a total of 2-5 µg of protein per sample were loaded. Shortly, four parts of sample were combined with one part of a 5 x Fluorescent Master Mix, and denatured by incubation at 95 °C for 5 min. The samples and a biotinylated molecular weight ladder, the primary antibodies (always diluted 1:50 in the antibody diluent of the WES module), horseradish peroxidase (HRP)-conjugated secondary detection antibodies for WES, the streptavidin-horseradish peroxidase conjugate, the chemiluminescent substrate, and the wash buffer were loaded into the plate. Samples were electrophoretically separated, with internal fluorescent standards used to normalize separation distances, and detected in a 25-capillary cartridge (12-230 kDa) as follows: 200-seconds (sec) loading time of the separation matrix, 15-sec loading time of the stacking

matrix, 9-sec loading time of the sample, 25-min separation time of the sample at 375 volt, 90-min incubation time with the primary antibody, and 30-min incubation time with the secondary antibody.

The detected chemiluminescent signals were analyzed with the Compass for Simple Western software. For quantification, the resulting signal intensities for the target proteins at the estimated molecular weights were shown as area under the curve (AUC).

2.2.6.6 RNA isolation and sequencing

For RNA isolation and sequencing, 2 x 10^5 cells were seeded and stimulated as described above. Next, cells were lysed directly in TRIzol, and lysates were either stored at -20 °C or used directly for RNA isolation, following the manufacturer's instructions, with 10 µg Glycogen used during RNA precipitation. Isolated RNA concentrations were assessed by UV spectroscopy to measure the absorbance at 260 nm using the NanoDrop. RNA was stored at -80 °C until full-length RNA-Seq. RNA quality control (Tape station 4200 system, Agilent), library preparation (Watchmaker RNA Library Prep Kit) and sequencing on the Ilumnia NovaSeq 6000 sequencing device (Illumina) (coverage of 15 M reads with a read length of 2x100 bp) was performed by the Next Generation Sequencing Core Facility.

2.2.7 Widefield fluorescence microscopy

2.2.7.1 Coating of microscopy plates

For microscopy experiments, 96-well F-bottom plates with black walls were used. To improve cell adhesion, plates were coated in-house with poly-L-lysine. Briefly, 75 µL/well of a 0.01 % aqueous poly-L-lysine solution were added, followed by a 30-90-min incubation at RT. Subsequently, the poly-L-lysine solution was removed, and the plates were dry-centrifuged upside-down (1-5 min, 1000 x g, RT).

2.2.7.2 Antibody staining

Upon fixation with formaldehyde (final concentration: 4 %) for 15 min at RT, formaldehyde was removed and cells were washed twice with 100 µL/well of DPBS. Either directly

afterwards or after storage at 4 °C overnight, the cells were then treated with 50-100 µL/well of permeabilization and blocking buffer (Table 6) and incubated for 30 min at 37 °C. This buffer was subsequently replaced by 50 µL/well of the primary antibody (ASC TMS-1 (Table 8); dilution 1:500) diluted in permeabilization and blocking buffer. The plate was incubated with the primary antibody for 1 h at 37 °C or overnight at 4 °C. Next, cells were gently washed three times with 100 µL/well of permeabilization and blocking buffer, and afterwards incubated for 1 h at 37 °C with 50 µL/well of the secondary antibody (goat anti-mouse IgG, Alexa Fluor 488 (Table 8); dilution 1:2000) and DRAQ5 (dilution 1:5000) in permeabilization and blocking buffer. Next, two washing steps with 100 µL/well of permeabilization and blocking buffer and one with 100 µL/well of DPBS were performed, and the cells were finally left with 200 µL/well of DPBS. The sealed plate was then stored at 4 °C until being imaged on the Zeiss Observer.Z1 fluorescence microscope.

2.2.7.3 Microscopy

After cell stimulation in black 96-well plates, and fixation with formaldehyde (final concentration: 4 %) mixed with DRAQ5 (final concentration: 5 µM) for HEK cells, or fixation and immunofluorescence staining (Method 2.2.7.2) for primary human monocytes, samples were stored at 4 °C until image acquisition. Imaging was performed at the Microscopy Core Facility, using the Zeiss Observer.Z1 widefield fluorescence microscope, with a dry 20 x Plan Apochromat objective (numerical aperture 0.8). The microscope was operated by the Zeiss Zen Pro 2.3 software.

Four images per well were acquired automatically, with the nuclear DRAQ5 channel as the reference channel for autofocus. Generally, a phase-contrast micrograph was acquired for every condition, using the Zeiss filter set #49 (DAPI) in the light path. For the fluorescent dyes, the following Zeiss filter sets were applied: 488, set #44; 568, set #43; 647, set #50.

The lower and upper limits of the lookup table of the acquired images were linearly adjusted, uniformly to all images within one experiment. Images were then exported as tagged image file format (TIFF) files with the Zeiss Zen Lite software.

For image quantification, raw imaging data were imported into the Cell Profiler software (Carpenter et al., 2006; Kamentsky et al., 2011; McQuin et al., 2018) with analysis pipelines

for both ASC speck and cell nuclei counting and mitochondrial granularity estimation. For each image, the DNA and ASC channels were extracted and submitted to an illumination correction, so that each primary object (DNA and ASC specks) can be identified with specific features and counted. In contrast, the granularity of the mitochondrial fluorescence signal was calculated in unprocessed images.

The percentual of specking cells (%) was determined by subtracting the values of the different conditions by the value of the unstimulated sample (None), which was thus determined as a negative control for percentual absence of ASC specks with 0 %. The percentual mitochondrial granularity (%) was determined by dividing the values of the different conditions by the value of the unstimulated sample (None), which was thus determined as a positive control for percentual mitochondrial granularity with 100 %.

2.2.8 Data analysis

2.2.8.1 RNA sequencing analysis

Paired-end RNA sequencing files were aligned using STAR (v2.7.11b) (Dobin et al., 2013). An index was generated using a combined genome file, concatenating the human GRCh38 genome with Moderna and Pfizer vector sequences obtained from UCSC (https://hgdownload.soe.ucsc.edu/goldenPath/wuhCor1/vaccines/), with genome annotation from the GENCODE v41 GTF file (Mudge et al., 2025)and with sjdbOverhang set to 100. Alignment was then performed to generate gene counts and co-ordinate sorted BAM files, using 20 sorting bins, with unique duplicate and multimapping reads marked.

Differential gene expression analyses were performed in R (v4.4.0) (The R Core Team, 2025). A DGEList was created using the edgeR package (v4.2.0) (Robinson et al., 2010) from the STAR gene counts, sample annotation and additional gene annotation obtained using the biomaRt package (v2.60.1) (Durinck et al., 2005, 2009) with Ensembl v107.

A design matrix was constructed with samples grouped according to treatment, including donor as a batch effect. Lowly expressed genes were removed using the filterByExpr function. In addition, the genes *HBA1* and *TLE5* were also excluded, as were two lncRNAs antisense to these genes (*ENSG00000290010* and *ENSG00000267469*), since 3’ UTR

sequences from these genes were included in the vectors (Moderna and Pfizer respectively). Normalisation factors were calculated using the TMM method (Robinson & Oshlack, 2010). Counts were transformed using the voom method (Law et al., 2014) and a linear model was fit using the edgeR voomLmFit function. Comparisons between groups were made using the contrasts.fit function from the limma package (v3.60.0) (Ritchie et al., 2015). Moderated *t*-statistics were calculated using a 1.2-fold change (FC) threshold and *p*-values obtained using the treat function (McCarthy & Smyth, 2009). Differentially expressed genes were defined as those with a false discovery rate (FDR)-adjusted *p*-value < 0.05. In addition, genes were ranked by confident effect size at this adjusted *p*-value threshold using the limma_confects function from the topconfects package (Harrison et al., 2019).

2.2.8.2 General data analysis

Upon collection, data was transferred to GraphPad Prism (Version 10) for visualization and statistical analysis. Quantitative pooled data are typically presented as mean and standard deviation (SD), with the number of independent experiments or biological repeats (minimum of two) stated in the figure legend. Individual data points represent means of technical replicates (usually duplicates) in each independent experiment, except when stated differently. P values were determined by two-way ANOVA with multiple comparison tests (Dunnett's or Šídák's) or paired t tests, and shown graphically and accurately stated in the figure legend.

3. Results

3.1 Inflammasomes sense Lipofectamine 2000

Like many other projects in the scientific world, my thesis research started with a serendipitous observation. Non-canonical activation of NLRP3 is triggered by intracellular LPS, which by binding to human caspases-4 and -5 (and the mouse homolog caspase-11) leads to GSDMD cleavage, K^+ efflux, and NLRP3 activation (Downs et al., 2020; Kayagaki et al., 2015; Rühl & Broz, 2015; Shi et al., 2014). We wanted to investigate this non-canonical inflammasome response in mouse primary BMDMs, delivering LPS with the transfection reagent LF2000. However, we found that WT BMDMs responded to LF2000 alone by secreting IL-1β (Figure (Fig.) 1A), and this was in the same range as the cytokine release produced upon a LF2000-mediated LPS transfection (Fig. 1A). This suggests that LPS itself does not contribute to inflammasome activation in this setting. Interestingly, the response to LF2000 was decreased in both AIM2- and NLRP3-KO BMDMs (Fig. 1A), indicating that both sensors could build an inflammasome upon recognizing LF2000. Very similar results were observed in WT, AIM2- and NLRP3-KO mouse iMacs (Supplementary (Suppl.) Fig. 1A). Moreover, pre-treatment with the NLRP3 inflammasome inhibitor CRID3 (Coll & O'Neill, 2011), also decreased, but not completely abolished the IL-1β response to LF2000 in WT BMDMs (Suppl. Fig. 1B), supporting the hypothesis that both the NLRP3 and the AIM2 inflammasomes play a role in this process.

Similarly, the human inflammasome sensors responded to LF2000. Primary human monocytes were purified from PBMCs. Purity of monocytes was determined, and, as shown previously (Hawwari et al., 2024), excluding platelets ($CD41^+$), which actually represent the highest number of cells upon purification, monocytes ($CD14^+$ cells) constituted 80-90% of cells, indicating low contamination of other leukocytes ($CD45^+CD14^-$ cells) (Suppl. Fig. 1C). Upon isolation, monocytes were primed with LPS for 3 hours and then stimulated with LF2000. This led to IL-1β secretion (Suppl. Fig. 1D), which was mostly NLRP3- and caspase-1-dependent, as it was inhibitable by CRID3 and VX-765 (caspase-1 inhibitor) (Wannamaker et al., 2007). Interestingly, poly(dA:dT) response, which in mouse cells is AIM2 mediated,

was also prevented by CRID3, suggesting solely NLRP3-dependent inflammasome activation in this setting. This is consistent with previous studies, showing that in human myeloid cells, cytosolic DNA is primarily sensed by cGAS-STING, which induces lysosomal cell death and consequent K^+ efflux, which in turn activates NLRP3 (Gaidt et al., 2017). The observations in the human system contrast with what was seen in mouse cells, which appeared to engage both NLRP3 and AIM2 in the LF2000 response, *i.e.*, the AIM2 inflammasome was also able to recognize the stimulus of interest. Unfortunately, there are no commercially available AIM2 inhibitors and it is not possible to perform KOs in this primary cell type (as the cells are too short-lived, or rather differentiate too quickly), so testing the relative contribution of AIM2 to LF2000-induced IL-1β secretion in primary human monocytes was not possible. Thus, the question remained whether in primary human cells both sensors (AIM2 and NLRP3) are involved in responding to LF2000, or if the response is strictly NLRP3-mediated. If the latter is the case, is the observed dependence on NLRP3 a result of a selective NLRP3 expression in the tested cell type (with lack of AIM2 expression), or does AIM2, even when present, not contribute to LF2000 sensing in human monocytes?

To answer this question, we first determined AIM2 protein (Suppl. Fig. 1E) and RNA (Suppl. Fig. 1F) expression in the monocytes' lysates. Of note, all RNA sequencing data performed in this thesis was with the help of the Next Generation Sequencing Core Facility of the Medical Faculty at the University of Bonn, and Jamie Gearing (from Eicke Latz's research group Immunobiology of Inflammation at the German Rheumatology Research Center) for the analysis. According to the literature (Gaidt et al., 2017; Veeranki et al., 2011; Y. Zhao et al., 2024), overnight pre-treatment of human monocytes with IFN-γ increases their AIM2 protein levels. Therefore, we decided to test AIM2 expression under these conditions. Indeed, compared to the steady-state AIM2 levels in untreated cells, AIM2 protein expression significantly increased in IFN-γ primed monocytes (Suppl. Fig. 1E). Similarly, at RNA level *AIM2* was found to be highly upregulated upon IFN-γ priming (Suppl. Fig. 1F). Interestingly, while *NLRP3* expression was also slightly upregulated by IFN-γ, *IL1B* and *NFKB1* levels were not affected by this treatment (Suppl. Fig. 1F).

We wanted to test whether enforcing higher expression of AIM2 would skew human monocytes away from NLRP3- and towards AIM2-mediated responses, and whether this would shift the LF2000-mediated inflammasome activation from being NLRP3-dependent to being NLRP3-independent – which would then be a strong hint for AIM2 activation, as AIM2 is upregulated in this cell type and we know it senses LF2000 in mouse cells (Fig. 1A). Thus, to characterize human monocyte response to LF2000 in a system expressing high levels of AIM2, we pre-stimulated human monocytes with IFN-γ overnight, and subsequently administered LPS and LF2000. This led to a stronger IL-1β secretion (Fig. 1B) compared to what was observed in the absence of IFN-γ stimulation (Suppl. Fig. 1D). However, CRID3 treatment, although not completely prevented, still strongly reduced the inflammasome response to LF2000, thus suggesting that the response in human cells is mainly NLRP3-mediated even in the presence of high levels of AIM2. Thus, the increased IL-1β secretion levels in the IFN-γ-primed cells cannot be fully explained by an additional AIM2-mediated response to the triggers. Instead, the increased *NLRP3* RNA levels observed upon IFN-γ treatment could provide the underlying mechanism (Suppl. Fig. 1F). Importantly, LF2000 treatment did not substantially reduce the viability of monocytes (Suppl. Fig. 1G).

To further untangle the question of which human inflammasomes could, directly or indirectly, sense LF2000, we employed a gain-of-function approach in a reductionist set-up of ASC speck-reporter HEK cells. We overexpressed human NLRP3 or AIM2 as well as fluorescently tagged human inflammasome adaptor protein ASC to allow investigation of inflammasome response to the agents of interest by monitoring ASC speck formation. Interestingly, we found that both human inflammasome sensors tested, AIM2 and NLRP3, recruit ASC to form an ASC speck upon LF2000 treatment (Fig. 1C).

Remarkably, in this setup NLRP3 is highly responsive in the poly(dA:dT)-treated condition (Fig. 1C), as seen in monocytes, in which CRID3 prevented the poly(dA:dT) induced IL-1β secretion (Fig. 1B). Since poly(dA:dT) is transfected into the cells with LF2000, it is possible that the NLRP3 inflammasome exclusively responds to LF2000, while the AIM2 inflammasome responds to both LF2000 and DNA. In IFN-γ-primed monocytes, most of the IL-1β response is contributed by NLRP3 – however, CRID3 does not fully prevent the response to poly(dA:dT) or to LF2000 (Fig. 1B). That small residual secretion of IL-1β could

indeed be driven by the AIM2 inflammasome, which might activate a weaker signal, as its expression is likely lower than the LPS-induced expression of NLRP3, even in the IFN-γ-primed monocytes (Gaidt et al., 2016; Kumari et al., 2020). Supporting this hypothesis could also be the data from monocytes without IFN-γ treatment (Suppl. Fig. 1D): In this case, where the AIM2 protein and RNA expressions are even lower (Suppl. Fig. 1E,F), CRID3 is indeed able to completely prevent the responses to poly(dA:dT) and to LF2000.

Taken together, both mouse and human NLRP3 and AIM2 inflammasomes are able to sense the transfection reagent LF2000 at endogenous expression levels in primary cells and in a simplified model of inflammasome activation in HEK cells overexpressing inflammasome components.

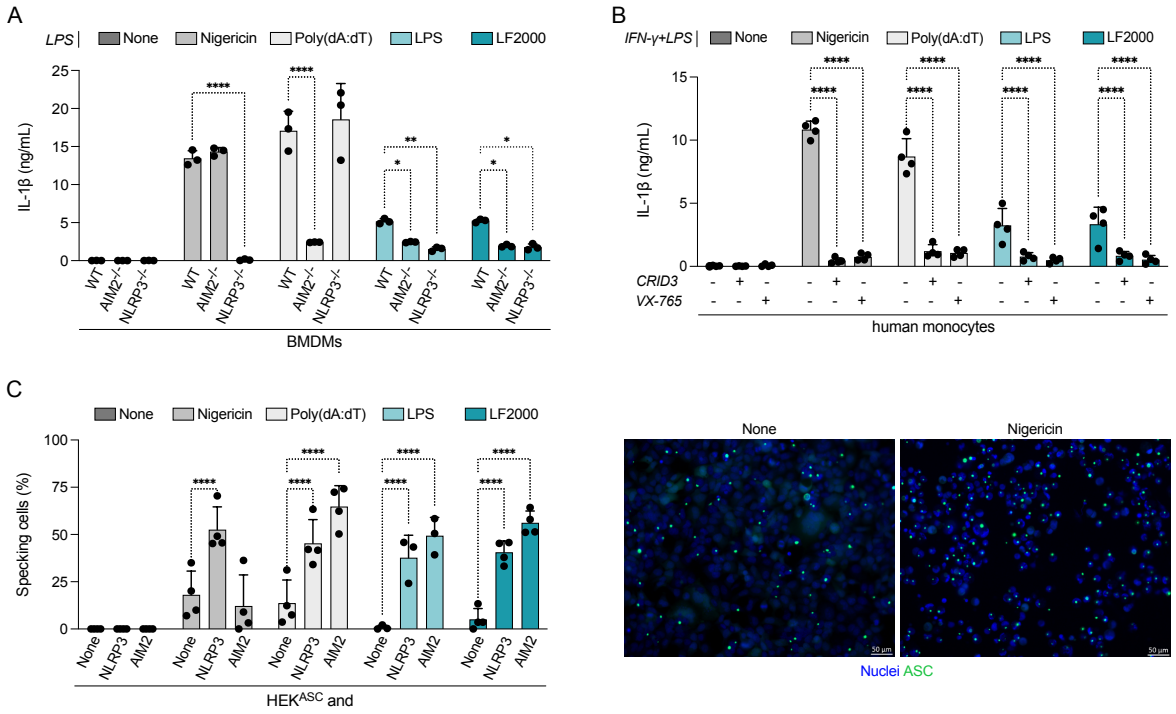

Fig. 1: NLRP3 and AIM2 inflammasomes sense lipofectamine (LF) 2000 in the human and mouse.
(**A**) IL-1β secretion from mouse wild-type (WT), AIM2- or NLRP3-knockout ($^{-/-}$) primary bone marrow-derived macrophages (BMDMs), primed with LPS (200 ng/mL) for 3 hours (h), and stimulated overnight (20-24 h) with nigericin (10 µM), poly(dA:dT) dsDNA (2 µg/mL), transfected LPS (5 ng/mL), and LF2000 (5 µg/mL).

(**B**) IL-1β secretion from human monocytes pre-treated with IFN-γ (10 ng/mL) overnight, and then primed with LPS (2 ng/mL) for 3 h, treated or not with CRID3 (5 μM) or VX-765 (50 μM) for 10-30 minutes (min), and stimulated overnight (20-24 h) with nigericin (10 μM), poly(dA:dT) dsDNA (2 μg/mL), transfected LPS (5 ng/mL), and LF2000 (5 μg/mL).
(**C**) Normalized ASC speck formation per cell (specking cells) (left) and visualization of ASC specks (right) in Human Embryonic Kidney 293T (HEK) cells expressing fluorescently tagged ASC and either no inflammasome (None) or NLRP3 or AIM2, stimulated overnight (20-24 h) with nigericin (10 μM) and poly(dA:dT) dsDNA (2 μg/mL), transfected LPS (5 ng/mL), and LF2000 (5 μg/mL).
N = 3 (A) or 4 (B) biological repeats or 3-4 independent experiments (C); individual data points are means of technical duplicates; all error bars represent SD.
P values were calculated using two-way ANOVA with Dunnett's multiple comparison test. **P* = 0.0261, ***P* = 0.0021, ****P* = 0.0007, *****P* < 0.0001; NS *P* = 0.1582–0.9999 (not shown).

3.2 Human inflammasomes also sense other transfection reagents

Next, we investigated the human inflammasome responses to other transfection reagents, testing different types of LF, DOTAP, and non-liposomal reagents such as GeneJuice and FuGENE HD (defined simply as FuGene).

Neither DOTAP nor GeneJuice and FuGene caused any inflammasome activation in monocytes (Fig. 2A) or reporter HEK cells (Fig. 2C).

In contrast, among the LF variants, LF MessengerMAX, RNAiMAX, and, to a lower extent, CRISPRMAX Cas9 led to inflammasome activation. Firstly, stimulation with these reagents in human monocytes resulted in NLRP3-dependent IL-1β (Fig. 2A) and LDH (Suppl. Fig. 2A) release. Although plasma membrane integrity of some cells must have been lost to some extent to allow the release of LDH, it could be only a modest membrane damage in a limited amount of cells, as the LFs do not appear to have affected the viability of most cells too strongly: LF-treated cells remain metabolically active (Suppl. Fig. 2B). Similar observations have been made previously, where specific nanoparticles led to strong LDH release, indicating membrane damage, but metabolic activity-based cell viability assays did not show differences at the same nanoparticle concentration (Bancos et al., 2012). Moreover, LF reagents led to ASC speck formation in HEK cells expressing NLRP3 or AIM2 (Fig. 2B).

Interestingly, while LF2000 consistently showed an inflammasome response in monocytes and inflammasome component-expressing HEK cells, LF3000 – the newer, improved version

of LF2000 – did not have that effect (Fig. 2A and B; Suppl. Fig. 2A). To better understand the difference in inflammasome responses upon treatment with the two LFs, we sequenced mRNA of monocytes treated with either LF2000 or LF3000 (Fig. 2D). While only some genes were upregulated upon treatment with LF3000 (49) or commonly upon treatment with both LFs (355), a larger subset was only upregulated upon LF2000 administration (1693). The same holds true for downregulated genes (19 vs. 176 vs. 1016, respectively). This suggests that LF2000 is not only inducing a stronger inflammasome response, but also a broader transcriptional response in monocytes compared to LF3000. While *IL1B* and *NFKB1* levels remained unchanged upon treatments, *NLRP3* was actually slightly downregulated upon stimulation with both LF2000 ($\log_2$(FC)) = -2.29, confect = -1) and LF3000 ($\log_2$(FC) = -1.51, confect = -1). Interestingly, *AIM2* was strongly upregulated upon stimulation with LF2000 ($\log_2$(FC) = 3.28, confect = +1) but not significantly with LF3000 ($\log_2$(FC) = 2.54, confect = 0). However, even though AIM2 is able to sense LF2000 in the overexpression-based HEK cell model (Fig. 2B), in monocytes the response to LF2000 appeared to exclusively rely on NLRP3, as it is preventable by CRID3 (Fig. 2A). Thus, this higher *AIM2* expression in LF2000-treated monocytes cannot explain the response difference between LF2000 and LF3000.

A broader look at the differentially expressed genes, there are some genes whose products are involved in stress responses and inflammation upregulated by both LF2000 and LF3000. More stress- and immune-related genes are also selectively upregulated upon LF2000 stimulation, in addition to *AIM2*. Yet, many immune-related genes are also found downregulated by both stimuli (*e.g.*, *NLRP3*). Furthermore, genes associated with the monocyte-macrophage lineage and immune regulation are also found selectively downregulated by LF2000. In contrast, upon LF3000 stimulation less immune-related genes are selectively regulated (compared to LF2000).

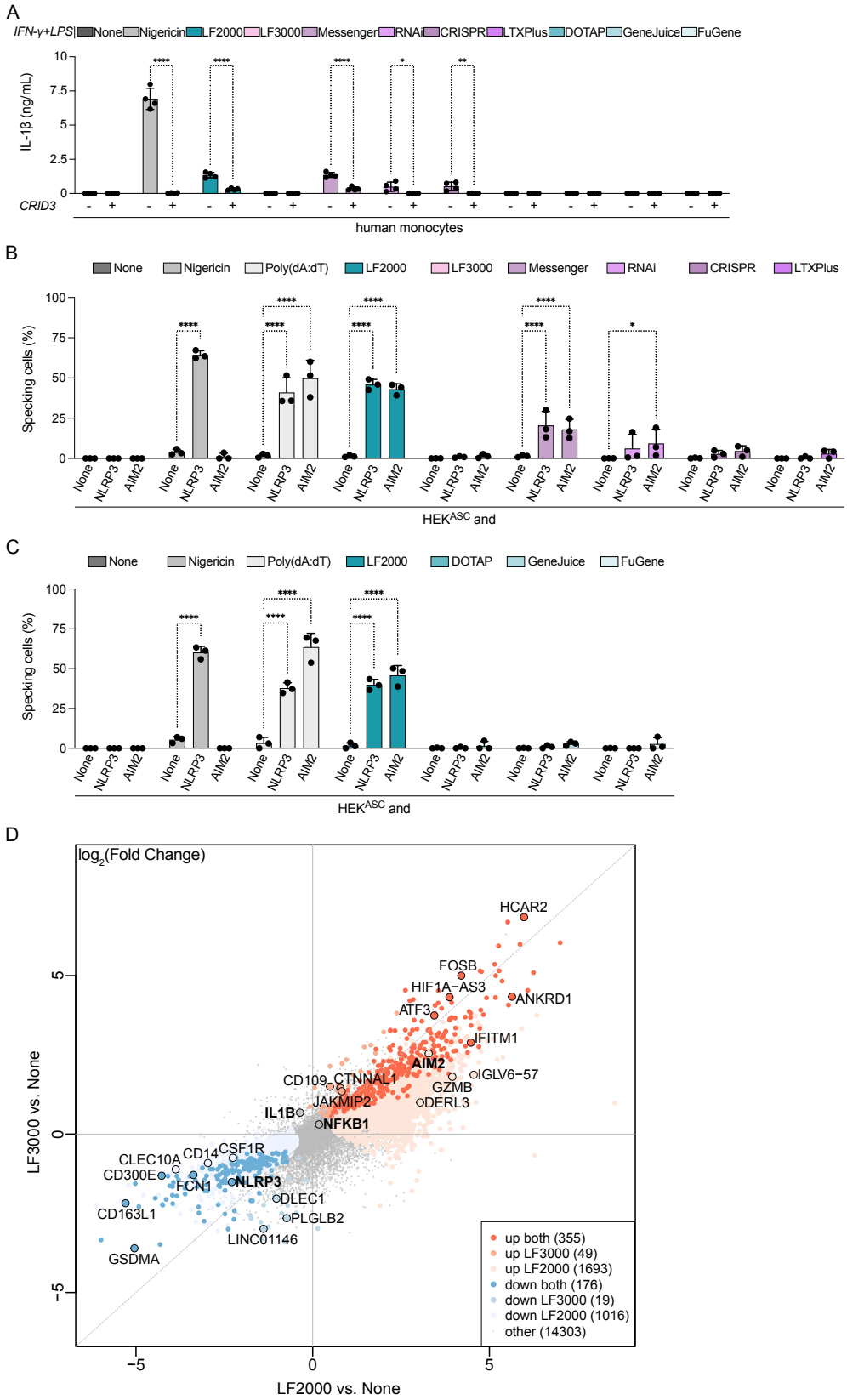
A
IFN-γ+LPS
None
Nigericin
LF2000
LF3000
Messenger
RNAi
CRISPR
LTXPlus
DOTAP
GeneJuice
FuGene
IL-1β (ng/mL)
CRID3
human monocytes
B
None
Nigericin
Poly(dA:dT)
LF2000
LF3000
Messenger
RNAi
CRISPR
LTXPlus
Specking cells (%)
None
NLRP3
AIM2
HEK^ASC and
C
None
Nigericin
Poly(dA:dT)
LF2000
DOTAP
GeneJuice
FuGene
Specking cells (%)
HEK^ASC and
D
log2(Fold Change)
HCAR2
FOSB
HIF1A−AS3
ANKRD1
ATF3
IFITM1
AIM2
IGLV6−57
CD109
CTNNAL1
GZMB
JAKMIP2
DERL3
IL1B
NFKB1
CLEC10A
CD14
CSF1R
CD300E
FCN1
NLRP3
DLEC1
CD163L1
PLGLB2
LINC01146
GSDMA
up both (355)
up LF3000 (49)
up LF2000 (1693)
down both (176)
down LF3000 (19)
down LF2000 (1016)
other (14303)
LF3000 vs. None
LF2000 vs. None

Fig. 2: Human inflammasomes sense some lipofectamines (LFs) (MessengerMAX, RNAiMAX, CRISPRMAX Cas9), but not LF3000.
(**A**) IL-1β secretion from human monocytes pre-treated with IFN-γ (10 ng/mL) overnight, and then primed with LPS (2 ng/mL) for 3 hours (h), treated or not with CRID3 (5 μM) for 10-30 minutes (min), and stimulated overnight (20-24 h) with nigericin (10 μM), LF2000, LF3000, and LF MessengerMAX (Messenger), RNAiMAX (RNAi), CRISRMAX Cas9 (CRISPR), LTX Plus, DOTAP, GeneJuice, FuGene (5 μg/mL).
(**B,C**) Normalized ASC speck formation per cell (specking cells) in Human Embryonic Kidney 293T (HEK) cells expressing fluorescently tagged ASC and NLRP3 or AIM2, stimulated overnight (20-24 h) with nigericin (10 μM), poly(dA:dT) dsDNA (2 μg/mL), and LF2000, LF3000, and LF MessengerMAX, RNAiMAX, CRISRMAX Cas9, LTX Plus (5 μg/ml) (B), or DOTAP, GeneJuice, FuGene (5 μg/mL) (C).
(**D**) Comparison of the $\log_2$ fold changes (FCs) of LF3000 and LF2000 treatments versus control. Genes are coloured according to whether they were significantly differentially expressed with either treatment or both. Certain example genes with high confect effect sizes are highlighted, as well as *AIM2*, *NLRP3*, *IL1B* and *NFKB1*.
N = 4 (A), 5 (D) biological repeats or 3 independent experiments (B,C); individual data points are means of technical duplicates; all error bars represent SD.
P values were calculated using two-way ANOVA with Šídák's (A) or Dunnett's (B,C) multiple comparison test. $*P = 0.0261$, $**P = 0.0021$, $***P = 0.0007$, $****P < 0.0001$; NS $P = 0.1582$–0.9999 (not shown).

In summary, inflammasomes expressed by human monocytes do not sense transfection reagents in general, but only some specific LFs. The strongest inflammasome response is induced by LF2000, while LF3000 does not activate any of the tested inflammasomes. RNA sequencing data shows that some immune-related genes are differentially expressed upon both LF2000 and LF3000. Yet, while LF2000 exclusively induced expression changes of genes involved in inflammation, LF3000 selectively affected more non-immune-related genes. As inflammasome components (*NLRP3*, *IL1B*), however, are not differentially regulated by LF2000 *vs.* LF3000, it is difficult to link the difference in inflammasome responses to both LFs to the differences in gene expression profiles that they induce. Potentially, some of the immune-related genes differentially expressed upon LF2000 administration only could still provide a more complex explanation.

3.3 Human inflammasomes sense LNP-based COVID-19 vaccines

In the aftermath of the COVID-19 pandemic, we have come to recognize the significance of newly developed LNP-based mRNA vaccines. Therefore, the potential capacity of inflammasomes to sense specific lipids or lipid-based formulations is of relevance to better understand the mechanism of action of these new vaccines. A pro-inflammatory response to these preparations would have to be followed up by determining whether this effect is beneficial (adjuvant-like) or risky, contributing to harmful side effects.

Consequently, we stimulated inflammasome-reporter HEK cells with COVID-19 vaccines manufactured by BioNTech/Pfizer and Moderna overnight. Indeed, NLRP3 and AIM2 sensed these stimuli, leading to ASC speck formation (Fig. 3A). Interestingly, inflammasome activation upon vaccine treatment seems to be a slow, potentially multi-step process, considering that shorter stimulations (90 min, Suppl. Fig. 3A; or 5 h, Suppl. Fig. 3B) only led to little ASC speck formation.

We also investigated the responses to LNP-based vaccines in diverse primary human cells, such as PBMCs, monocytes, GM-CSF monocyte-derived macrophages and isolated DCs. PBMCs pre-treated overnight with IFN-γ, primed with LPS for 3 h and then stimulated with the vaccines overnight secreted IL-1β (Fig. 3B) in the cleaved form (Fig. 3C). Cleaved caspase-1 could also be detected in the supernatants of LNP-mRNA vaccine-treated PBMCs (Suppl. Fig. 3E). Of note, the purpose of the IFN-γ pre-treatment was to upregulate expression of AIM2 (Suppl. Fig. 3C), which occurred in PBMCs in a way similar to what was seen in monocytes (Suppl. Fig. 1D and E). Despite that, the response to LNP-mRNA vaccines in human PBMCs was completely dependent on NLRP3, as previously also seen in the LF2000-stimulated monocytes (Fig. 1B). Short stimulations (90 min) with the vaccines also led to an inflammasome response in PBMCs, though lower IL-1β levels were released compared to the overnight stimulations (Suppl. Fig. 3D).

Next, we depleted $CD14^+$ cells from PBMCs to see whether this could abrogate inflammasome activation in PBMCs. A positive outcome of such an experiment (lack of inflammasome activation in CD14-depleted PBMCs) would suggest that monocytes

are the fraction of PBMCs responsible for this inflammatory activation. Indeed, CD14-depleted PBMCs did not secrete any IL-1β in response to any of the tested stimuli (Fig. 3D). To corroborate this finding, we purified monocytes, pre-treated them with IFN-γ, and observed IL-1β secretion (Fig. 3E) as well as ASC speck formation (Fig. 3F, Suppl. Fig. 3F) and GSDMD cleavage (Fig. 3G), in the conditions stimulated with the vaccines manufactured by Pfizer and Moderna. The IL-1β levels in monocyte supernatants were generally much higher compared to those of PBMCs; and consistent with the observations made in PBMCs, the response to LNP-mRNA vaccine in monocytes was NLRP3-dependent, since it was completely prevented by CRID3. Similar to PBMCs, short vaccine stimulations (90 min) also led to a monocyte inflammasome response, though the detected IL-1β concentrations were slightly lower in this case compared to the longer stimulation (Suppl. Fig. 3H). Notably, ASC speck formation was also observed in vaccine-treated THP-1 monocytes expressing a fluorescent ASC fusion protein (Suppl. Fig. 3G).

Lastly, we tested other human cell types known to express inflammasome components. Human GM-CSF derived macrophages also exhibited strong NLPR3-dependent IL-1β secretion upon vaccine stimulation, both under IFN-γ treated (Fig. 3H) and not pre-treated (Suppl. Fig. 3I) conditions. In contrast, IFN-γ treated pan DCs only slightly responded to both preparations of Pfizer and Moderna (Fig. 3I), with IL-1β levels similar to the ones secreted upon nigericin administration. Very interestingly, DCs without IFN-γ pre-treatment showed much higher IL-1β release on treatment with nigericin or poly(dA:dT), but for the LNP-mRNA vaccines, the levels of secreted cytokine were similar to the unstimulated condition (Suppl. Fig. 3J). This suggests that IFN-γ might trigger DCs to be less prone to inflammasome stimulation in general, but not in regard to the vaccine treatment conditions.

Taken together, we identified diverse primary human cell types in which NLRP3 was able to sense the LNP-mRNA COVID-19 vaccines produced by Pfizer and Moderna, with longer stimulations correlating to higher inflammasome responses.

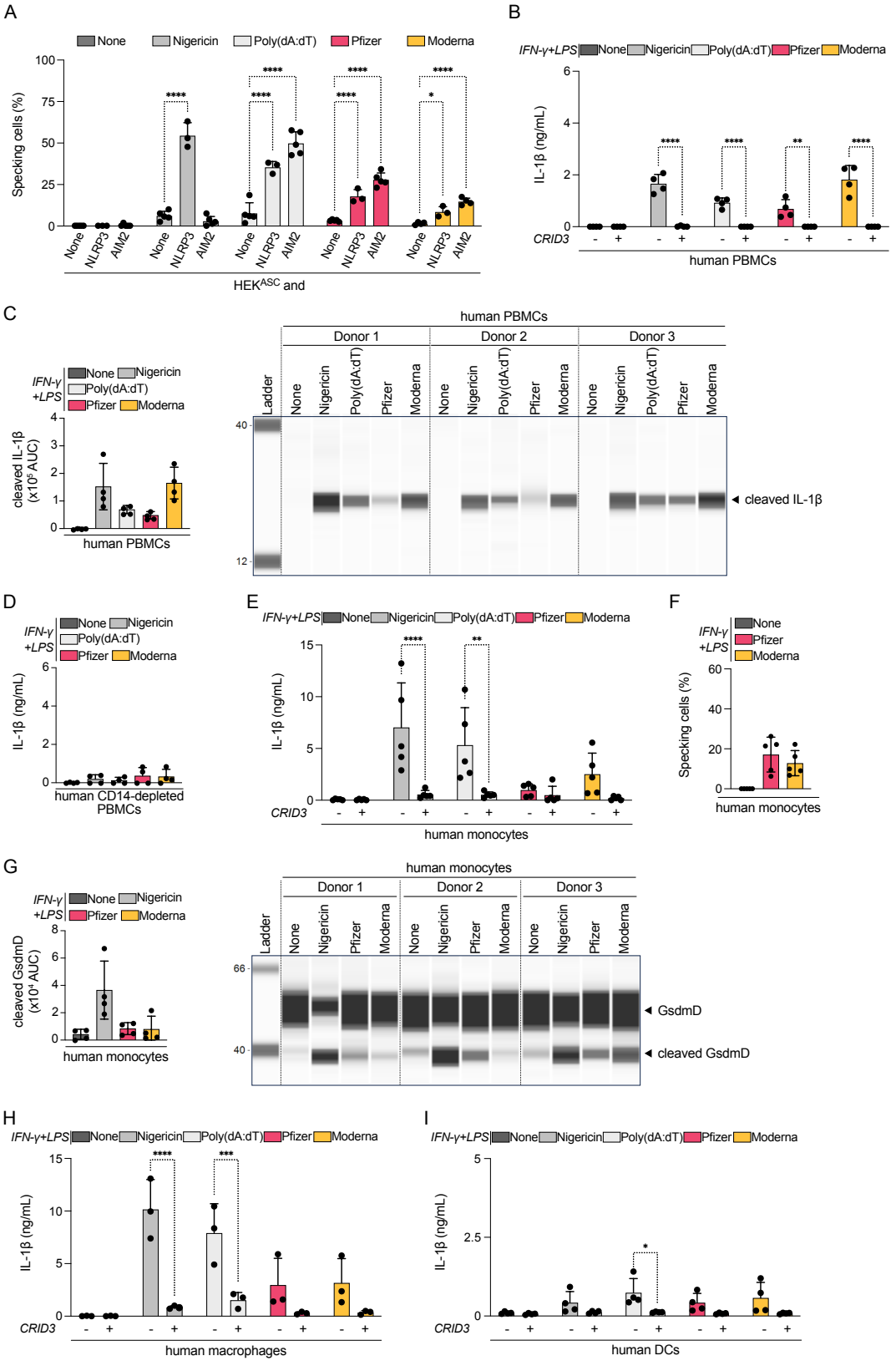
A
None
Nigericin
Poly(dA:dT)
Pfizer
Moderna
Specking cells (%)
HEK^ASC and
B
IFN-γ+LPS
IL-1β (ng/mL)
CRID3
human PBMCs
C
IFN-γ +LPS
cleaved IL-1β (x10⁶ AUC)
human PBMCs
human PBMCs
Donor 1
Donor 2
Donor 3
Ladder
cleaved IL-1β
D
human CD14-depleted PBMCs
E
human monocytes
F
human monocytes
G
cleaved GsdmD (x10⁴ AUC)
human monocytes
human monocytes
GsdmD
cleaved GsdmD
H
human macrophages
I
human DCs

Fig. 3: Human inflammasomes sense lipid nanoparticle (LNP)-based COVID-19 vaccines.
(**A**) Normalized ASC speck formation per cell (specking cells) in Human Embryonic Kidney 293T (HEK) cells expressing fluorescently tagged ASC and NLRP3 or AIM2, stimulated overnight (20-24 hours (h)) with nigericin (10 μM), poly(dA:dT) dsDNA (2 μg/mL), and Pfizer and Moderna vaccines (50 μg/mL).
(**B**) IL-1β secretion from human peripheral blood mononuclear cells (PBMCs), pre-treated with IFN-γ (10 ng/mL) overnight, then primed with LPS (2 ng/mL) for 3 h, treated or not with CRID3 (5 μM) for 10-30 minutes (min), and stimulated overnight (20-24 h) with nigericin (10 μM), poly(dA:dT) dsDNA (2 μg/mL), and Pfizer and Moderna vaccines (50 μg/mL).
(**C**) Simple Western analysis (area under the curve (AUC)) and virtual lane view of cleaved IL-1β detected in the cell culture supernatants of (B).
(**D,E**) IL-1β secretion from human PBMCs depleted of $CD14^+$ cells (D) or purified primary human monocytes (E), primed and stimulated as in (B).
(**F**) Normalized ASC speck formation per cell (specking cells) in primary human monocytes, pre-treated with IFN-γ (10 ng/mL) overnight, then primed with LPS (2 ng/mL) for 3 h, treated with VX-765 (50 μM) for 10-30 min, and stimulated overnight (20-24 h) with Pfizer and Moderna vaccines (50 μg/mL).
(**G**) Simple Western analysis (AUC) and virtual lane view of full-length and cleaved gasdermin D (GsdmD) expression in cell lysates of primary human monocytes, pre-treated with IFN-γ (10 ng/mL) overnight, then primed with LPS (2 ng/mL) for 3 h, and stimulated overnight (20-24 h) with nigericin (10 μM), and Pfizer and Moderna vaccines (50 μg/mL).
(**H,I**) IL-1β secretion from primary human macrophages (H) or dendritic cells (DCs) (I), primed and stimulated as in (B).
N = 3-5 (A) independent experiments or 3 (H), 4 (B,C,D,F,G,I), 5 (E,F) biological repeats; individual data points are means of technical duplicates (except in C,F,G); all error bars represent SD.
P values were calculated using two-way ANOVA with Dunnett's (A) or Šídák's (B,E,H,I) multiple comparison test. $*P = 0.0261$, $**P = 0.0021$, $***P = 0.0007$, $****P < 0.0001$; NS $P = 0.1582–0.9999$ (not shown).

3.4 Pro-inflammatory, inflammasome-independent responses of monocytes to LNP-based COVID-19 vaccines

In addition to inflammasome activation, LNP-mRNA vaccines could also have additional effects on innate immune cells. To study this inflammasome-independent activity, we characterized the inflammatory responses in unprimed (neither IFN-γ nor LPS-primed) monocytes stimulated with LNP-based vaccines. To this end, we ran the ProcartaPlex Mix&Match Human 33-plex on the supernatants of vaccine-treated monocytes to investigate the cytokine responses (Fig. 4A) and performed bulk RNA sequencing to explore intracellular events (Fig. 4B).

Among the cytokines released into the supernatant, we found CXCL8 as the most highly secreted analyte by monocytes treated with the Pfizer and Moderna vaccines (Fig. 4A). CXCL8 is a pro-inflammatory chemoattractant secreted by monocytes and macrophages to attract and activate neutrophils. Other chemoattractants were also found to be secreted at high levels, including those acting on monocytes and T cells, like CCL2 (also known as MCP1) or CXCL12. IL-1RA, an anti-inflammatory antagonistic agent that blocks IL-1β or -1α binding to their receptor, was also highly secreted. A similar IL-1RA release to liposome-based cancer vaccines has also been previously observed (Tahtinen et al., 2022). Moreover, diverse growth factors (*e.g.*, M-CSF, PIGF-1 or Vascular Endothelial Growth Factor A (VEGF-A)), chemokines (*e.g.*, CXCL5, CXCL1) and cytokines (*e.g.*, TNF-α, IL-1α) were found in the supernatants of vaccine-treated monocytes. In contrast, some other proteins were not detected, such as the anti-inflammatory cytokine IL-10 or IFN-α, which could be considered as surprising as they are usually involved in the antiviral response, but is actually in accordance with previously published data that the Pfizer and Moderna COVID-19 vaccines do not lead to IFN-α release (Arunachalam et al., 2021; Jiang et al., 2023). To ensure that the lack of detected IFN-α secretion was not an analytical problem, we also analyzed the supernatants of vaccine-stimulated monocytes after IFN-γ- and LPS-priming (same as those shown in Fig. 3E) by HTRF, and no IFN-α release was detectable (data not shown).
All in all, we concluded that the vaccines by themselves generate a mostly pro-inflammatory response in monocytes, with clear functions such as pro-inflammatory signaling, chemotaxis, and tissue remodeling. Very similar results were found in PBMCs (data not shown).

To determine what happens at the mRNA level (upstream of cytokine secretion) in monocytes treated with the vaccines, bulk RNA sequencing was performed (Fig. 4B). While *NLRP3* (Pfizer: $\log_2(FC) = -1.27$, confect = 0; Moderna: $\log_2(FC) = -0.30$, confect = 0) and *AIM2* (Pfizer: $\log_2(FC) = 1.45$, confect = 0; Moderna: $\log_2(FC) = 1.84$, confect = 0) expression levels remained unchanged, *NFKB1* (Pfizer: $\log_2(FC) = 1.23$, confect = +1; Moderna: $\log_2(FC) = 1.35$, confect = +1) and, at a much higher level, *IL1B* (Pfizer: $\log_2(FC) = 5.49$, confect = +1;

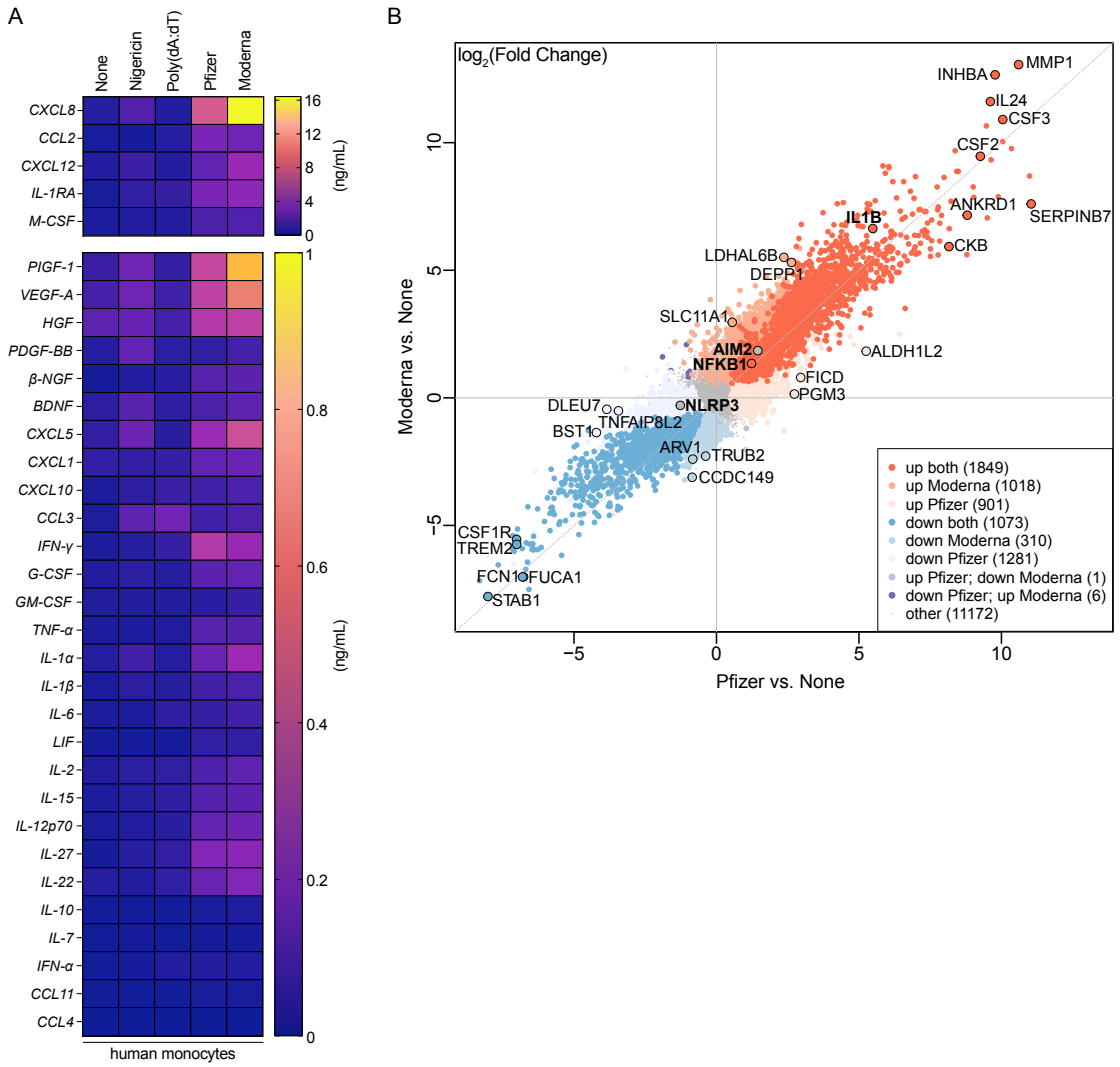

Fig. 4: Pro-inflammatory, inflammasome-independent responses of monocytes to lipid nanoparticle (LNP)-based COVID-19 vaccines.
(**A**) Secretion levels of a panel of chemokines, cytokines and growth factors from the ProcartaPlex Mix&Match Human 33-plex, released by primary human monocytes rested overnight, and then stimulated overnight (20-24 hours (h)) with nigericin (10 μM), poly(dA:dT) dsDNA (2 μg/mL), and Pfizer and Moderna vaccines (50 μg/mL).
(**B**) Comparison of the $\log_2$ fold changes (FCs) of Moderna and Pfizer treatments versus control. Genes are coloured according to whether they were significantly differentially expressed with either treatment or both. Certain example genes with high confect effect sizes are highlighted, as well as *AIM2*, *NLRP3*, *IL1B* and *NFKB1*.
N = 5 biological repeats.

Moderna: $\log_2$(FC) = 6.64, confect = +1) are upregulated by both Pfizer and Moderna vaccines. Also upregulated by both vaccines are genes involved in inflammation (*e.g.*, other cytokine signaling). Different genes involved in cellular adaptation to oxidative and metabolic stress in activated/hypoxic immune cells are found upregulated upon Moderna as well as Pfizer vaccine stimulation. On the other hand, genes associated with immune regulation and signaling, phagocytosis, lysosomal degradation, lipid homeostasis and mitochondrial RNA processing are found to be downregulated in response to one or both vaccines.

Taken together, the RNA sequencing data indicate that genes related to inflammation and oxidative/metabolic stress are upregulated upon vaccine treatments, while other immune regulatory genes were found downregulated.

3.5 Human inflammasomes also sense non-LNP-based COVID-19 vaccines and lipids alone

Next to the LNP-mRNA vaccines sold by Pfizer and Moderna, there are also other COVID-19 vaccines on the market, such as the ones from AstraZeneca and Novavax. While the AstraZeneca vaccine is based on an adenoviral vector, where the spike protein genetic material is inserted into a modified chimpanzee adenovirus (Folegatti et al., 2020), the Novavax vaccine is a protein subunit vaccine, which includes only the purified spike protein combined with adjuvants (Keech et al., 2020).

The AstraZeneca vaccine activated HEK cells expressing NLRP3 and, even more so, AIM2 (Fig. 5A), which was expected, as adenoviruses contain dsDNA genome (Eichholz et al., 2016). In human monocytes, however, the AstraZeneca vaccine was able to strongly activate NLRP3, leading to substantial IL-1β release (Fig. 5B), also in agreement with previously published data (Barlan et al., 2011). The Novavax vaccine could also be sensed by both inflammasomes (NLRP3 and AIM2) expressed in HEK cells (Fig. 5A), predominantly by NLRP3, as was predicted based on prior publications showing the adjuvant Matrix-M activating NLRP3-mediated IL-1β release (Stertman et al., 2023; Zarnegar et al., 2025). Unexpectedly, though, it did not lead to very high IL-1β secretion (Fig. 5B) in human monocytes. Importantly, none of the vaccines (Pfizer, Moderna, AstraZeneca, Novavax) affected cell viability (Fig. 5C), as measured by metabolic activity.

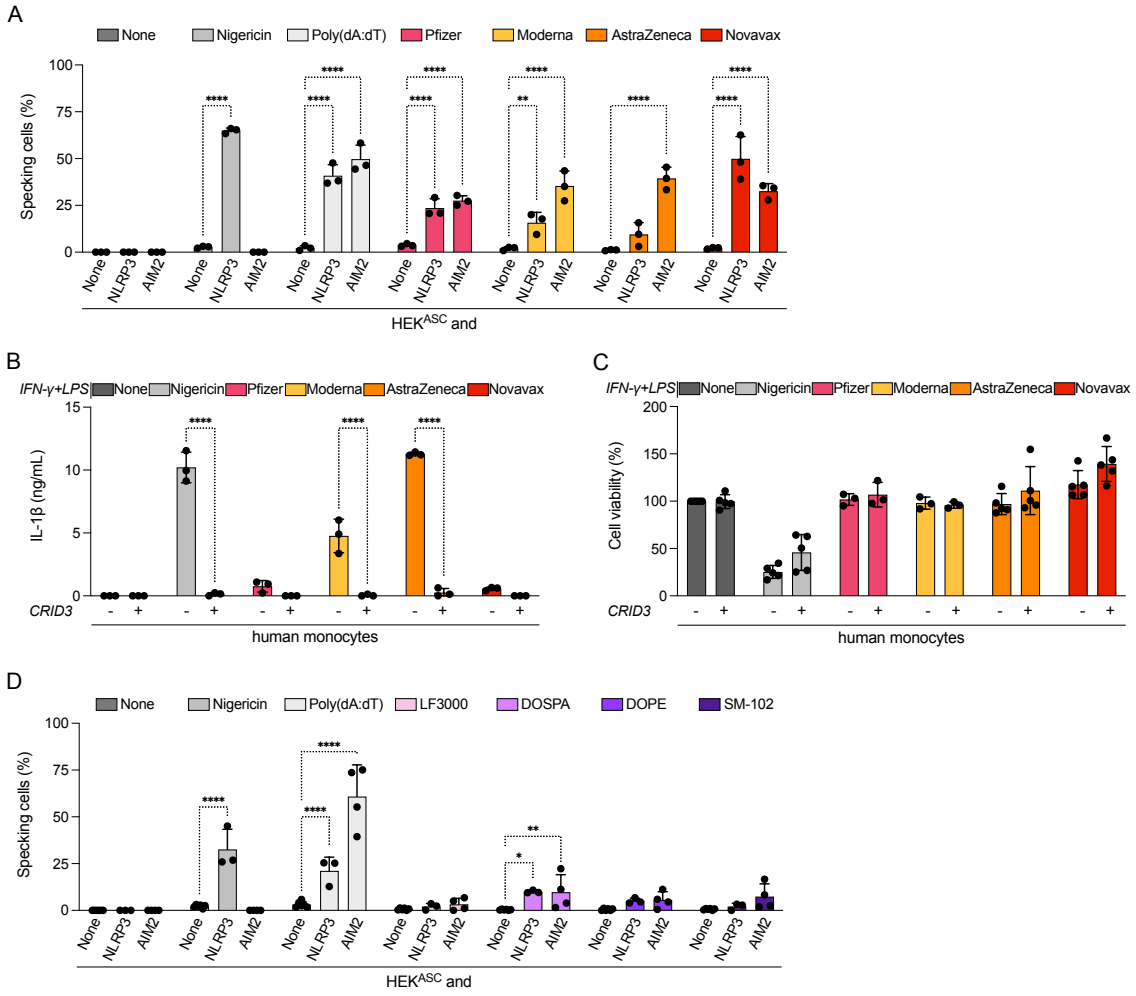

Fig. 5: Human inflammasomes sense non-lipid nanoparticle (LNP)-based COVID-19 vaccines and lipids alone.

(**A**) Normalized ASC speck formation per cell (specking cells) in Human Embryonic Kidney 293T (HEK) cells expressing fluorescently tagged ASC and NLRP3 or AIM2, stimulated overnight (20-24 hours (h)) with nigericin (10 μM) and poly(dA:dT) dsDNA (2 μg/mL), and Pfizer and Moderna (50 μg/mL), AstraZeneca ($2.5x10^8$ iu/mL) and Novavax (5 μg/mL) vaccines.

(**B,C**) IL-1β secretion from (B) or cell viability of (C) primary human monocytes, pre-treated with IFN-γ (10 ng/mL) overnight, then primed with LPS (2 ng/mL) for 3 h, treated or not with CRID3 (5 μM) for 10-30 minutes (min), and stimulated overnight (20-24 h) with nigericin (10 μM), and Pfizer and Moderna (50 μg/mL), AstraZeneca ($2.5x10^8$ iu/mL) and Novavax (5 μg/mL) vaccines.

(**D**) Normalized ASC speck formation per cell (specking cells) in Human Embryonic Kidney 293T (HEK) cells expressing fluorescently tagged ASC and NLRP3 or AIM2, stimulated overnight (20-24 h) with nigericin (10 μM) and poly(dA:dT) dsDNA (2 μg/mL), and 2,3-

dioleyloxy-N-[2-(sperminecarboxamido)ethyl]-N,N-dimethyl-1-propanaminium (DOSPA) (5 µg/mL), dioleoylphosphatidylethanolamine (DOPE) (5 µg/mL) or SM-102 (10 µg/mL) lipids.
N = 3-4 independent experiments (A,D) or 3 biological repeats (B,C); individual data points are means of technical duplicates; all error bars represent SD.
P values were calculated using two-way ANOVA with Dunnett's (A,D) or Šídák's (B,C) multiple comparison test. **P* = 0.0261, ***P* = 0.0021, ****P* = 0.0007, *****P* < 0.0001; NS *P* = 0.1582–0.9999 (not shown).

In addition to whole vaccine preparations, we also wanted to test whether inflammasomes were able to sense some of the lipids present in LF2000 and/or LNP-based vaccines. We chose the neutral phospholipid DOPE present in LF2000 (and very similar to distearoylphosphatidylcholine (DSPC), the phospholipid present in both Moderna and Pfizer COVID-19 vaccines), and the (ionizable) cationic lipids DOSPA present in LF2000 and SM-102 present in the Moderna vaccine. We transfected them into the HEK cells with help of LF3000, as we knew from previous data that this transfection reagent would not activate any inflammasomes on its own. Both DOSPA and DOPE induced ASC speck formation in NLRP3- and AIM2-expressing reporter HEK cells, while SM-102 only activated AIM2 (Fig. 5D). The fact that the lipids alone induced a bit less ASC speck formation, compared to the levels we usually observe with LF2000 or Moderna vaccine stimulations, suggests that inflammasome-mediated sensing of the combinations of lipids in LNPs could be stronger.

All in all, we can conclude that both NLRP3 and AIM2 sensed all tested COVID-19 vaccines, both LNP-based and not. Moreover, the inflammasomes were also able to respond, although at lower levels, to single lipids present in LF2000 or the Moderna vaccine.

3.6 The LNP-mRNA COVID-19 vaccines enter through micropinocytosis, do not seem to induce lysosomal or mitochondrial damage and to require spike protein expression for inflammasome activation

Next, the question arose of how the LNP-based vaccines actually enter the cells, which they then activate. To answer it, we decided to test inhibitors of different phago- and pinocytosis pathways in primary human monocytes to untangle which is the one used by these vaccines.

We started by blocking early endocytic stages, such as cytoskeletal rearrangement and vesicle formation. Firstly, we tested CytoD, an inhibitor of actin polymerization and thus of phagocytosis and micropinocytosis (Dutta & Donaldson, 2012).

Of note, CytoD was commonly used in the field to characterize phagocytosis-dependent NLRP3 activators, such as silica, alum, MSU crystals and cholesterol crystals. As it did not affect the viability of unstimulated cells (Suppl. Fig. 4A), a potential cytotoxic effect of the compound can be excluded. Although CytoD did slightly decrease the IL-1β response to nigericin (Fig. 6A), it did not affect its associated LDH release (Fig. 6B) or cell viability loss (Suppl. Fig. 4A). In contrast, CytoD significantly decreased the monocyte response to MSU crystals, as expected (Hornung et al., 2008), and substantially to the Pfizer vaccine, both at the IL-1β (Fig. 6A) and LDH (Fig. 6B) levels. For the Moderna vaccine, although not significant, a clear CytoD-mediated inhibition of IL-1β and LDH responses is also visible (Fig. 6A,B). At the cell viability level, we can see a significant rescue by CytoD for both Pfizer and Moderna vaccines (Suppl. Fig. 4A).

Next, we tested wortmannin, a phosphoinositide 3-kinase (PI3K) inhibitor, which also inhibits phagocytosis and micropinocytosis (Araki et al., 1996). Wortmannin did not affect cell viability (Suppl. Fig. 4B). While this compound did not rescue cell viability in any of the tested inflammasome stimulations (Suppl. Fig. 4B), it did significantly prevent the LDH release not only triggered by the MSU crystals but also the Pfizer and Moderna vaccine-stimulated cells (Fig. 6D). The IL-1β release was only significantly reduced by wortmannin upon Moderna vaccine treatment, but a decrease is also clearly seen for the MSU crystals stimulation and, to a lesser extent, for the Pfizer vaccine stimulation (Fig. 6C).

To exclude a clathrin-mediated process, we pre-treated monocytes with the inhibitor PitStop2, which interferes with the binding of proteins to the N-terminal domain of clathrin and thus blocks receptor-mediated uptake (von Kleist et al., 2011). Again, the compound did not affect cell viability of unstimulated cells (Suppl. Fig. 4E). As expected, this compound did neither prevent any IL-1β (Suppl. Fig. 4C) or LDH (Suppl. Fig. 4D) release nor did it rescue cell viability (Suppl. Fig. 4E) upon any of the tested inflammasome stimulations. Very similar results were also observed with dynasore, an inhibitor of dynamin and clathrin-mediated as well as caveolar endocytosis (Macia et al., 2006; Oh et al., 2012) (data not shown).

The data obtained with these inhibitors suggest that the LNP-mRNA vaccine entry is likely mediated by phagocytosis/micropinocytosis, both of which are actin-driven, large-particle uptake processes.

For further characterization of the vaccine-mediated inflammasome response, we also tested inhibitors that do not directly block uptake pathways but target some later processing stages. Chloroquine inhibits the endo-/lysosomal acidification, thus blocking the maturation of endocytic vesicles and lysosomal degradation (Schaer et al., 2013). While this compound did decrease the IL-1β levels secreted from MSU crystals-treated monocytes – as expected, considering that the crystals require lysosomal acidification and lysosomal damage for NLRP3 activation – it did not affect the cytokine secretion mediated by the vaccines (Fig. 6E). Similarly, chloroquine showed no effect on either LDH release (Fig. 6F) or cell viability (Suppl. Fig. 4F) of vaccine-stimulated monocytes. Importantly, this inhibitor did not affect viability of unstimulated cells (Suppl. Fig. 4F).

Next, we tested CA-074Me, an inhibitor of cathepsin B, a lysosomal cysteine protease, which prevents cathepsin-catalyzed proteolysis inside of the lysosome (Montaser et al., 2002). The NLRP3 activator nigericin only acts through K^+ efflux and does not directly require lysosomal damage (Muñoz-Planillo et al., 2013) – however, surprisingly, cathepsin B inhibitors have been shown to be able to prevent nigericin-induced NLRP3 activation. Some studies show how even subtle cathepsin B release into the cytosol, not necessarily dependent on strong lysosomal damage, can contribute to NLRP3 inflammasome activation (Guicciardi & Gores, 2013). The nigericin-induced K^+ efflux can lead to some secondary lysosomal and mitochondrial stress (Heid et al., 2013), which can potentially lead to the release of Cathepsin B into the cytosol and generation of mitochondrial ROS, known triggers/amplifiers of NLRP3. Moreover, CA-074Me can have some off-target effects, such as altering lysosomal pH and membrane properties (potentially indirectly also affecting ion fluxes), or reducing mitochondrial damage. Indeed, we also observed the inhibitory effect of CA-074Me on nigericin-stimulated cells, as evidenced by the decreased IL-1β secretion (Fig. 6G), although no inhibition of LDH release (Fig. 6H) nor rescue of cell viability (Suppl. Fig. 4G) were otherwise observed. As expected, the inhibitor prevented cytokine release of MSU crystals-

treated monocytes, which undergo dramatic lysosomal damage (Fig. 6G). Interestingly, although no effect had been observed for chloroquine treatment in vaccine-treated cells (Fig. 6E), suggesting lack of lysosomal damage involvement, we did observe decreased IL-1β secretion in CA-074Me pre-treated cells (Fig. 6G). This can potentially have the same explanation as CA-074Me-mediated inhibition of nigericin-induced NLRP3 activation, whereby, in the absence of direct lysosomal damage, cathepsin B is still released into the cytosol at low level, amplifying the NLRP3 response.

All in all, the chloroquine data suggest that the inflammasome response to vaccines does not depend on lysosomal damage. Yet, the CA-074Me-related results point to a potential role of cathepsin B. Due to this inhibitor's unspecific effects, also targeting nigericin-induced activation, a clear conclusion cannot be drawn.

Next, we wanted to investigate whether mitochondria could be damaged by the vaccines. If yes, this could also explain the activation of both inflammasomes: AIM2 recognizes dsDNA (so including mtDNA) (Bae et al., 2019; Hornung et al., 2009), and NLRP3 activation has been linked to mitochondria, oxidized mtDNA, and mitochondrial ROS (Abais et al., 2015; Martinon, 2010; Shimada et al., 2012; Zhou et al., 2011).

To analyze whether Pfizer and Moderna vaccines induce disruption of mitochondria, we used HEK cells that express a fluorescent mitochondrial reporter, which acts as an indicator for mitochondrial integrity. This could be monitored by microscopy and quantified based on the granularity of the mitochondrial signal: a decreased granularity indicating a decrease in mitochondrial integrity. While thapsigargin – a compound previously shown to lead to mitochondrial damage (Próchnicki et al., 2023) – clearly decreased the mitochondrial granularity, this was not the case for the Moderna vaccine, and there was only a slight decrease of mitochondrial granularity seen with the Pfizer vaccine (Fig. 6J).

A second technique to investigate the possible role of mitochondrial damage in the inflammasome-mediated sensing of LNP-based vaccines was to deplete mtDNA using ddC. The mtDNA depletion approach would allow us to determine whether the loss of mtDNA prevents the AIM2 response to the vaccines. A positive control here was again thapsigargin, which, by damaging the mitochondria, can activate AIM2 in an mtDNA-dependent fashion

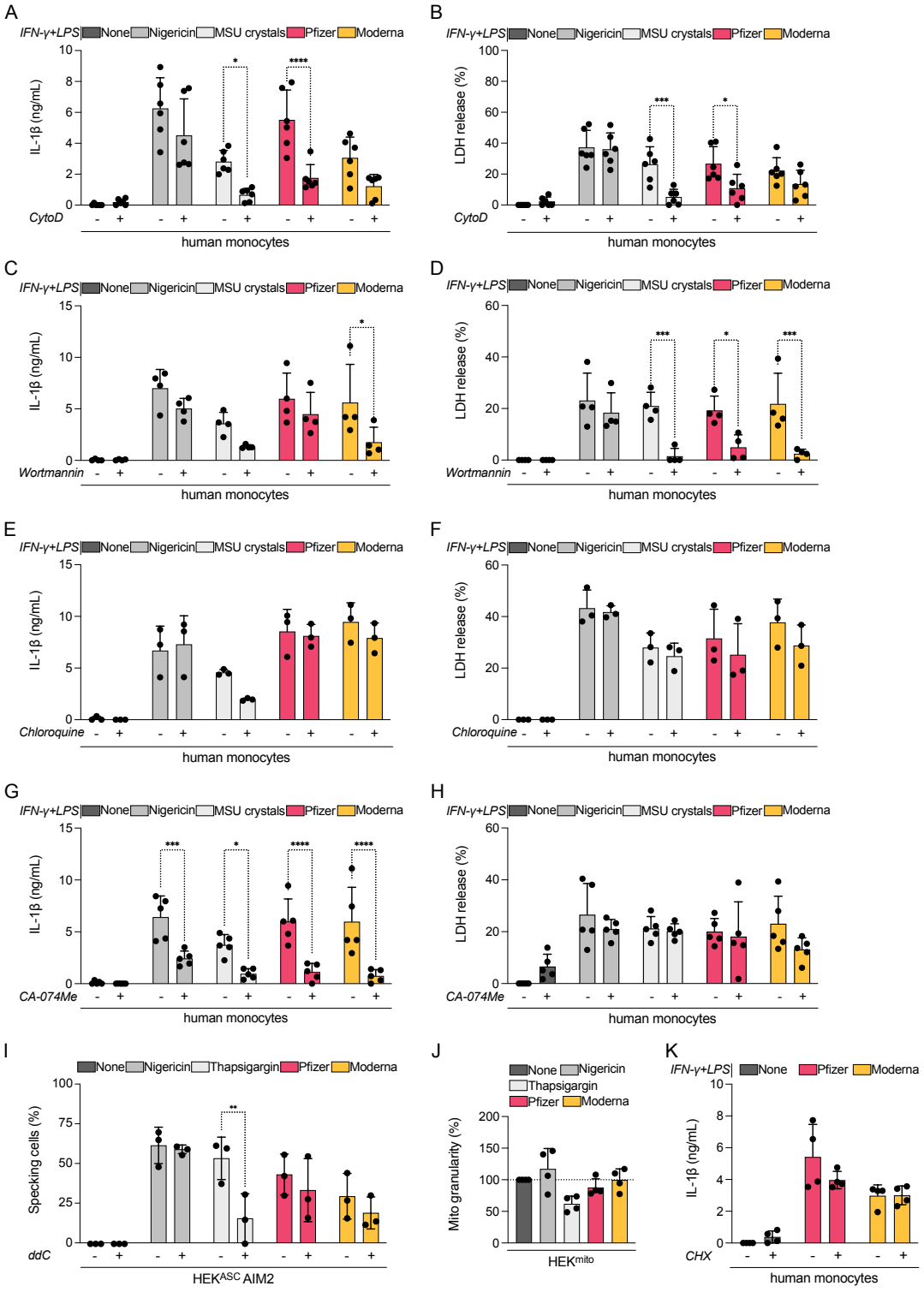
A
IFN-γ+LPS
None
Nigericin
MSU crystals
Pfizer
Moderna
IL-1β (ng/mL)
CytoD
human monocytes
B
LDH release (%)
C
Wortmannin
D
E
Chloroquine
F
G
CA-074Me
H
I
Thapsigargin
Specking cells (%)
ddC
HEKASC AIM2
J
HEKmito
Mito granularity (%)
K
CHX

Fig. 6: Lipid nanoparticle (LNP)-based COVID-19 vaccines enter through micropinocytosis, do not induce lysosomal or mitochondrial damage, and do not require spike protein expression for inflammasome activation.
(**A-H**) IL-1β (A,C,E,G) and lactate dehydrogenase (LDH) (B,D,F,H) secretion from primary human monocytes, pre-treated with IFN-γ (10 ng/mL) overnight, then primed with LPS (2 ng/mL) for 3 hours (h), treated or not with cytochalasin D (CytoD) (1 μg/mL) (A,B), wortmannin (100 nM) (C,D), chloroquine (10 μM) (E,F), CA-074Me (50 μM) (G,H) for 10-30 minutes (min), and stimulated overnight (20-24 h) with nigericin (10 μM), MSU crystals (250 μg/mL), and Pfizer and Moderna (50 μg/mL) vaccines.
(**I**) Normalized ASC speck formation per cell (specking cells) in Human Embryonic Kidney 293T (HEK) cells expressing fluorescently tagged ASC and AIM2, pre-incubated with 2′,3′-dideoxycytidine (ddC) (80 μg/mL) for 72 h, and then stimulated overnight (20-24 h) with nigericin (10 μM), thapsigargin (20 μM), and Pfizer and Moderna (50 μg/mL) vaccines.
(**J**) Normalized mitochondrial (mito) granularity in HEK cells expressing a fluorescent mitochondrial reporter, stimulated overnight (20-24 h) with nigericin (10 μM), thapsigargin (20 μM), and Pfizer and Moderna (50 μg/mL) vaccines.
(**K**) IL-1β secretion from primary human monocytes, pre-treated with IFN-γ (10 ng/mL) overnight, then primed with LPS (2 ng/mL) for 3 h, treated or not with cycloheximide (CHX) (50 μg/mL), and stimulated overnight (20-24 h) with Pfizer and Moderna (50 μg/mL) vaccines.
N = 3 (E,F), 4 (C,D,K), 5 (G,H) 6 (A,B) biological repeats or 3 (I), 4 (J) independent experiments; individual data points are means of technical duplicates; all error bars represent SD.
P values were calculated using two-way ANOVA with Šídák's multiple comparison test. **P* = 0.0261, ***P* = 0.0021, ****P* = 0.0007, *****P* < 0.0001; NS *P* = 0.1582–0.9999 (not shown).

(Próchnicki et al., 2023). Therefore, we used HEK cells expressing fluorescently labeled ASC and human AIM2 and depleted mtDNA in these cells by incubation with ddC. While the 72h-long depletion of mtDNA considerably decreased ASC speck formation in cells stimulated with thapsigargin, it did not significantly affect the inflammasome response to the vaccines (Fig. 6I).

Taken together, the vaccines do not induce dramatic mitochondrial damage (although subtler alterations in mitochondrial function and integrity cannot be excluded based on our results), and mtDNA is unlikely to be released into the cytosol in vaccine-stimulated cells or to serve as the inflammasome agonist in this context.

Lastly, we wanted to investigate whether expression of the vaccines' spike protein was required for inflammasome activation. Therefore, we pre-treated human monocytes with

CHX, a translation inhibitor which blocks protein synthesis elongation (Obrig et al., 1971), before stimulation with the vaccines. Although the inhibitor was slightly toxic at the concentration used in this experiment and decreased cell viability (Suppl. Fig. 4H), it still did not significantly block IL-1β secretion upon Pfizer or Moderna vaccines treatment (Fig. 6K), suggesting that inhibition of translation of the spike protein did not impair inflammasome activation.

Taken all these observations together, vaccines likely enter the cells through micropinocytosis, they do not seem to trigger strong lysosomal or mitochondrial damage, and the human inflammasomes do not require spike protein expression – all in all suggesting that they could sense either the vaccines directly or some other changes in cellular homeostasis triggered by the administration of these stimuli.

3.7 Mouse inflammasomes do not sense LNP-based COVID-19 vaccines

As we have seen that primary mouse cells responded to LF2000 (Fig. 1A), we wanted to investigate whether they were also able to sense the LNP-based vaccines. To this end, we tested three primary cell types – PBMCs, macrophages and splenocytes – with or without an overnight pre-stimulation with either IFN-γ or GM-CSF, followed by LPS priming and stimulation with the different potential activators (Fig. 7).

Firstly, mouse PBMCs were isolated from peripheral blood, among which different types of leukocytes ($CD45^+$ cells) are found, including B cells ($CD19^+$ cells), T cells ($CD3^+$) and monocytes ($CD11b^+Ly6C^{high/low}$ cells) (Suppl. Fig. 5A). While mouse PBMCs pre-treated with IFN-γ and even more so with GM-CSF did respond to the NLRP3 trigger nigericin, they did not secrete any IL-1β upon LF2000 or vaccine stimulations (Fig. 7A). Oddly, neither in PBMCs at steady-state nor in IFN-γ- or GM-CSF-pre-treated PBMCs, AIM2 or NLRP3 protein expression could be detected (Suppl. Fig. 5B). Notably, one would expect that at least GM-CSF primed PBMCs express NLRP3, as they responded to nigericin – possibly, there is low NLRP3 expression that is just below detection limit.

As previous publications showed that mouse blood cells release the anti-inflammatory protein IL-1RA upon vaccine treatment (Tahtinen et al., 2022), we also tested the release of this cytokine – however, we were not able to detect any IL-1RA secretion (Fig. 7B).

In contrast to PBMCs, BMDMs did respond to LF2000, as expected from the previous data (Fig. 1), but still did not respond to neither Pfizer nor Moderna vaccines (Fig. 7C) – not even upon GM-CSF pre-treatment, which generally rendered the cells more responsive and secreting higher IL-1β levels. It is not obvious why this GM-CSF pre-treatment leads to higher IL-1β secretion in these cells, considering that neither AIM2 nor NLRP3 expression increases compared to their already high levels under steady-state conditions (Suppl. Fig. 5C). Perhaps pro-IL-1β levels get upregulated under these conditions (not tested). Nevertheless, even though NLRP3 is highly expressed in BMDMs even at steady state, the inflammasome in these cells still does not seem to sense the vaccines. Next, we decided to test iMacs overexpressing mouse NLRP3 and a fluorescently-tagged ASC protein to look at the ASC speck formation readout. While these cells did form ASC specks upon LF2000 stimulation, they did not upon vaccine treatments (Fig. 7E).

As with PBMCs, we also investigated IL-1RA secretion in BMDMs. LPS-stimulated BMDMs secreted high levels (approximately 4 ng/mL) of this cytokine already in the absence of stimuli, which was decreased upon nigericin and poly(dA:dT) treatments (likely due to cell death of the cells upon overnight treatment with these compounds). Previous studies had observed a similar IL-1RA release by LPS-stimulated L929-differentiated BMDMs (J.-X. Yang et al., 2017). BMDMs treated with LF2000 or LNP-mRNA vaccines secreted high levels of IL-1RA, similar to what was seen in the unstimulated conditions, indicating that the vaccines themselves do not lead to an increased IL-1RA secretion (Fig. 7D).

To look at a broader cytokine release panel, we performed a ProcartaPlex Custom Mouse 22-plex (Fig. 7F) on supernatants of BMDM cultures. The cytokine with the strongest induction by Pfizer and Moderna vaccines was CXCL2, a pro-inflammatory chemoattractant secreted by monocytes and macrophages to attract and activate neutrophils – similar to

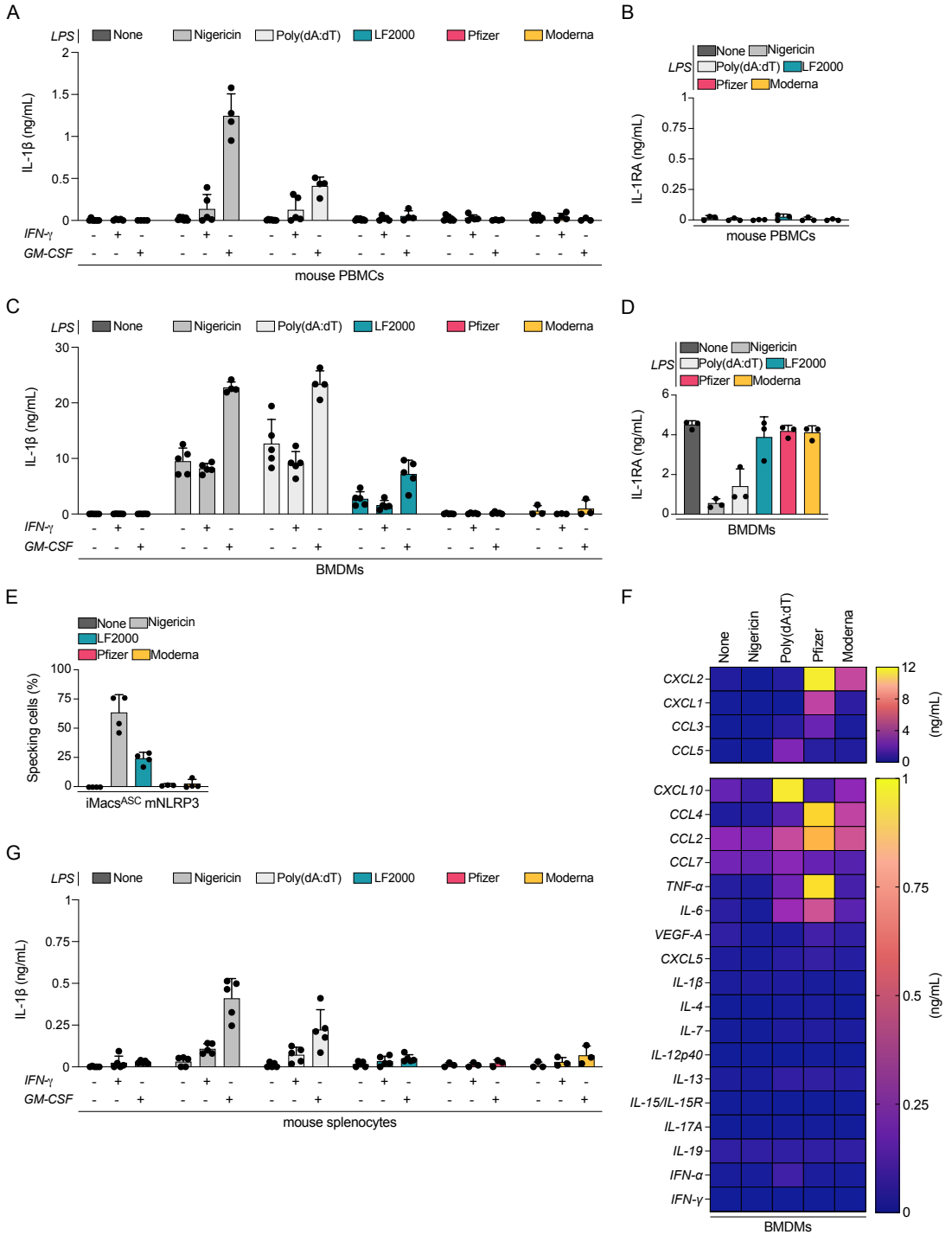

Fig. 7: Mouse inflammasomes do not sense lipid nanoparticle (LNP)-based COVID-19 vaccines.

(**A,C,G**) IL-1β secretion from primary mouse peripheral blood mononuclear cells (PBMCs) (A), bone marrow-derived macrophages (BMDMs) (C), or splenocytes (G), pre-treated or not

with mouse IFN-γ (10 ng/mL) or GM-CSF (1 ng/mL) overnight, then primed with LPS (200 ng/mL) for 3 hours (h), and stimulated overnight (20-24 h) with nigericin (10 μM), poly(dA:dT) dsDNA (2 μg/mL), lipofectamine (LF) 2000 (5 μg/mL), and Pfizer and Moderna vaccines (50 μg/mL).
(**B,D**) IL-1RA secretion from primary mouse PBMCs (B) and BMDMs (D) without pre-treatment of Fig. 7A,C.
(**E**) Normalized ASC speck formation per cell (specking cells) in mouse immortalized macrophages (iMacs) expressing mouse NLRP3 and fluorescently tagged ASC, stimulated overnight (20-24 h) with nigericin (10 μM), LF2000 (5 μg/mL), and Pfizer and Moderna vaccines (50 μg/mL).
(**F**) Secretion levels of a panel of chemokines, cytokines and growth factors from a ProcartaPlex Custom Mouse 22-plex, released by primary mouse BMDMs rested overnight, and then stimulated overnight (20-24 h) with nigericin (10 μM), poly(dA:dT) dsDNA (2 μg/mL), and Pfizer and Moderna vaccines (50 μg/mL).
N = 3 (B,D), 4 (A), 5 (F), 3-5 (C,G) biological repeats or 4 (E) independent experiments; individual data points are means of technical duplicates; all error bars represent SD.

CXCL1, also highly secreted by Pfizer-vaccine stimulated BMDMs. Other chemokines (sensed by monocytes and T cells, for example, CCL3 and CCL5) were also found in abundance in the supernatants. TNF-α and IL-6 were released at high levels in response to the Pfizer vaccine. Many other analytes like growth factors (*e.g.*, VEGF-A), chemokines (*e.g.*, CXCL5) and cytokines (*e.g.*, IL-1β) were not detected.

Finally, we tested splenocytes, which upon pre-treatment with IFN-γ or GM-CSF did release low concentrations of IL-1β upon nigericin and poly(dA:dT) stimulations, but showed almost no inflammasome response to LF2000 or the vaccines (Fig. 7G). For these cells, IFN-γ and GM-CSF seemed to increase an already substantial AIM2 expression, while NLRP3 expression only got upregulated by GM-CSF treatment (Suppl. Fig. 5D). However, NLRP3 expression levels are much lower compared to BMDMs. Considering that the BMDM response to LF2000 is already much lower than the response to nigericin, this could explain why splenocytes are effectively insensitive to LF2000.

All in all, while diverse human inflammasomes seem to sense LNP-based COVID-19 vaccines, mouse inflammasomes in diverse primary cells do not. Additionally, only BMDMs respond to LF2000 by secreting IL-1β, as seen in Fig. 1.

3.8 Differential human *vs.* mouse sensing of LNP-based COVID-19 vaccines

To better understand the difference between human and mouse inflammasomes in sensing LNP-based COVID-19 vaccines, we decided to directly compare the activity of the human and mouse NLRP3 proteins in the same cell type.

We started with NLRP3-KO mouse iMacs, which were reconstituted with mCitrine tag only (None) or the human (hum) or mouse (mou) NLRP3, expressed at similar levels (Fig. 8B, Suppl. Fig. 6A). While all three cell types responded similarly to the AIM2 stimulus poly(dA:dT) (including the KO, as in the mouse system it is AIM2 and not NLRP3 that responds to this trigger (Hornung et al., 2009)), human NLRP3 showed higher IL-1β release compared to mouse NLRP3 in response to nigericin (Fig. 8A), suggesting a higher sensitivity of the human NLRP3 to specific triggers. Similarly, only the human ortholog was able to respond with IL-1β secretion to LF2000 as well as to the vaccines (Fig. 8A).

At the same time, the experiment shown in Fig. 8A was also a method to check whether the mouse background could play a role in LNP-mRNA vaccine sensing, since all mouse cells shown in the prior figures (Fig. 1, 7) came from the C57BL/6 background, while the cells in Fig. 8A were derived from BALB/c mice. As these two backgrounds do have genetic differences, also in regard to immune mechanisms, different phenotypes can sometimes be observed (Aoki et al., 2019; Jakic et al., 2021). However, we can note that the NLRP3-KO iMacs reconstituted with mouse NLRP3 are also not able to respond to vaccines in this scenario, indicating that the background does not play a role in the inflammasome sensing of vaccines.

Next, we tested NLRP3 from other species (macaque (mac) and rat) in the same context – unfortunately only with respect to the response to the Pfizer vaccine, since we had no Moderna vaccine left anymore. In this setting, all five cell lines not only responded similarly to poly(dA:dT) but also to nigericin and LF2000 (Fig. 8C). This comparable nigericin response between human and mouse NLRP3 (contrasting with the result in Fig. 8A) can potentially be explained by the fact that, in these remade cell lines, the mouse NLRP3 expression was higher than the human one (Fig. 8D, Suppl. Fig. 6B). Nonetheless, in the comparison of

NLRP3 orthologs from the four species only the human NLRP3-reconstituted cells showed a robust response to the Pfizer vaccine (Fig. 8C). The lowest response was seen in the cells reconstituted with mouse NLRP3, while the reconstitutions with macaque and rat NLRP3 led to secreted IL-1β levels that were in-between human and mouse, suggesting that the human NLRP3 has the highest sensitivity to the Pfizer vaccine.

To unravel the mechanism behind this difference in sensitivity, we generated two mutated variants of the mouse NLRP3 construct with parts of the human NLRP3 sequence, enabling expression of mouse NLRP3 with either the human linker or a human mutation.

NLRP3 consists of three domains: the N-terminal PYD, the nucleotide-binding oligomerization (NACHT) domain in the middle, and the C-terminal leucine-rich repeat (LRR) domain (Akbal et al., 2022). The human linker region that is of interest for our study is the stretch between the C-terminal end of the PYD and the N-terminal end of the NACHT domain, from amino acids (aa) 91-219, although slightly different boundaries can be found in the literature. It comprises a short flexible linker, followed by a small subdomain called fish-specific NACHT-associated (FISNA) (Akbal et al., 2022). It has been shown that this linker region helps NLRP3 sense its stimuli (especially the ones via K^+ efflux) (Rahman et al., 2020; Tapia-Abellán et al., 2021), and deleting diverse parts of this region reduced or completely prevented NLRP3 activation (*e.g.*, by nigericin) (Tapia-Abellán et al., 2021). The linker contains a positively-charged polybasic region, which binds to phosphatidylinositol-4-phosphate (PI4P) on the dispersed trans-golgi network (J. Chen & Chen, 2018). Upon different NLRP3 stimuli, PI4P-rich vesicles are created by the trans-golgi network, to which NLRP3 gets recruited through the polybasic region in the linker and forms the inflammasome (J. Chen & Chen, 2018). Interestingly, mouse and human NLRP3 show sequence differences in this polybasic region (Tapia-Abellán et al., 2021): human NLRP3 has some residues that are positively charged, whereas the residues in the corresponding positions are uncharged in mouse NLRP3.

Based on this and on III-internal data, we decided to test the two mutated variants of the mouse NLRP3 mentioned before. It has been observed that mouse NLRP3 with the human linker region (aa 91-220) showed stronger activation and different cellular localization (more

bound to the plasma membrane, similar to the human NLRP3). Anil Akbal specifically found that mouse NLRP3 ‘humanized’ at residues 133 and 135 (resulting in positive charges reminiscent of the polybasic region, C133R and M135K) also displayed increased activation. In contrast, human NLRP3 ‘murinized’ at residues 137 and 139 (leading to the loss of positive charges through the following mutations: R137C, K139M) showed decreased activation potential and less plasma membrane localization. Thus, we wanted to check whether these two ‘hybrid’ proteins – mouse NLRP3 with the human linker (aa 91-220) (mou N3_hlink) and mouse NLRP3 with the two positively charged human residues (C133R, M135K) (mou N3_hmut) – were able to sense the Pfizer and Moderna vaccines. As in previous tests, all reconstituted NLRP3-KO iMac cells responded similarly to poly(dA:dT) and to nigericin (Fig. 8E), probably because in this series of experiments mouse NLRP3 expression levels are higher than the human one (Fig. 8F, Suppl. Fig. 6C; similar to the phenomenon observed in Fig. 8D, Suppl. Fig. 6B). Interestingly, however, not only reconstitution with human NLRP3 but also with mouse NLRP3 containing the human linker conferred responsiveness to LF2000 and to the Pfizer vaccine (Fig. 8E). In contrast, mouse NLRP3 with the humanized C133R and M135K residues did not have that effect (Fig. 8E).
This suggests that the higher sensitivity of human NLRP3 to LNP-mRNA vaccines, compared to mouse NLRP3, does not depend on just the two specific human residues in the linker region, but instead on the entire linker region.

Finally, we decided to compare human and mouse NLRP3 in a human system, using NLRP3-KO U937 cells differentiated to macrophages, reconstituted with an mCitrine tag only (None) or the human or mouse NLRP3. Interestingly, mouse NLRP3 responded with higher IL-1β secretion to nigericin and to the higher of the two tested concentrations of R837 (imiquimod), another commonly used NLRP3 activator (Fig. 8G) (Kanneganti et al., 2006). This could be due to the fact that mouse NLRP3 is expressed at slightly higher levels (Fig. 8H, Suppl. Fig. 6D). However, at the lower tested R837 concentration, human NLRP3 responds robustly, while mouse NLRP3 does not respond at all. This could hint that human NLRP3 is more sensitive, responding faster also to lower trigger concentrations, and then saturating, while mouse NLRP3 only responds to stronger triggers. Mouse NLRP3 also responded slightly

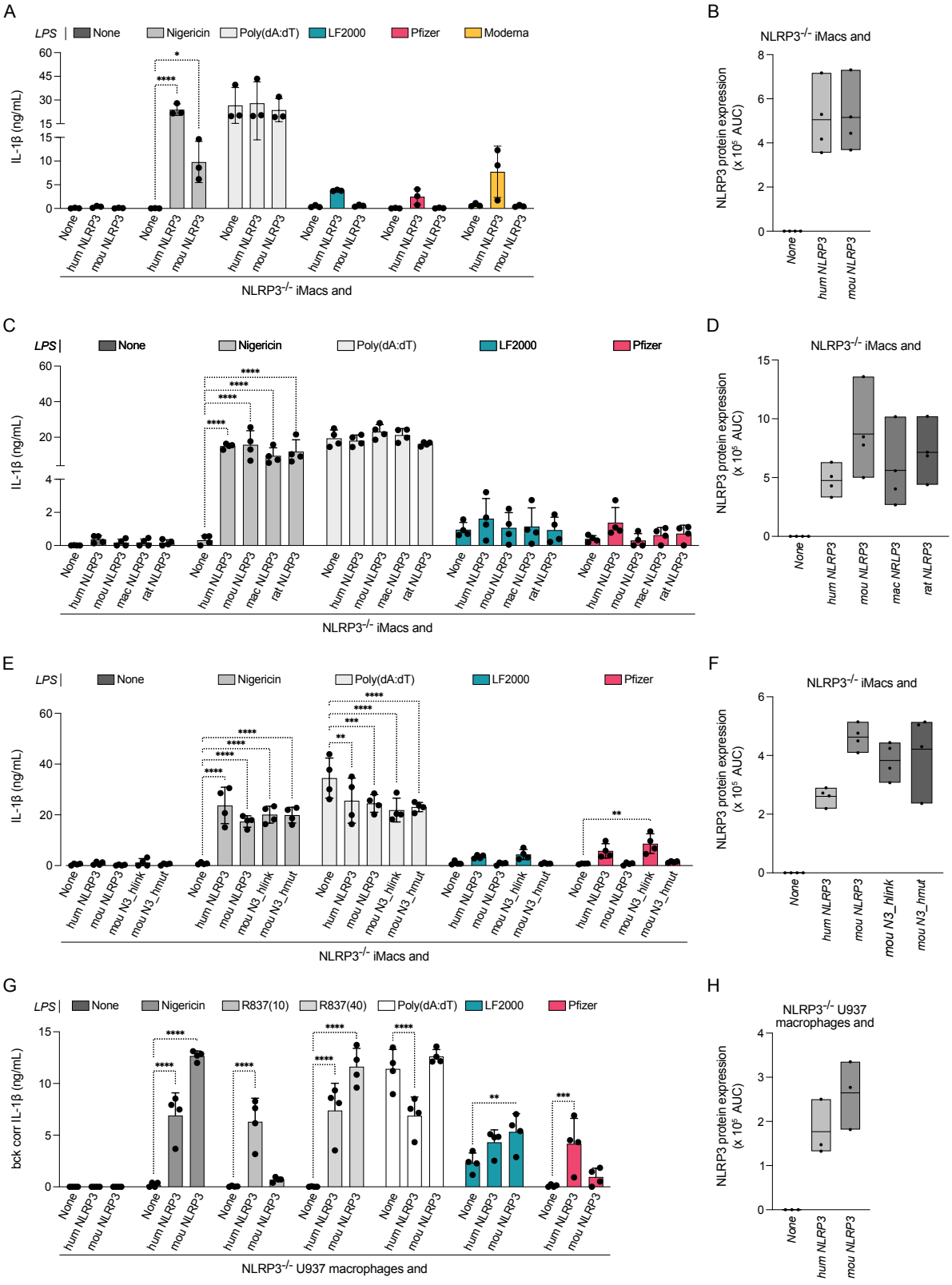
A
LPS | None Nigericin Poly(dA:dT) LF2000 Pfizer Moderna
IL-1β (ng/mL)
None hum NLRP3 mou NLRP3
NLRP3-/- iMacs and
B
NLRP3-/- iMacs and
NLRP3 protein expression (x 10⁶ AUC)
None hum NLRP3 mou NLRP3
C
LPS | None Nigericin Poly(dA:dT) LF2000 Pfizer
IL-1β (ng/mL)
None hum NLRP3 mou NLRP3 mac NLRP3 rat NLRP3
NLRP3-/- iMacs and
D
NLRP3-/- iMacs and
NLRP3 protein expression (x 10⁶ AUC)
None hum NLRP3 mou NLRP3 mac NRLP3 rat NLRP3
E
LPS | None Nigericin Poly(dA:dT) LF2000 Pfizer
IL-1β (ng/mL)
None hum NLRP3 mou NLRP3 mou N3_hlink mou N3_hmut
NLRP3-/- iMacs and
F
NLRP3-/- iMacs and
NLRP3 protein expression (x 10⁶ AUC)
None hum NLRP3 mou NLRP3 mou N3_hlink mou N3_hmut
G
LPS | None Nigericin R837(10) R837(40) Poly(dA:dT) LF2000 Pfizer
bck corr IL-1β (ng/mL)
None hum NLRP3 mou NLRP3
NLRP3-/- U937 macrophages and
H
NLRP3-/- U937 macrophages and
NLRP3 protein expression (x 10⁶ AUC)
None hum NLRP3 mou NLRP3

Fig. 8: Difference in inflammasome sensing of lipid nanoparticle (LNP)-based COVID-19 vaccines between the human and mouse systems.
(**A,C,E**) Mouse IL-1β secretion from NLRP3-knockout ($^{-/-}$) mouse immortalized macrophages (iMacs), reconstituted with an mCitrine tag only (None), or human (hum), mouse (mou) (A), macaque (mac), or rat NLRP3 (C), or mouse NLRP3 with the human linker (hlink) or the human mutation (hmut) (E), primed with LPS (200 ng/mL) for 3 hours (h), and stimulated overnight (20-24 h) with nigericin (10 μM), poly(dA:dT) dsDNA (2 μg/mL), lipofectamine (LF) 2000 (5 μg/mL), and Pfizer and Moderna vaccines (50 μg/mL).
(**B,D,F,H**) Simple Western quantification analysis (area under the curve (AUC)) of NLRP3 expression in cell lysates of the cells from Fig. 8A (B), 8C (D), 8E (F), 8G (H).
(**G**) Background corrected (bck corr) human IL-1β secretion from NLRP3-knockout ($^{-/-}$) U937 macrophages, reconstituted with an mCitrine tag only (None), or hum or mou NLRP3, primed with LPS (40 ng/mL) for 3 h, and stimulated overnight (20-24 h) with nigericin (10 μM), R837 (10 or 40 μg/mL), poly(dA:dT) dsDNA (2 μg/mL), LF2000 (5 μg/mL), and Pfizer vaccine (50 μg/mL).
N = 3 (A, H) or 4 (B-G) independent experiments; individual data points are means of technical duplicates; all error bars represent SD.
P values were calculated using two-way ANOVA with Dunnett's multiple comparison test. **P* = 0.0261, ***P* = 0.0021, ****P* = 0.0007, *****P* < 0.0001; NS *P* = 0.1582–0.9999 (not shown).

stronger to poly(dA:dT) and LF2000 (Fig. 8G). Interestingly, in this scenario also the KO responded to LF2000, hinting, for the first time, at a human cell type in which AIM2 could sense LF2000 independent of NLRP3 (until now only seen in AIM2-overexpressing HEK cells) (Fig. 1C). Still, upon Pfizer vaccine stimulation, only the expression of human NLRP3 conferred inflammasome responsiveness, suggesting that, at least at these vaccine concentrations, only the human but not the mouse NLRP3 is sensitive enough to respond to the trigger.

Previously published data, which show similar differences between the human *vs.* mouse inflammasome responses to liposome-based vaccines, explain these dissimilarities by the distinctive IL-1β/IL-1RA release patterns: mice release higher levels of IL-1RA and lower levels of IL-1β (Tahtinen et al., 2022). Here, however, we observe an additional contributing factor, related to different sensitivities of human and mouse NLRP3 protein to vaccine-related triggers. This finding could be important to consider when, for example, testing doses of newly developed LNP-based vaccines in mice. Mechanistically, we suggest that this difference in inflammasome sensitivity could be related to the human NLRP3 linker region.

4. Discussion

4.1 Inflammasomes sense specific transfection reagents

Although inflammasomes play a pivotal role in innate immunity, the exact ligand and activation mechanisms of some of the inflammasome-forming sensors and receptors remain unknown and to be studied. While AIM2 is known to bind to dsDNA (Hornung et al., 2009), several direct NLRP3 ligands have been proposed over the years, but none is universally considered as the one NLRP3 ligand (Y. He et al., 2016; Shimada et al., 2012).

At the beginning of my thesis work, we attempted to perform a non-canonical NLRP3 activation experiment following published protocols in mouse BMDMs, *i.e.*, treat the cells with intracellular LPS, which is known to activate NLRP3 in this fashion. We tested WT, NLRP3- and AIM2-KO C57BL/6J mice, and delivered LPS with the help of the transfection reagent LF2000. As a control, we also delivered LF2000 alone, not complexed with LPS. We expected LPS to exclusively activate NLRP3 and not AIM2, and LF2000 to not activate any inflammasome. However, LF2000 alone activated the cells as strongly as LPS itself, and this activation was not only dependent on NLRP3 but also on AIM2. In immortalized mouse macrophages as well as HEK cells expressing human NLRP3 and AIM2, the same patterns were observed. In human monocytes, NLRP3 was also able to sense LF2000 (Fig.1B). Both in the reporter HEK cells and in monocytes, we could observe strong NLRP3 response to poly(dA:dT), which has been previously explained through intracellular DNA activating STING-lysosomal damage-NLRP3 pathway in human monocytes (Gaidt et al., 2017). Moreover, poly(dA:dT) is also transfected into the cells using LF2000, which could provide an additional explanation for the NLRP3 activation (Fig.1B). The Gaidt et al. (2017) study also transfects DNA with LF2000, and while the authors do not detect much IL-1β secretion in the supernatants of LF2000-treated monocytes by ELISA, they do detect cleaved IL-1β by immunoblotting, which was prevented by CRID3 (MCC950).

Although LF2000 treatment induced cytokine secretion, it did not substantially reduce the viability of the monocytes (Suppl. Fig. 1G). This seems to have similar outcomes (although likely different mechanisms) as previous observations in DCs, in which oxidized

phospholipids (Zanoni et al., 2016) lead to NLRP3 activation with IL-1β secretion but no pyroptosis. In human monocytes, extracellular LPS administered overnight also led to NLRP3-dependent IL-1β release without cell death (Gaidt et al., 2016).

Seeing as LF2000 was a bona fide inflammasome agonist, we wanted to test if other transfection reagents show similar effects (Fig. 2). Interestingly, while LF2000 was a potent activator of diverse inflammasomes, its newer, improved version LF3000 was not. By performing RNA sequencing of LF2000- and LF3000-stimulated monocytes (Fig. 2D), we found that monocyte treatment with LF2000 induced differential expression of more genes than LF3000 did, in particular genes related to cellular stress and inflammation. However, neither *NLRP3* nor *IL1B* were differentially upregulated by LF2000, so at least this potentially straightforward explanation for LF2000-induced NLRP3 activation does not apply in our model. Interestingly, *AIM2* was expressed at higher levels in LF2000-treated monocytes compared to LF3000-treated cells - but, as in monocytes the response to LF2000 appeared to exclusively rely on NLRP3, this higher *AIM2* expression is unlikely to explain the response difference between LF2000 and 3000, unless, of course, both NLRP3 and AIM2 are non-redundantly required for this answer.

Whereas some other LFs, such as LF MessengerMAX and LF RNAiMAX, had a weak pro-inflammatory activity, other lipid- (*e.g.*, DOTAP) and non-liposome-based (*e.g.*, GeneJuice, FuGeneHD) transfection reagents did not induce any inflammasome activation.

One paper describing NLRP3 inflammasome activation, occurring downstream of cytoplasmic LPS recognition by caspases-4/5, also transfects LPS with LF2000, and reports IL-1β secretion in THP-1 monocytes – however, the study only includes the LPS alone and not the LF alone control (Baker et al., 2015). Other articles do indeed report the LF2000 control. One study does not detect IL-1β upon LF2000 treatment in primary human monocytes – however, while we use 5 µg/mL LF2000, they use 2 µg/mL for the first 6 h and then reduce it to 1 µg/mL by diluting the assay volume 2-fold for overnight incubation (Diamond et al., 2017). In another report, increased IL-1β and LDH secretion in mouse microglia is shown upon 3-h stimulation with LF2000 alone, but the effect is not strong and therefore ignored (Afzal et al., 2025). LF2000 is also used for transfecting many other

molecules in immunology research, such as DNA (*e.g.*, poly(dA:dT)) or RNA (*e.g.*, poly(I:C)), and most studies do not include the LF2000 alone control. Interestingly, some papers that have this control, as they are using LF2000 to transfect dsDNA for AIM2 activation, also observe IL-1β secretion either by primary human monocytes (Hawwari et al., 2024) or by mouse macrophages (Luheshi et al., 2012). Another report of intratracheal LF2000 administration in mice shows strong neutrophil influx and high LDH levels in the bronchoalveolar lavage, with significant lung toxicity – interestingly, DOTAP, which was tested in parallel, did not have the same effect (Dokka et al., 2000). The study does not link this observation to inflammasome activation, considering also that the foundational study first describing the inflammasome was only published two years later (Martinon et al., 2002), but one could hypothesize that the membrane and cellular damage occurring in this context could very well generate DAMPs capable of activating NLRP3.

4.2 Human cells respond to COVID-19 vaccines in a pro-inflammatory manner

Transfection reagents and LNPs have similar functions: they are used as vehicles to deliver substances, *e.g.*, LPS or nucleic acids, inside of cells. So, we quickly got interested in testing the potential inflammasome recognition of and response to the newly developed, more biologically relevant LNP-based mRNA vaccines, specifically those against COVID-19 manufactured by BioNTech/Pfizer and Moderna. If inflammasomes can sense specific lipids or lipid-based formulations, such as LF2000, they might also respond in a pro-inflammatory fashion to the vaccine preparations. Moreover, next to our serendipitous finding, another line of evidence in the form of a recent publication (Tahtinen et al., 2022) served as the starting point for our investigation. The article showed that human PBMCs and monocytes respond to the liposome-based RNA-LPX cancer vaccine by releasing IL-1β in an NLRP3-dependent manner. This IL-1β secretion in turn triggers production of various other pro-inflammatory cytokines (*e.g.*, IL-6) and transient systemic reactions (*e.g.*, fever and chills). In contrast, mice do not show this pro-inflammatory signature, since they mainly respond to the vaccines with secretion of high levels of the anti-inflammatory agent IL-1RA, protecting the animals from uncontrolled inflammatory reactions and toxicities at higher vaccine doses. Lastly, this study

suggests that the main driver of the inflammatory reaction to the vaccine are the lipid components recognized by inflammasomes and not the RNA – since IL-1β release was also observed upon treatment with LNPs containing modified RNA or even no RNA at all, formulated with specific lipids (*e.g.*, the SM-102 lipid, which is used in the Moderna COVID-19 vaccine) (Tahtinen et al., 2022).

To characterize LNP-mRNA vaccine sensing by inflammasomes, we first tested the two LNP-mRNA COVID-19 vaccines in a reductionist setup of fluorescent ASC-reporter HEK cells overexpressing inflammasome-forming sensors. We found that human NLRP3 as well as AIM2 were able to nucleate ASC specks upon treatments with both vaccines (Fig. 3). Interestingly, longer incubations with these stimuli enhanced the strength of inflammasome response (Suppl. Fig. 3). We next investigated primary human cells and found that the Pfizer and Moderna vaccines led to IL-1β secretion by both PBMCs and monocytes, a response which, based on experiments with an NLRP3 inhibitor, was shown to be mediated non-redundantly by NLRP3 (Fig. 3). Previous human studies also reported NLRP3 activation and IL-1β secretion upon treatment with LNPs (Rizzo et al., 2024; Tahtinen et al., 2022).
Collectively, the likelihood of AIM2 involvement is lower in these processes, as it has not been formally shown to bind to any of the components of the stimuli that we use (*i.e.*, lipid components or RNA) and it is atypical for two inflammasomes to act together in the same inflammasome assembly cascade. Yet, the non-redundant involvement of NLRP3 in the response does not exclude that AIM2 could also be required, as mentioned before for the NLRP3-dependent LF2000 response in human monocytes. Unfortunately, there is no available AIM2 inhibitor on the market that could be tested in primary cells and no accessible AIM2 deficiency model in these cells, not allowing for the final AIM2 loss-of-function experiment that would be a proof of the exclusive role of NLRP3 in the response to LNP-mRNA vaccines. Nonetheless, NLRP3 is non-redundantly required for the response to the vaccines even in IFN-γ pre-treated cells, which upregulate AIM2 (as demonstrated in my thesis and corroborated by the literature) (Suppl. Fig. 1) (Gaidt et al., 2017), further suggesting a dominant role for NLRP3. Note that priming with IFN-γ is physiologically translatable to the human system, as diverse papers have shown that there is a strong

IFN-γ increase in the blood, especially after the second dose of the Pfizer vaccine, both in mice (C. Li et al., 2022) and humans (Arunachalam et al., 2021). To investigate the impact of IFN-γ on inflammasome activation, we performed RNA sequencing of untreated monocytes and monocytes treated overnight with IFN-γ: While *NLRP3* expression was slightly upregulated by IFN-γ, *IL1B* and *NFKB1* levels were not affected (Suppl. Fig. 1). Instead of IFN-γ-primed monocytes and overexpression-based HEK cells, one could try to investigate AIM2 activation by LNP-mRNA vaccines in other cell types that, at endogenous levels, selectively express AIM2 and not NLRP3, such as B cells (Svensson et al., 2017). Moreover, it would be valuable to test specific cell types that are of interest regarding undesirable pro-inflammatory reactions, such as NLRP3-expressing cardiomyocytes (G. Chen et al., 2018), since some of the most severe side effects of the vaccines were cardiomyopathies and studies have shown that circa 90% of the myocarditis cases following COVID-19 vaccination occurred upon mRNA vaccine administration (BioNTech/Pfizer and Moderna) (Paknahad et al., 2023). The exact mechanism behind this side effect has not been completely understood, and, for now, only residual dsRNA of the mRNA vaccine nanoparticles has been proposed to play an inflammatory role (Paknahad et al., 2023).

In regard to the cell types responsible for the inflammasome reaction to the vaccines, the observation that monocytes are the vaccine-responsive PBMC fraction (Fig. 3) is in agreement with published data, which, similar to our data, show loss of inflammasome response to the vaccines in CD14-depleted PBMCs (Tahtinen et al., 2022). Interestingly, other studies also show that the frequency of inflammatory monocytes increases in the blood after Pfizer COVID-19 vaccine administration (Arunachalam et al., 2021), but also more broadly the numbers of innate immune cells rise at the injection site and in the draining LNs, due to cell recruitment (Liang et al., 2017; Ndeupen et al., 2021). Therefore, we also tested other primary human innate immune cell types, such as macrophages and DCs: IFN-γ-primed DCs slightly and primed or unprimed macrophages strongly responded to both Pfizer and Moderna vaccines (Fig. 3). Interestingly, isolated DCs without IFN-γ pre-treatment responded strongly to nigericin and poly(dA:dT), but almost not at all to the vaccines (Suppl. Fig. 3). It has been previously shown that IFN-γ dampens NLRP3-dependent IL-1β mRNA

levels and protein secretion (and upregulates IL-1RA, which further blunts IL-1-driven positive feedback) in human monocyte-derived DCs (Cardone et al., 2014).

Without prior LPS priming, the vaccines did not induce any IL-1β secretion in monocytes (data not shown), indicating that the LNPs act as the second NLRP3 activation signal, but do not provide the first priming stimulus. Similar observations have been previously reported (Rizzo et al., 2024; Tahtinen et al., 2022). In contrast to the LNP-mRNA vaccines, empty LNPs made of SM-102 were sufficient as both the first and the second signal for NLRP3 activation (Tahtinen et al., 2022). Notably, in the physiological setting *in vivo*, where LPS is not present, the first signal might derive from among the DAMPs generated at the immunization site. In such a scenario, the LNP-mRNA vaccine might efficiently act as the second, triggering NLRP3 stimulus.

To get a broader overview of the inflammatory responses of monocytes treated with LNP-mRNA vaccines, supernatants of these cells were analyzed for different cytokines and chemokines (Fig. 4). Indeed, many chemoattracts for monocytes and neutrophils (*e.g.*, CXCL8, CCL2), as well as growth factors (*e.g.*, M-CSF, VEGF-A) and cytokines (*e.g.*, TNF-α, IL-1α) could be detected. This release of pro-inflammatory factors is strongly in agreement with many previous studies in humans (Arunachalam et al., 2021; Jiang et al., 2023; Lonez et al., 2014; Tahtinen et al., 2022; Tanaka et al., 2008). Interestingly, we detect high levels of the anti-inflammatory agent IL-1RA. Release of both IL-1RA and IL-1β had also been detected in a previous study in human PBMCs and monocytes treated with liposome-based mRNA (cancer) vaccines, with both cytokines induced similarly at low vaccine doses, but IL-1RA plateauing and IL-1β continuously strongly increasing at high doses (Tahtinen et al., 2022). On the other hand, we were not able to detect type I IFN, such as IFN-α (neither by multiplex nor HTRF) – surprising at first glance, as these cytokines are involved in the antiviral responses to nucleic acids. Remarkably, while previous studies in mouse and macaque were able to detect IFN-α (C. Li et al., 2022; Liang et al., 2017), potentially released by DCs, one previous human study using the Pfizer COVID-19 vaccine was also not able to detect IFN-α (Arunachalam et al., 2021). Another only reported IFN-α production upon AstraZeneca

adenoviral vaccine administration, but neither with the Pfizer nor Moderna COVID-19 vaccines (Jiang et al., 2023).

We also performed RNA sequencing of human monocytes treated with the LNP-mRNA COVID-19 vaccines to explore more intracellular events that are presumably upstream of cytokine secretion (Fig. 4). While *NLRP3* and *AIM2* expression levels were unchanged by the vaccines, *NFKB1* and, at a much higher level, *IL1B* were upregulated upon both Pfizer and Moderna vaccine administration. In addition, also genes involved in inflammation and oxidative/metabolic stress were upregulated. In contrast, other immune regulatory genes were downregulated.

Having looked at inflammasome activation by the LNP-mRNA vaccines from Pfizer and Moderna, we wanted to compare them to some of the other COVID-19 vaccines, such as the ones manufactured by AstraZeneca, an adenoviral vector vaccine, and Novavax, a protein subunit vaccine (Fig. 5). As expected, the AstraZeneca vaccine, consisting of an adenovirus which contains dsDNA genome (encoding COVID-19 spike protein), activated the AIM2, and also slightly the NLRP3 inflammasomes in the inflammasome-expressing reporter HEK cells. Interestingly, the AstraZeneca vaccine was able to strongly activate NLRP3 in monocytes. Although no previous publication explicitly shows this, there are studies that demonstrate that the same adenoviral vector for vaccines, ChAdOx1, expressing other antigens, leads to NLRP3-dependent IL-18 secretion by $CD14^+$ monocytes (Provine et al., 2021). Another study shows that AstraZeneca COVID-19 vaccine induces inflammatory effects in human cells – however, they do not look into inflammasome activation (Jiang et al., 2023). On the other hand, the Novavax vaccine, which comprises the Matrix-M adjuvant, activated predominantly NLRP3. Interestingly, this activation was very potent in the HEK cell overexpression system, but only minimal in primary monocytes. This NLRP3 activation is in agreement with previous publications describing Matrix-M-induced activation of NLRP3 (Stertman et al., 2023; Zarnegar et al., 2025). The Zarnegar et al. (2025) paper shows that Matrix-M induces lysosomal membrane permeabilization and consequent cathepsin B- and NLRP3-dependent IL-1β secretion by mouse BM-derived DCs. However, as NLRP3-KO mice still mount strong

adaptive responses to recombinant SARS-CoV-2 spike protein formulated with Matrix-M, they suggest that NLRP3 contributes to but is not essential for adjuvanticity.

To gain a better insight into the mechanism of LNP-based vaccine-mediated inflammasome activation, we tested whether inflammasomes could sense some of the lipids present in LF2000 and/or LNP-based vaccines (Fig. 5). The neutral phospholipid DOPE, present in LF2000 and very similar to DSCP (the phospholipid present in both Moderna and Pfizer COVID-19 vaccines), was able to induce weak activation of NLRP3 and AIM2. DOSPA, the cationic lipid present in LF2000, activated both inflammasomes at marginally higher levels, while the cationic ionizable lipid SM-102, used in the Moderna vaccine, only activated AIM2. The lower activation levels compared to LF2000 or the vaccines might be linked to poorer efficiency of intracellular delivery of the single lipids or to the biological scenario that inflammasomes sense the combinations of lipids in lipid formulations the strongest.

4.3 Mechanistic insights into inflammasome-mediated sensing of LNP-mRNA COVID-19 vaccines in the human system

A very challenging but interesting part of this study was to identify the mechanism behind the LNP-mRNA vaccine sensing by the diverse inflammasomes. This is also an aspect previous publications have not addressed. How do the vaccines enter the immune cells, and what happens afterwards? Do NLRP3 and AIM2 directly recognize lipids/lipid formulations, or is it an indirect activation mechanism? Unraveling how and what exactly different inflammasomes sense upon vaccine administration is of utmost importance.

We started by addressing the question of how the vaccines get taken up by monocytes (Fig. 6). As CytoD and Wortmannin inhibited cytokine and/or LDH release, and/or rescued cell viability, while PitStop2 and Dynasore did not, we suspect phago-/micropinocytosis to be the entry pathway for the vaccines. A study that investigated entry of specific nanoparticles into human macrophages similarly observed a CytoD-sensitive phagocytosis pathway (Rizzo et al., 2024).

Next, we looked at later intracellular distribution and translocation stages, more precisely if lysosomes and their damage could be involved in inflammasome activation (Fig. 6). As chloroquine, an inhibitor of lysosomal acidification and lysosome-mediated degradation, did not have any effect on the inflammatory response, we initially excluded the involvement of these organelles. Nonetheless, we did observe an inhibitory effect by CA-074Me, a cathepsin B inhibitor that dampened vaccine-induced inflammasome activation. Yet, this compound also inhibits the response to nigericin (which had also already been reported previously (Orlowski et al., 2015)), which is mediated by K^+ efflux and not lysosomal damage. Thus, this activity of CA-074Me could be either due to off-target effects of the drug, or because cathepsin B indeed is released at low levels into the cytosol, without major lysosomal damage occurring, as suggested in a previous publication (Bae et al., 2019; Guicciardi & Gores, 2013). Interestingly, a study of a newly developed nanoparticle targeted for vaccination reported co-localization of the nanoparticle with early and late endosomes, lysosomal membrane destabilization, cathepsin B release and subsequent NLRP3 activation (Rizzo et al., 2024). Another study investigating the ability of different mRNA-LNP formulations to activate NLRP3 in mice, has shown that some NLRP3-activating formulations induced high lysosomal rupture and cathepsin B maturation – but interestingly, these formulations also delayed the endosomal escape of mRNA into the cytoplasm and thus had poor mRNA transfection efficiency. These specific LNPs displayed delayed endosomal rupture, progressing to late endosome/early lysosome stages, where the mRNA got degraded (instead of translocating to the cytoplasm to be translated); then, the ionizable lipid component of the LNP disrupted the lysosomal membrane, and this caused NLRP3 activation. Based on this model, the LNP composition has to be carefully evaluated, since it has to balance early mRNA release and immunogenicity on the one hand, but also NLRP3 activation for a possible adjuvanticity on the other hand (Forster III et al., 2022).

Subsequently, we investigated the role of another organelle, the mitochondria, in inflammasome activation by the vaccines (Fig. 6). If mitochondria get damaged, (oxidized) mitochondrial dsDNA can be released to the cytosol, which may activate AIM2 (Bae et al., 2019) as well as NLRP3 (A. Cabral et al., 2023), and mitochondrial ROS are produced, which have also been linked to NLRP3 activation (Heid et al., 2013; Zhou et al., 2011). A previous

study has also reported mitochondrial ROS production and cytosolic calcium influx upon treatment with specific mRNA-LNP formulations in mouse macrophages (Forster III et al., 2022). However, in HEK cells, mitochondria do not seem to get (dramatically) damaged by the tested vaccines, and mtDNA does not appear to be required for the AIM2 response. Yet, other experiments could be performed to completely exclude a role of mitochondria, such as measurement of mitochondrial ROS or of cytochrome c release into the soluble cytosol.

Lastly, we wanted to investigate whether COVID-19 spike protein expression was required for inflammasome activation, but, as blocking translation of spike mRNA did not impede cytokine secretion by vaccine-treated monocytes, we conclude that this is not the case. This is also in agreement with previously published data in human cells treated with the AstraZeneca COVID-19 vaccine (Jiang et al., 2023). They report that the adenovirus vector (ChAdOx1), and not the COVID-19 spike protein or soluble components of the formulation, is responsible for the inflammatory response, as they observe that the adenoviral vector without the spike insert induces strong cytokine response in human PBMCs. Moreover, in a differential centrifugation experiment that separates the ChAdOx1 virus fraction containing the adenovirus particles (insoluble) from the supernatant fraction with the soluble components, the authors show that only the virus-containing fraction induces a cytokine response.

Based on the available literature and our results (*e.g.*, lipids alone activating inflammasomes (Fig. 5), the potential connection to lysosomal damage (which would be induced by the LNP lipids, and not the mRNA) (Fig. 6), the lack of requirement for the spike protein (Fig. 6)), we speculate that inflammasomes somehow sense the lipids, and not the mRNA component of the vaccines. Hence, it is valuable to have a closer look at the different LNP components. Many studies show that the ionizable lipid component of LNPs is necessary for innate immune responses, as replacing or removing these lipids leads to decreased inflammation (Ndeupen et al., 2021) and also adaptive responses (Alameh et al., 2021). Additionally, some empty (*i.e.*, RNA-free) LNPs, constructed with individual specific lipids (such as the SM-102 lipid used in the Moderna COVID-19 vaccine), have been described as sufficient to elicit a

NLRP3-dependent IL-1β-driven immune response in human PBMCs (Tahtinen et al., 2022). In future efforts, it will be useful to assemble a range of empty LNPs consisting of different types of (ionizable) lipids to help untangle whether specific types of lipids are able to activate inflammasomes, by testing them in our various cellular systems. This would allow closer investigation of the individual role of lipids in innate immune responses and vaccine reactogenicity, and to understand how differences in LNP composition lead to differences in adaptive responses and immunogenicity.

4.4 Mouse *vs.* human NLRP3 differences in LNP-mRNA COVID-19 vaccine sensing

As mice are the standard model for testing newly developed vaccines, we wanted to investigate whether mouse inflammasomes were also able to sense the LNP-based COVID-19 vaccines (Fig. 7). While mouse macrophages responded to LF2000, as previously seen, mouse PBMCs and splenocytes did not. Interestingly, the LNP-mRNA vaccines were not sensed by any of these cell types, including GM-CSF pre-treated cells, despite GM-CSF mediated upregulation of NLRP3 protein and the consequent generally higher IL-1β secretion in response to regular inflammasome activators. Regarding the PBMC data, one potential explanation could be that the frequency of monocytes in PBMCs in humans is 10-20 %, while in mice it is only 4-6 %. The lack of sensitivity to the vaccines in mouse macrophages is more surprising, as these cells were able to respond to LF2000, and also express the highest levels of NLRP3 among the tested cell types. Yet, two different readouts, IL-1β secretion in BMDMs and ASC speck formation in iMacs, yielded the same negative results. Nonetheless, these results are consistent with the study by Tahtinen et al., which shows that, compared to humans, mice release much lower levels of IL-1β upon treatment with a liposomal cancer vaccine (Tahtinen et al., 2022). Instead, they release much higher levels of the anti-inflammatory IL-1RA. In our case, however, we prime BMDMs with LPS before treating them with the vaccines, and LPS priming already leads to high IL-1RA secretion in BMDMs, as reported by J.-X. Yang et al. (2017). The levels of LPS-induced IL-1RA do not increase with the subsequent vaccine treatment. Nonetheless, IL-1RA, constitutively present in the

extracellular milieu, could act as an anti-inflammatory agent counteracting a possible inflammasome-driven response to the vaccines.

Still, BMDMs release other inflammatory chemokines (such as CXCL1 and CXCL2) and cytokines (*e.g.*, TNF-α and IL-6) (Fig. 7), consistent with previous mouse studies (Alameh et al., 2021; C. Li et al., 2022; Lonez et al., 2014; Ndeupen et al., 2021; Tahtinen et al., 2022; Tanaka et al., 2008). Similar to the supernatants of human cells (Fig. 4), also in mouse BMDMs we were not able to detect IFN-α. Although *in vivo* mice (C. Li et al., 2022) and macaque (Liang et al., 2017) studies demonstrated IFN-α secretion, the lack of IFN-α production by BMDMs could be explained by cell type differences: diverse paper suggest IFN-α is likely coming from plasmacytoid DCs (Liang et al., 2017; Provine et al., 2021).

To understand whether the *in vitro* sensitivity difference between mice and humans is only related to the IL-1 family balance (IL-1β vs. IL-1RA), as previously described (Tahtinen et al., 2022), or if there are additional mechanistic differences, we decided to directly compare human and mouse NLRP3-driven responses in the same cell type. We started with NLRP3-KO iMacs reconstituted with NLRP3 proteins from different species. While human NLRP3 was able to sense LF2000 and the vaccines, mouse, macaque and rat NLRP3 did not respond strongly or at all. Interestingly, mouse NLRP3 containing the human linker (aa 91-220, between the PYD and the NACHT domains) became responsive to all triggers. In contrast, mouse NLRP3 with only specific residues of the polybasic region humanized (C133R, M135K) was not activated by LNP-mRNA vaccines, while it remained responsive to the canonical NLRP3 activator nigericin. This suggests that the higher sensitivity of the human NLRP3, compared to mouse NLRP3, does not originate in the two specific human residues in the polybasic region, but instead likely depends on the entire linker region. As the human positively-charged NLRP3 polybasic region binds to PI4P, a negatively-charged Golgi lipid (J. Chen & Chen, 2018), it is not surprising to envisage that this region does not interact with the LNPs, which contain neutral or positively-charged lipids. However, the entire human linker could, potentially, still be responsible for the interaction with the hydrophobic parts of lipid molecules, and thus, when inserted into the mouse NLRP3 sequence, provide mouse NLRP3 with the sensitivity to LNP-mRNA based vaccines. Of note, AIM2, which is present in

the mouse iMacs used for the reconstitution and targeted mutagenesis experiments, does not seem to be able to sense the vaccines, even though it mounted inflammasome responses to poly(dA:dT) in NLRP3-KO cells.

Next, we compared human and mouse NLRP3 in the human U-937 monocytic cell line, differentiated to macrophages. Firstly, it was interesting that in these cells human AIM2 is very likely able to respond to LF2000, as the NLRP3-KO cells are also releasing IL-1β upon poly(dA:dT) and LF2000 treatment. Until now, except in the overexpression-based HEK cell system, we had only observed NLRP3-dependent sensing of LF2000 in primary human cells. Regarding the response to the vaccines in U-937 macrophages, we only found human NLRP3 responding to the Pfizer vaccine, similar to the observations in other test systems. This pattern whereby human NLRP3 was sensitive, and mouse NLRP3 was not, resembled what we have observed with the low concentration of R837 (10 μM). Interestingly, at a higher R837 concentration (40 μM), mouse NLRP3 becomes able to sense this stimulus and mount the IL-1β response. Potentially, human NLRP3 is thus more sensitive, also responding to lower trigger concentrations, while mouse NLRP3 requires stronger activators. Possibly, this difference originates from the linker region.

In this case, the question arises how the different linker region sequences modulate NLRP3 sensitivity to LNP-mRNA vaccines. If NLRP3 directly binds to the LNP lipids, could the linker regions differentially allow ligand binding? An interesting experiment would be to encapsulate fluorescently labeled nucleic acids (DNA or RNA) in the LNP – not only to confirm delivery into the cells and allow for intracellular (organelle) tracking, but also to look at potential co-localization with human *vs.* mouse NLRP3 inflammasome, for example by microscopy. Another option is running a proteome integral solubility alteration (PISA) thermal stabilization assay or a cellular thermal shift assay (CETSA) to assess possible thermal stability shifts of NLRP3 (Batth et al., 2024). In such an experiment, direct binding of vaccine-derived lipids to NLRP3 or other proteins could result in thermal stabilization or destabilization of these proteins, indicating that they are a candidate receptor recognizing these lipids.

This inflammasome-mediated sensing of lipids in LNP-based vaccines could explain the inflammatory side effects of these vaccines, as IL-1β is, for example, known to be a key pyrogen responsible for inducing fever (Dinarello et al., 1977). Thus, it would be relevant to gain a deeper understanding of this response, to possibly help with the development of improved LNPs which would elicit a fine-tuned inflammatory response.

On the other hand, it is important to remember that IL-1β was first described as a lymphocyte-activating factor, playing a role in an effective T cell response, enhancing their proliferation in response to antigens (Gery et al., 1972; Gery & Waksman, 1972; Mizel & Ben-Zvi, 1980). Moreover, other adjuvants, such as alum (Franchi & Núñez, 2008; Hornung et al., 2008; H. Li et al., 2008), Quil A (H. Li et al., 2008) and chitosan (H. Li et al., 2008) have been shown to activate NLRP3, and while one study suggests that NLRP3 is not involved in alum's adjuvanticity (Franchi & Núñez, 2008), another one suggests that NLRP3 activation does contribute to adjuvanticity (H. Li et al., 2008). Also another adjuvant, GLA-SE, has been linked to NLRP3 activation and consequent dependent adaptive responses (Seydoux et al., 2018). Finally, diverse studies also show that LNPs can activate NLRP3 (C. Li et al., 2022; Liang et al., 2017; Lonez et al., 2014; Tahtinen et al., 2022). Taken together, these data suggest that the inflammasome response to the LNP-mRNA COVID-19 vaccines could also potentially contribute to the adjuvant effect of these vaccines. On the other hand, there are three agents in the clinic (anakinra, canakinumab, rilonacept) which block IL-1 signaling, but the patients, although officially classified as immunosuppressed, can be effectively vaccinated, mounting normal antibody responses, including upon administration of the COVID-19 vaccines (Atagündüz et al., 2022; Geck et al., 2023). Also, NLRP3 is an attractive drug target, and already has antagonists in human clinical trials (J. E. Cabral et al., 2025; Kaur et al., 2025), which are expected to control inflammation without broad immunosuppression (Klück et al., 2020; Madurka et al., 2023; Pinzón-Fernández et al., 2025; Y. Yang et al., 2019; Zahid et al., 2019). Moreover, NLRP3-, ASC-, or caspase-1-KO animals are also not broadly immunosuppressed (Lin & Porto, 2025; Liu et al., 2009; Stitham et al., 2020; Svandova et al., 2024). This would suggest that IL-1 secretion might not be crucial for successful adaptive defenses, neither for vaccination nor disease protection. Still, one interesting experiment would be to treat human monocytes with the LNP-mRNA vaccines, with or without CRID3

pre-treatment, and upon overnight incubation add them to human T cells. If vaccine-treated monocytes induce T cell activation, and CRID3 pre-treatment blocks it, that would suggest that NLRP3 contributes to adjuvanticity of the vaccines. Moreover, it could be of high clinical interest to test whether NLRP3 inhibition by CRID3 affects the adaptive immune response upon vaccine administration into a humanized immune system mouse model (or a mouse model expressing human NLRP3 under the endogenous promoter), as mouse inflammasomes do not respond to the vaccines in the same way that human NLRP3 does. If the results of such future studies indicate that NLRP3 is necessary for LNP-mRNA vaccine adjuvanticity and NLRP3 inhibition dampens the adaptive immune response, a new important role of inflammasomes in LNP-based vaccination would be demonstrated. Such findings would have an important impact on future rational vaccine development.

5. Abstract

The innate immune system is the first line of host defense. Upon detecting pathogens or cell stress, some NOD-like receptors (NLRs) and absent in melanoma (AIM)-like receptors (ALRs) recruit the adaptor protein ASC and consecutively the protease pro-caspase-1, forming an intracellular complex called an inflammasome. Inflammasome formation induces pro-caspase-1 activation, which in turn triggers gasdermin D-dependent pyroptotic cell death and the subsequent release of the pro-inflammatory cytokines interleukin (IL)-1β and IL-18. The exact triggers and activation mechanisms of several inflammasome-forming sensors remain a topic of active research.

Recently, lipid-based mRNA vaccines have been shown to induce the production of IL-1β in human peripheral blood mononuclear cells (PBMCs). Here we show that several human inflammasomes, such as NLRP3 and AIM2, can sense the lipid nanoparticle (LNP)-mRNA Pfizer and Moderna COVID-19 vaccines as well as the transfection reagent lipofectamine 2000, causing ASC speck formation and cytokine release. We speculate that the inflammasomes could sense the lipid nanoparticles and not the mRNA component of these vaccines. Interestingly, mouse inflammasomes do not seem to have the same sensitivity to these vaccines, as they do not activate inflammasomes upon vaccine treatment.

Our findings might explain the inflammatory side effects of LNP-mRNA vaccines, such as fever and arm swelling, but also, potentially, the adjuvant mechanism of these novel vaccines. Better characterization of inflammasome-activating lipids could aid the development of improved LNP-based mRNA vaccines that elicit a fine-tuned inflammatory response. Finally, due to differences in inflammasome sensing of LNP-mRNA vaccines between humans and mice, we propose that wild-type mice may not be the best model to study immuno- and reactogenicity of newly developed mRNA vaccines.

6. List of figures

7. List of tables

8. Supplementary figures

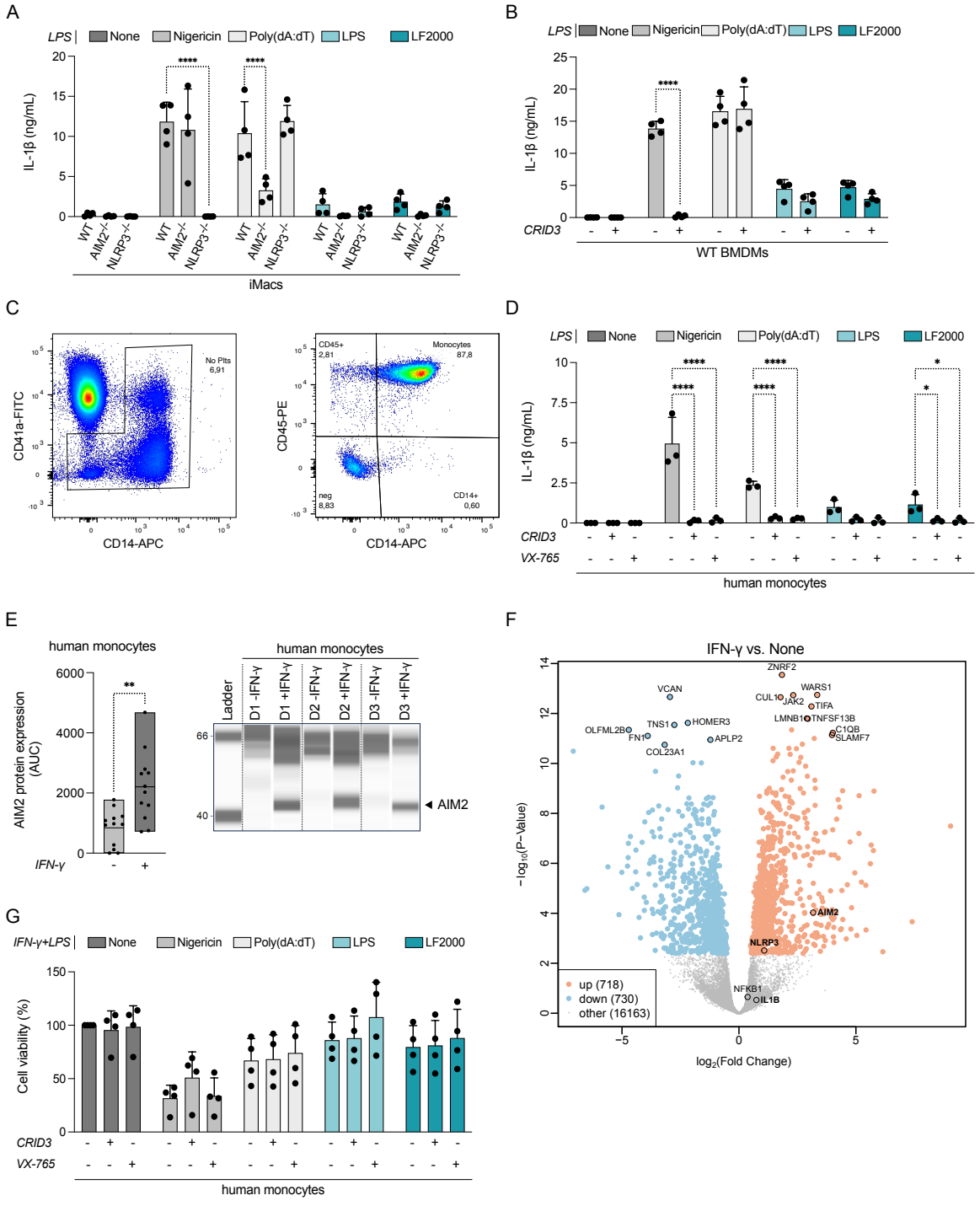

Suppl. Fig. 1: NLRP3 and AIM2 inflammasomes sense lipofectamine (LF) 2000 in the human and mouse.
(**A**) IL-1β secretion from wild-type (WT), AIM2- or NLRP3-knockout ($^{-/-}$) mouse immortalized macrophages (iMacs), primed with LPS (200 ng/mL) for 3 hours (h), and stimulated overnight (20-24 h) with nigericin (10 µM), poly(dA:dT) dsDNA (2 µg/mL), transfected LPS (5 ng/mL), and LF2000 (5 µg/mL).
(**B**) IL-1β secretion from mouse WT primary bone marrow-derived macrophages (BMDMs), primed with LPS (200 ng/mL) for 3 h, treated or not with CRID3 (5 µM) for 10-30 minutes (min), and stimulated overnight (20-24 h) with nigericin (10 µM), poly(dA:dT) dsDNA (2 µg/mL), transfected LPS (5 ng/mL), and LF2000 (5 µg/mL).
(**C**) Purity of isolated monocytes shown by flow cytometry dot plots of one representative donor. Monocytes were defined as $CD14^+$ cells, platelets as $CD41a^+$ cells, and leukocytes as $CD45^+$ cells.
(**D**) IL-1β secretion from human monocytes rested overnight, and then primed with LPS (2 ng/mL) for 3 h, treated or not with CRID3 (5 µM) or VX-765 (50 µM) for 10-30 min, and stimulated overnight (20-24 h) with nigericin (10 µM), poly(dA:dT) dsDNA (2 µg/mL), transfected LPS (5 ng/mL), and LF2000 (5 µg/mL).
(**E**) Simple Western quantification analysis (area under the curve (AUC)) and image of AIM2 expression in cell lysates of primary human monocytes, treated or not with IFN-γ (10 ng/mL) overnight.
(**F**) Volcano plot showing significance (negative $\log_{10}$ un-adjusted p-values) versus $\log_2$ fold changes (FCs) of all genes comparing IFN-γ treatment to control. Significantly upregulated genes are shown in red and downregulated genes are shown in blue. Selected highly significant genes are highlighted, as well as *AIM2*, *NLRP3*, *IL1B* and *NFKB1*.
(**G**) Normalized cell viability of human monocytes from the experiment shown in Fig. 1B.
N = 2 (B), 3 (C), 4 (A,F), 5 (E), 12 (D) biological repeats or 3 (G,H) or 4 (A) independent experiments; individual data points are means of technical duplicates (except in D); all error bars represent SD.
P values were calculated using two-way ANOVA with Šídák's (A,G,H) or Dunnett's (A,C,F) multiple comparison test or paired t test (D). $*P = 0.0261$, $**P = 0.0021$, $***P = 0.0007$, $****P < 0.0001$; NS $P = 0.1582–0.9999$ (not shown).

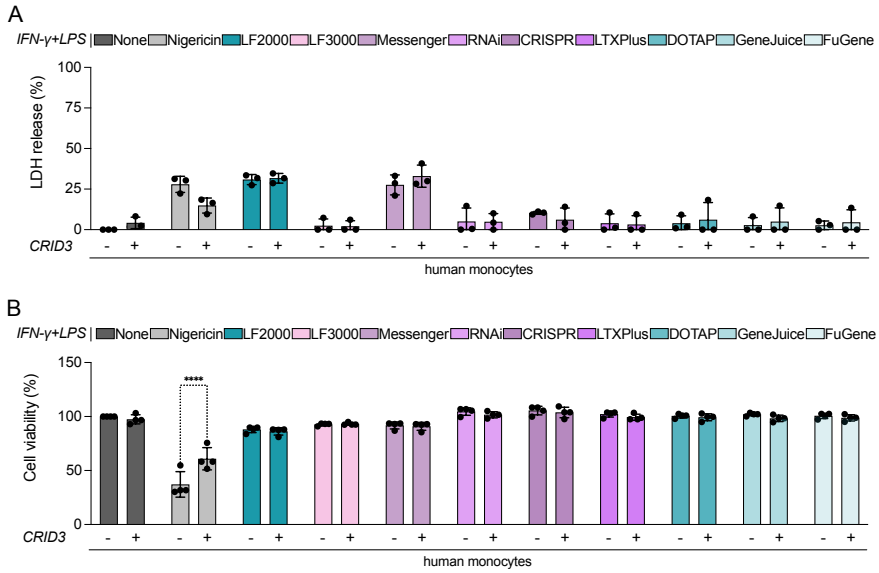

Suppl. Fig. 2: Human inflammasomes sense some lipofectamines (LFs) (MessengerMAX, RNAiMAX, CRISPRMAX Cas9), but not LF3000.

(**A,B**) Lactate dehydrogenase (LDH) secretion from (A) and cell viability of (B) human monocytes of Fig. 2A, *i.e.*, human monocytes pre-treated with IFN-γ (10 ng/mL) overnight, and then primed with LPS (2 ng/mL) for 3 hours (h), treated or not with CRID3 (5 µM) for 10-30 minutes (min), and stimulated overnight (20-24 h) with nigericin (10 µM), LF2000, LF3000, and LF MessengerMAX (Messenger), RNAiMAX (RNAi), CRISRMAX Cas9 (CRISPR), LTX Plus, DOTAP, GeneJuice, FuGene (5 µg/mL).

N = 3 (A), 4 (B) biological repeats; individual data points are means of technical duplicates; all error bars represent SD.

P values were calculated using two-way ANOVA with Šídák's multiple comparison test. **P* = 0.0261, ***P* = 0.0021, ****P* = 0.0007, *****P* < 0.0001; NS *P* = 0.1582–0.9999 (not shown).

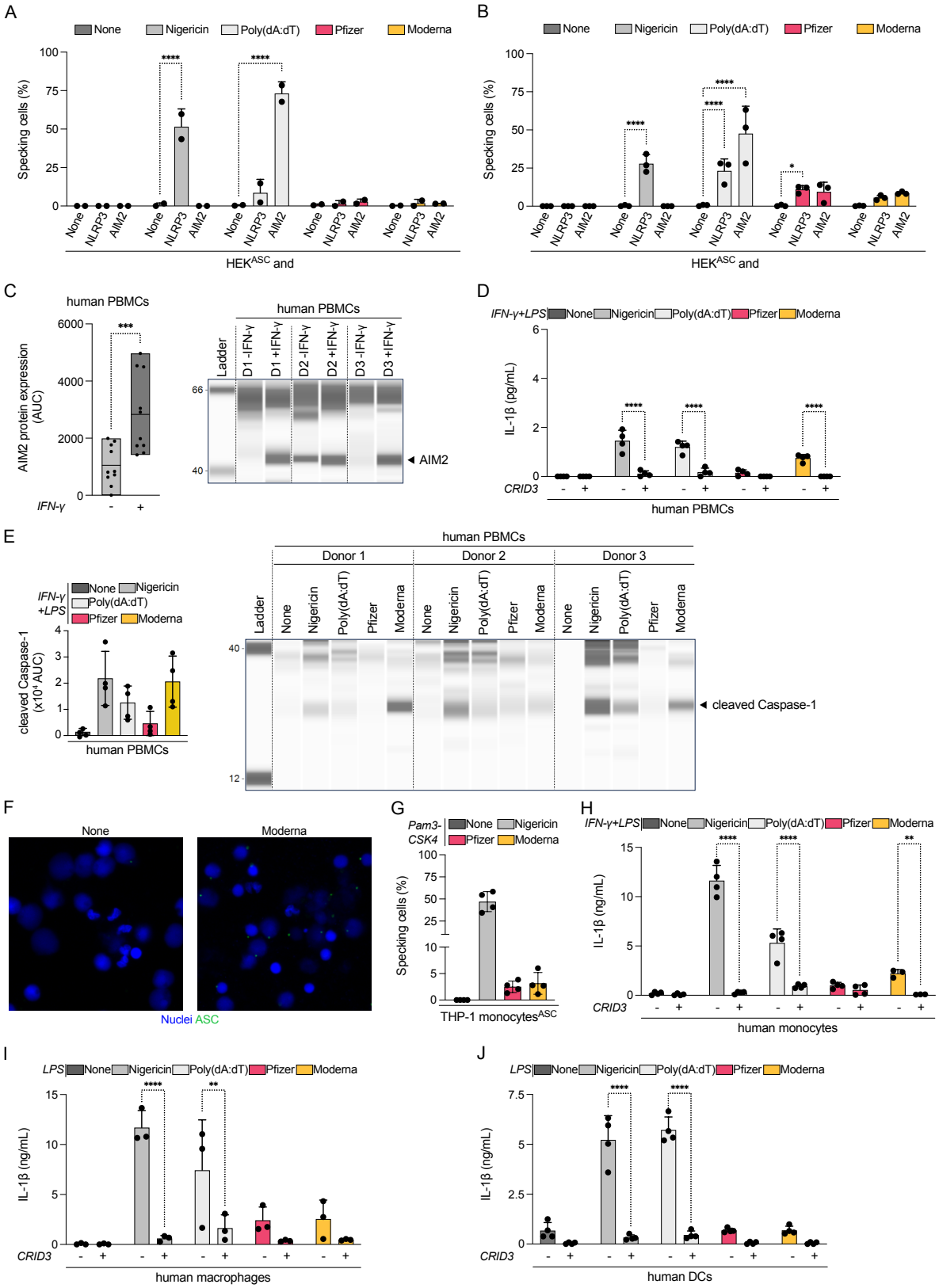
A
None
Nigericin
Poly(dA:dT)
Pfizer
Moderna
Specking cells (%)
NLRP3
AIM2
HEK^ASC and
B
C
human PBMCs
AIM2 protein expression (AUC)
IFN-γ
Ladder
D1 -IFN-γ
D1 +IFN-γ
D2 -IFN-γ
D2 +IFN-γ
D3 -IFN-γ
D3 +IFN-γ
AIM2
D
IFN-γ+LPS
IL-1β (pg/mL)
CRID3
E
IFN-γ +LPS
cleaved Caspase-1 (x10⁴ AUC)
Donor 1
Donor 2
Donor 3
F
Nuclei ASC
G
Pam3-CSK4
THP-1 monocytes^ASC
H
IL-1β (ng/mL)
human monocytes
I
LPS
human macrophages
J
human DCs

Suppl. Fig. 3: Human inflammasomes sense lipid nanoparticle (LNP)-based COVID-19 vaccines.
(**A,B**) Normalized ASC speck formation per cell (specking cells) in Human Embryonic Kidney 293T (HEK) cells expressing fluorescently tagged ASC and NLRP3 or AIM2, stimulated for 90 minutes (min) (A) or 5 hours (h) (B) with nigericin (10 μM), poly(dA:dT) dsDNA (2 μg/mL), and Pfizer and Moderna vaccines (50 μg/mL).
(**C**) Simple Western quantification analysis (area under the curve (AUC)) and virtual lane view of AIM2 expression in cell lysates of human peripheral blood mononuclear cells (PBMCs), treated or not with IFN-γ (10 ng/mL) overnight.
(**D,H**) IL-1β secretion from human PBMCs (D) or monocytes (H), pre-treated with IFN-γ (10 ng/mL) overnight, then primed with LPS (2 ng/mL) for 3 h, treated or not with CRID3 (5 μM) for 10-30 min, and stimulated for 90 min with nigericin (10 μM), poly(dA:dT) dsDNA (2 μg/mL), and Pfizer and Moderna vaccines (50 μg/mL).
(**E**) Simple Western analysis (AUC) and virtual lane view of cleaved Caspase-1 detected in the cell supernatants of Fig. 3B.
(**F**) Visualization of ASC specks of Fig. 3F.
(**G**) Normalized ASC speck formation per cell (specking cells) in THP-1 monocytes expressing fluorescently tagged ASC, primed with Pam3CSK4 (1 μg/mL) for 3 h, treated with VX-765 (50 μM) for 10-30 min, and stimulated overnight (20-24 h) with nigericin (10 μM), Pfizer and Moderna vaccines (50 μg/mL).
(**I,J**) IL-1β secretion from primary human macrophages (I) or dendritic cells (DCs) (J), rested overnight, and then primed with LPS (2 ng/mL) for 3 h, treated or not with CRID3 (5 μM) for 10-30 min, and stimulated overnight (20-24 h) with nigericin (10 μM), poly(dA:dT) dsDNA (2 μg/mL), and Pfizer and Moderna vaccines (50 μg/mL).
N = 2 (A), 3 (B), 4 (G) independent experiments or 3 (I), 4 (D,E,H,J), 5 (F), 10 (C) biological repeats; individual data points are means of technical duplicates (except in C,E,F); all error bars represent SD.
P values were calculated using paired t test (C) or two-way ANOVA with Dunnett's (A,B) or Šídák's (D,G,H,I) multiple comparison test. $*P = 0.0261$, $**P = 0.0021$, $***P = 0.0007$, $****P < 0.0001$; NS $P = 0.1582–0.9999$ (not shown).

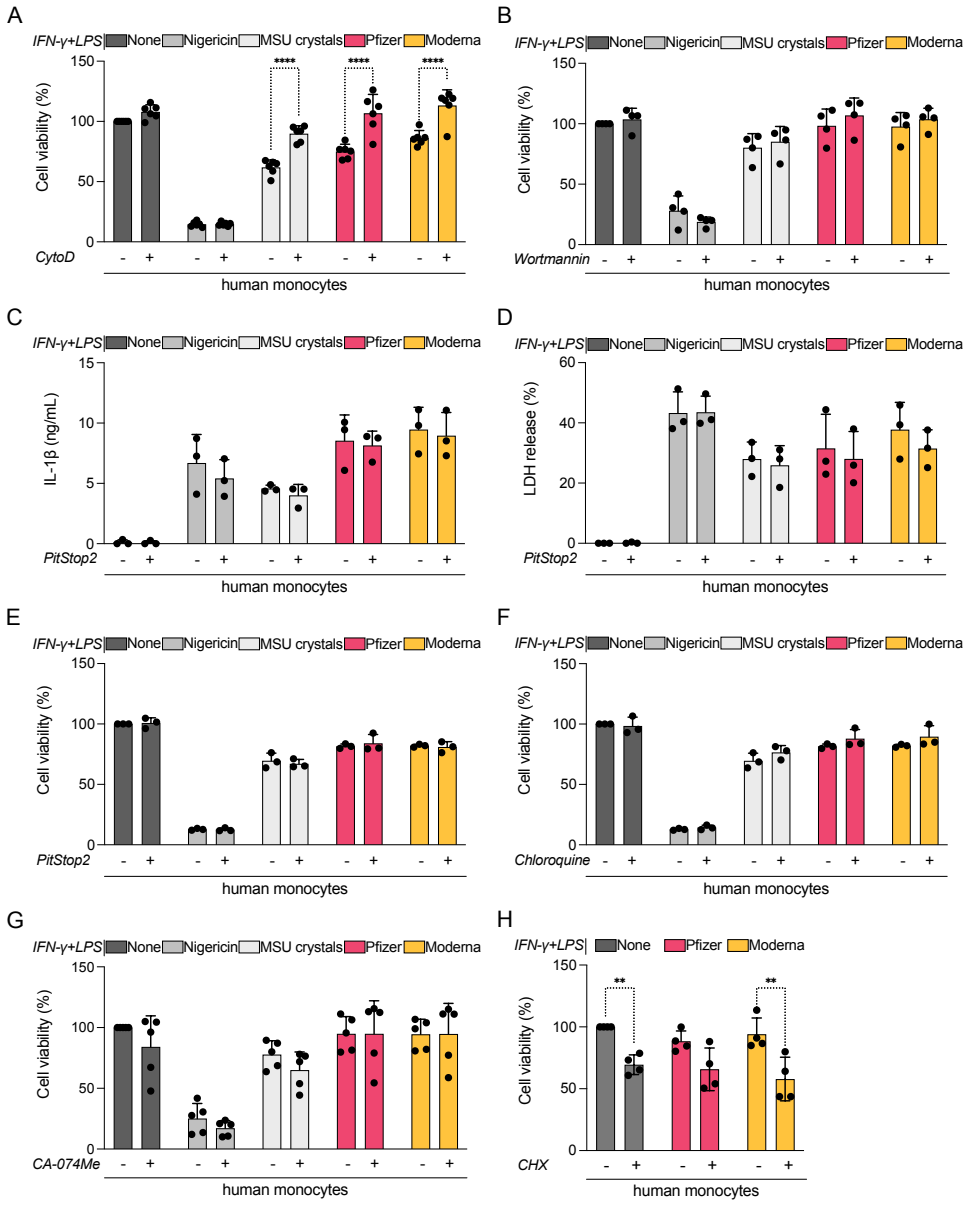

Suppl. Fig. 4: Lipid nanoparticle (LNP)-based COVID-19 vaccines enter through micropinocytosis, do not induce lysosomal or mitochondrial damage, and do not require spike protein expression for inflammasome activation.
(**A,B,F,G,H**) Cell viability of the human monocytes of Fig. 6A (A), Fig. 6C (B), Fig. 6E (F), Fig. 6G (G), Fig. 6K (H).
(**C-E**) IL-1β (C) and lactate dehydrogenase (LDH) (D) secretion from and cell viability (E) of primary human monocytes, pre-treated with IFN-γ (10 ng/mL) overnight, then primed with LPS (2 ng/mL) for 3 hours (h), treated or not with PitStop2 (30 µM) for 10-30 minutes (min), and stimulated overnight (20-24 h) with nigericin (10 µM), MSU crystals (250 µg/mL), and Pfizer and Moderna (50 µg/mL) vaccines.

N = 3 (C,D,E,F), 4 (B,H), 5 (G), 6 (A) biological repeats; individual data points are means of technical duplicates; all error bars represent SD.
P values were calculated using two-way ANOVA with Šídák's multiple comparison test. **P* = 0.0261, ***P* = 0.0021, ****P* = 0.0007, *****P* < 0.0001; NS *P* = 0.1582–0.9999 (not shown).

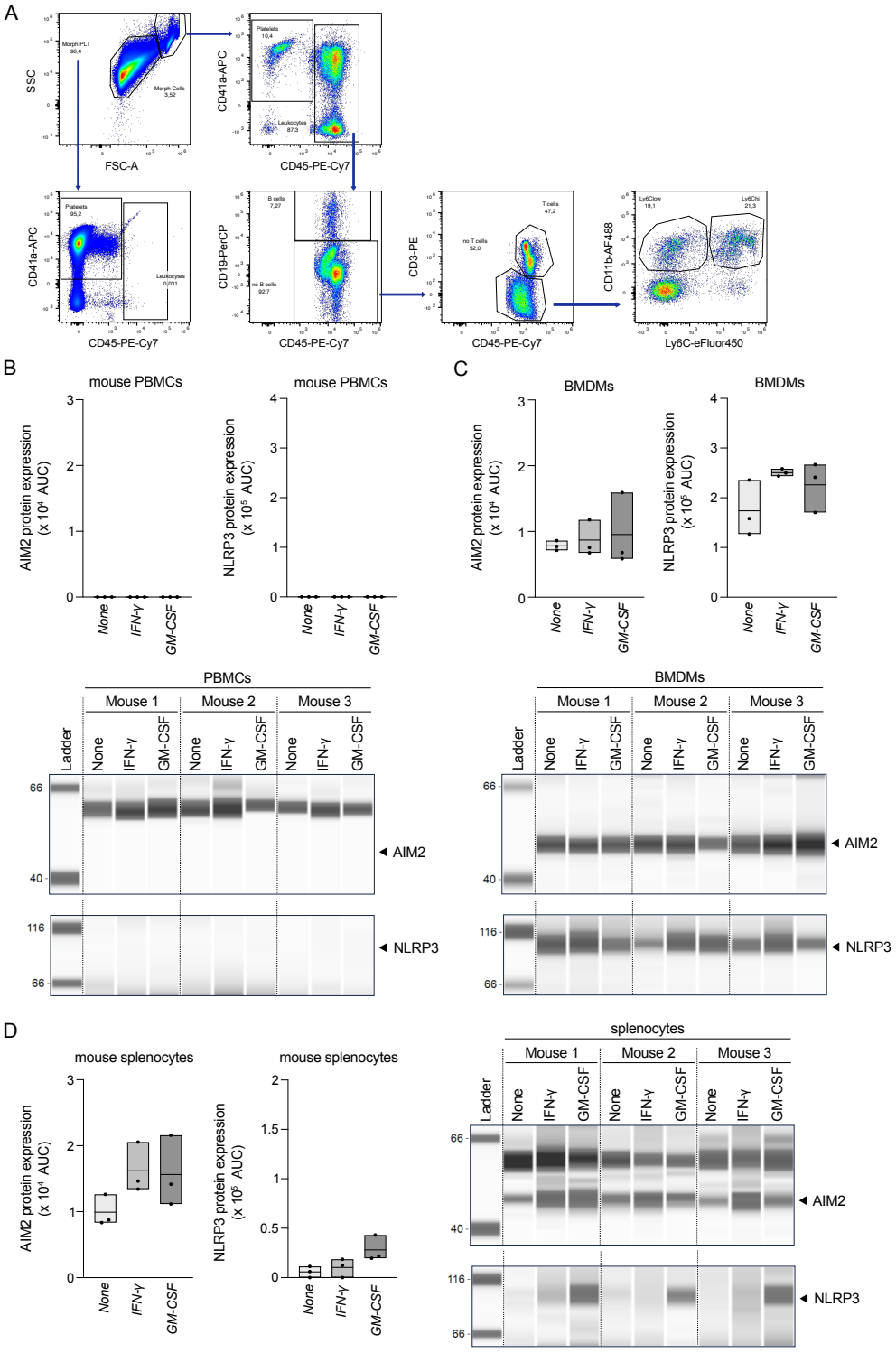
A
SSC
FSC-A
Morph PLT
96,4
Morph Cells
3,52
CD41a-APC
CD45-PE-Cy7
Platelets
10,4
Leukocytes
87,3
Platelets
95,2
Leukocytes
0,031
CD19-PerCP
B cells
7,27
no B cells
92,7
CD3-PE
T cells
47,2
no T cells
52,0
CD11b-AF488
Ly6C-eFluor450
Ly6Clow
19,1
Ly6Chi
21,3
B
mouse PBMCs
AIM2 protein expression
(x 10⁴ AUC)
NLRP3 protein expression
(x 10⁵ AUC)
None
IFN-γ
GM-CSF
C
BMDMs
NLRP3 protein expression
(x 10⁶ AUC)
PBMCs
BMDMs
Mouse 1
Mouse 2
Mouse 3
Ladder
None
IFN-γ
GM-CSF
66
40
116
AIM2
NLRP3
D
mouse splenocytes
splenocytes

Suppl. Fig. 5: Mouse inflammasomes do not sense lipid nanoparticle (LNP)-based COVID-19 vaccines.
(**A**) Compositional overview of isolated mouse peripheral blood mononuclear cells (PBMCs) shown by flow cytometry dot plots of one representative mouse. Platelets were defined as $CD41a^+$, leukocytes as $CD45^+$, B cells as $CD19^+$, T cells as $CD3^+$, and monocytes as $CD11b^+$ cells (with $Ly6C^{high}$ or $Ly6C^{low}$ subsets).
(**B-D**) Simple Western quantification analysis (area under the curve (AUC)) and virtual lane view of AIM2 and NLRP3 expression in cell lysates of primary mouse PBMCs (B), bone marrow-derived macrophages (BMDMs) (C) or splenocytes (D), treated or not with mouse IFN-γ (10 ng/mL) or GM-CSF (1 ng/mL) overnight.
N = 3 (B-D) biological repeats.

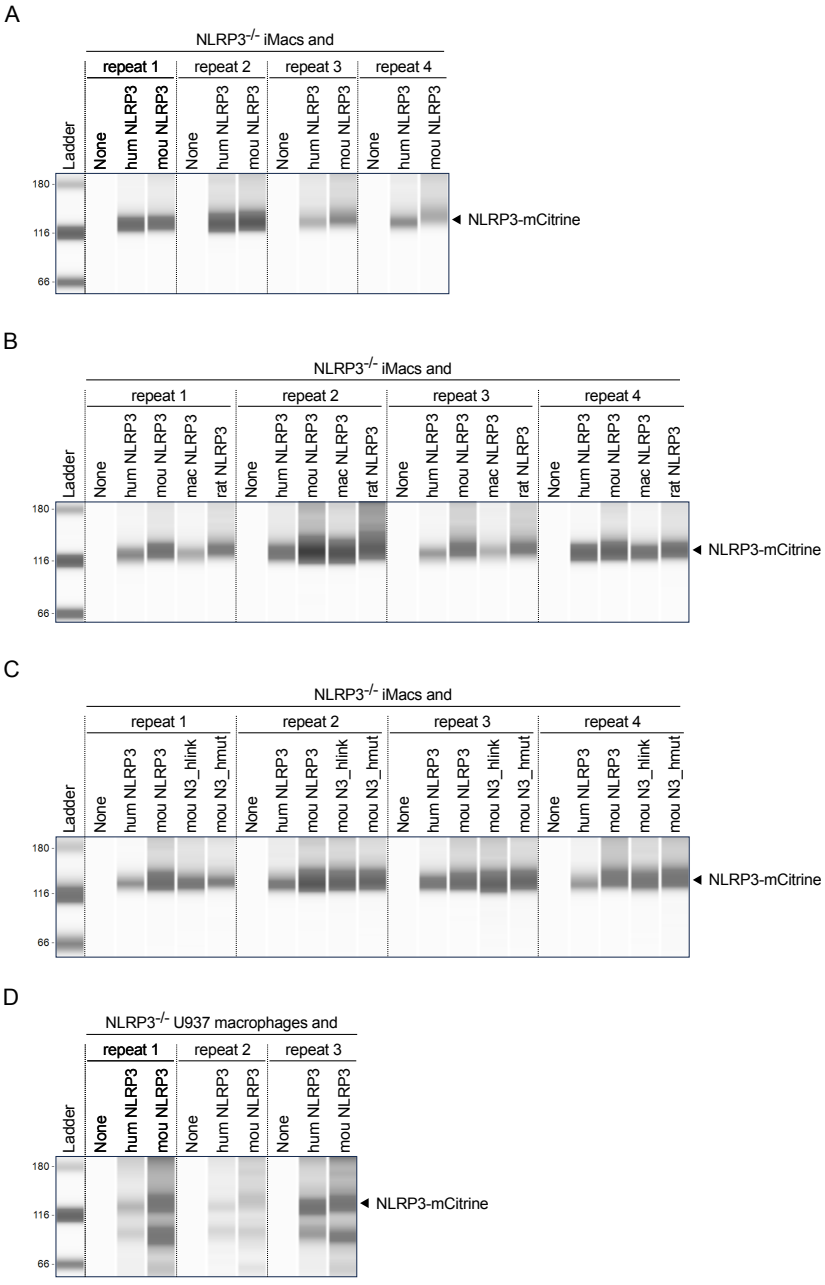

Suppl. Fig. 6: Difference in inflammasome sensing of lipid nanoparticle (LNP)-based COVID-19 vaccines between the human and mouse systems.
(**A-D**) Simple Western virtual lane view of NLRP3 expression in cell lysates of the cells from Fig. 8A (A), 8C (B), 8E (C), 8G (D).
N = 3 (D) or 4 (A-C) independent experiments.

9. References

Abais, J. M., Xia, M., Zhang, Y., Boini, K. M., & Li, P.-L. (2015). Redox Regulation of NLRP3 Inflammasomes: ROS as Trigger or Effector? *Antioxidants & Redox Signaling*, *22*(13), 1111–1129. https://doi.org/10.1089/ars.2014.5994

Ablasser, A., Goldeck, M., Cavlar, T., Deimling, T., Witte, G., Röhl, I., Hopfner, K.-P., Ludwig, J., & Hornung, V. (2013). cGAS produces a 2′-5′-linked cyclic dinucleotide second messenger that activates STING. *Nature*, *498*(7454), 380–384. https://doi.org/10.1038/nature12306

Afzal, M. A., Ghait, M., Hussain, A., Siegmund, A., Tuchscherr, L., Babic, P., Press, A. T., Hardt, R., Winter, D., Rödiger, A., Schüle, R., Fielitz, J., Bauer, M., & Hübner, C. A. (2025). Hyperactivity of the non-canonical inflammasome in SPG11 and SPG48. *EBioMedicine*, *121*, 105985. https://doi.org/10.1016/j.ebiom.2025.105985

Akbal, A., Dernst, A., Lovotti, M., Mangan, M. S. J., McManus, R. M., & Latz, E. (2022). How location and cellular signaling combine to activate the NLRP3 inflammasome. *Cellular & Molecular Immunology*, *19*(11), 1201–1214. https://doi.org/10.1038/s41423-022-00922-w

Al Fayez, N., Nassar, M. S., Alshehri, A. A., Alnefaie, M. K., Almughem, F. A., Alshehri, B. Y., Alawad, A. O., & Tawfik, E. A. (2023). Recent Advancement in mRNA Vaccine Development and Applications. *Pharmaceutics*, *15*(7), 1972. https://doi.org/10.3390/pharmaceutics15071972

Alameh, M.-G., Tombácz, I., Bettini, E., Lederer, K., Ndeupen, S., Sittplangkoon, C., Wilmore, J. R., Gaudette, B. T., Soliman, O. Y., Pine, M., Hicks, P., Manzoni, T. B., Knox, J. J., Johnson, J. L., Laczkó, D., Muramatsu, H., Davis, B., Meng, W., Rosenfeld, A. M., … Pardi, N. (2021). Lipid nanoparticles enhance the efficacy of mRNA and protein subunit vaccines by inducing robust T follicular helper cell and humoral responses. *Immunity*, *54*(12), 2877-2892.e7. https://doi.org/10.1016/j.immuni.2021.11.001

Alexopoulou, L., Holt, A. C., Medzhitov, R., & Flavell, R. A. (2001). Recognition of double-stranded RNA and activation of NF-κB by Toll-like receptor 3. *Nature*, *413*(6857), 732–738. https://doi.org/10.1038/35099560

Anand, P. K. (2020). Lipids, inflammasomes, metabolism, and disease. *Immunological Reviews*, *297*(1), 108–122. https://doi.org/10.1111/imr.12891

Anderson, E. J., Rouphael, N. G., Widge, A. T., Jackson, L. A., Roberts, P. C., Makhene, M., Chappell, J. D., Denison, M. R., Stevens, L. J., Pruijssers, A. J., McDermott, A. B., Flach, B., Lin, B. C., Doria-Rose, N. A., O'Dell, S., Schmidt, S. D., Corbett, K. S., Swanson, P. A., Padilla, M., … Beigel, J. H. (2020). Safety and Immunogenicity of SARS-CoV-2 mRNA-1273 Vaccine in Older Adults. *New England Journal of Medicine*, *383*(25), 2427–2438. https://doi.org/10.1056/NEJMoa2028436

Andries, O., Mc Cafferty, S., De Smedt, S. C., Weiss, R., Sanders, N. N., & Kitada, T. (2015). N1-methylpseudouridine-incorporated mRNA outperforms pseudouridine-incorporated mRNA by providing enhanced protein expression and reduced immunogenicity in mammalian cell lines and mice. *Journal of Controlled Release*, *217*, 337–344. https://doi.org/10.1016/j.jconrel.2015.08.051

Aoki, J. I., Muxel, S. M., Zampieri, R. A., Müller, K. E., Nerland, A. H., & Floeter-Winter, L. M. (2019). Differential immune response modulation in early Leishmania amazonensis infection of BALB/c and C57BL/6 macrophages based on transcriptome profiles. *Scientific Reports*, *9*(1), 19841. https://doi.org/10.1038/s41598-019-56305-1

Araki, N., Johnson, M. T., & Swanson, J. A. (1996). A role for phosphoinositide 3-kinase in the completion of macropinocytosis and phagocytosis by macrophages. *The Journal of Cell Biology*, *135*(5), 1249–1260. https://doi.org/10.1083/jcb.135.5.1249

Arunachalam, P. S., Scott, M. K. D., Hagan, T., Li, C., Feng, Y., Wimmers, F., Grigoryan, L., Trisal, M., Edara, V. V., Lai, L., Chang, S. E., Feng, A., Dhingra, S., Shah, M., Lee, A. S., Chinthrajah, S., Sindher, S. B., Mallajosyula, V., Gao, F., … Pulendran, B. (2021). Systems vaccinology of the BNT162b2 mRNA vaccine in humans. *Nature*, *596*(7872), 410–416. https://doi.org/10.1038/s41586-021-03791-x

Bae, J. H., Jo, S. I., Kim, S. J., Lee, J. M., Jeong, J. H., Kang, J. S., Cho, N.-J., Kim, S. S., Lee, E. Y., & Moon, J.-S. (2019). Circulating Cell-Free mtDNA Contributes to AIM2 Inflammasome-Mediated Chronic Inflammation in Patients with Type 2 Diabetes. *Cells*, *8*(4), 328. https://doi.org/10.3390/cells8040328

Baker, P. J., Boucher, D., Bierschenk, D., Tebartz, C., Whitney, P. G., D'Silva, D. B., Tanzer, M. C., Monteleone, M., Robertson, A. A. B., Cooper, M. A., Alvarez-Diaz, S., Herold, M. J., Bedoui, S., Schroder, K., & Masters, S. L. (2015). NLRP3 inflammasome activation downstream of cytoplasmic LPS recognition by both caspase-4 and caspase-5. *European Journal of Immunology*, *45*(10), 2918–2926. https://doi.org/10.1002/eji.201545655

Barlan, A. U., Griffin, T. M., McGuire, K. A., & Wiethoff, C. M. (2011). Adenovirus membrane penetration activates the NLRP3 inflammasome. *Journal of Virology*, *85*(1), 146–155. https://doi.org/10.1128/JVI.01265-10

Black, R. A., Kronheim, S. R., & Sleath, P. R. (1989). Activation of interleukin- 1β by a co-induced protease. *FEBS Letters*, *247*(2), 386–390. https://doi.org/10.1016/0014-5793(89)81376-6

Broderick, L., De Nardo, D., Franklin, B. S., Hoffman, H. M., & Latz, E. (2015). The inflammasomes and autoinflammatory syndromes. *Annual Review of Pathology: Mechanisms of Disease*, *10*, 395–424. https://doi.org/10.1146/annurev-pathol-012414-040431

Broz, P., & Dixit, V. M. (2016). Inflammasomes: mechanism of assembly, regulation and signalling. *Nature Reviews Immunology*, *16*(7), 407–420. https://doi.org/10.1038/nri.2016.58

Cabral, A., Cabral, J. E., Wang, A., Zhang, Y., Liang, H., Nikbakht, D., Corona, L., Hoffman, H. M., & McNulty, R. (2023). Differential Binding of NLRP3 to non-oxidized and Ox-mtDNA mediates NLRP3 Inflammasome Activation. *Communications Biology*, *6*(1), 578. https://doi.org/10.1038/s42003-023-04817-y

Cai, X., Chen, J., Xu, H., Liu, S., Jiang, Q.-X., Halfmann, R., & Chen, Z. J. (2014). Prion-like Polymerization Underlies Signal Transduction in Antiviral Immune Defense and Inflammasome Activation. *Cell*, *156*(6), 1207–1222. https://doi.org/10.1016/j.cell.2014.01.063

Cardone, M., Dzutsev, A. K., Li, H., Riteau, N., Gerosa, F., Shenderov, K., Winkler-Pickett, R., Provezza, L., Riboldi, E., Leighty, R. M., Orr, S. J., Steinhagen, F., Wewers, M. D., Sher, A., Anderson, S. K., Goldszmid, R., McVicar, D. W., Lyakh, L., & Trinchieri, G.

(2014). Interleukin-1 and Interferon-γ Orchestrate β-Glucan-Activated Human Dendritic Cell Programming via IκB-ζ Modulation. *PLoS ONE*, *9*(12), e114516. https://doi.org/10.1371/journal.pone.0114516

Carpenter, A. E., Jones, T. R., Lamprecht, M. R., Clarke, C., Kang, I., Friman, O., Guertin, D. A., Chang, J., Lindquist, R. A., Moffat, J., Golland, P., & Sabatini, D. M. (2006). CellProfiler: image analysis software for identifying and quantifying cell phenotypes. *Genome Biology*, *7*(10), R100. https://doi.org/10.1186/gb-2006-7-10-r100

Chapin-Bardales, J., Gee, J., & Myers, T. (2021). Reactogenicity Following Receipt of mRNA-Based COVID-19 Vaccines. *JAMA*, *325*(21), 2201. https://doi.org/10.1001/jama.2021.5374

Chen, G., Chelu, M. G., Dobrev, D., & Li, N. (2018). Cardiomyocyte Inflammasome Signaling in Cardiomyopathies and Atrial Fibrillation: Mechanisms and Potential Therapeutic Implications. *Frontiers in Physiology*, *9*. https://doi.org/10.3389/fphys.2018.01115

Chen, G. Y., & Nuñez, G. (2010). Sterile inflammation: sensing and reacting to damage. *Nature Reviews Immunology*, *10*(12), 826–837. https://doi.org/10.1038/nri2873

Chen, J., & Chen, Z. J. (2018). PtdIns4P on dispersed trans-Golgi network mediates NLRP3 inflammasome activation. *Nature*, *564*(7734), 71–76. https://doi.org/10.1038/s41586-018-0761-3

Civril, F., Deimling, T., de Oliveira Mann, C. C., Ablasser, A., Moldt, M., Witte, G., Hornung, V., & Hopfner, K.-P. (2013). Structural mechanism of cytosolic DNA sensing by cGAS. *Nature*, *498*(7454), 332–337. https://doi.org/10.1038/nature12305

Coggins, S. A., Laing, E. D., Olsen, C. H., Goguet, E., Moser, M., Jackson-Thompson, B. M., Samuels, E. C., Pollett, S. D., Tribble, D. R., Davies, J., Illinik, L., Hollis-Perry, M., Maiolatesi, S. E., Duplessis, C. A., Ramsey, K. F., Reyes, A. E., Alcorta, Y., Wong, M. A., Wang, G., … Mitre, E. (2022). Adverse Effects and Antibody Titers in Response to the BNT162b2 mRNA COVID-19 Vaccine in a Prospective Study of Healthcare Workers. *Open Forum Infectious Diseases*, *9*(1). https://doi.org/10.1093/ofid/ofab575

Coll, R. C., & O'Neill, L. A. J. (2011). The Cytokine Release Inhibitory Drug CRID3 Targets ASC Oligomerisation in the NLRP3 and AIM2 Inflammasomes. *PLoS ONE*, *6*(12), e29539. https://doi.org/10.1371/journal.pone.0029539

Cooper, M. D. (2010). 99th Dahlem Conference on Infection, Inflammation and Chronic Inflammatory Disorders: Evolution of adaptive immunity in vertebrates. *Clinical and Experimental Immunology*, *160*(1), 58–61. https://doi.org/10.1111/j.1365-2249.2010.04126.x

Degen, M., Santos, J. C., Pluhackova, K., Cebrero, G., Ramos, S., Jankevicius, G., Hartenian, E., Guillerm, U., Mari, S. A., Kohl, B., Müller, D. J., Schanda, P., Maier, T., Perez, C., Sieben, C., Broz, P., & Hiller, S. (2023). Structural basis of NINJ1-mediated plasma membrane rupture in cell death. *Nature*, *618*(7967), 1065–1071. https://doi.org/10.1038/s41586-023-05991-z

Diamond, C. E., Leong, K. W. K., Vacca, M., Rivers-Auty, J., Brough, D., & Mortellaro, A. (2017). Salmonella typhimurium-induced IL-1 release from primary human monocytes requires NLRP3 and can occur in the absence of pyroptosis. *Scientific Reports*, *7*(1), 6861. https://doi.org/10.1038/s41598-017-07081-3

Diebold, S. S., Kaisho, T., Hemmi, H., Akira, S., & Reis e Sousa, C. (2004). Innate Antiviral Responses by Means of TLR7-Mediated Recognition of Single-Stranded RNA. *Science*, *303*(5663), 1529–1531. https://doi.org/10.1126/science.1093616

Dinarello, C. A., Renfer, L., & Wolff, S. M. (1977). Human leukocytic pyrogen: purification and development of a radioimmunoassay. *Proceedings of the National Academy of Sciences*, *74*(10), 4624–4627. https://doi.org/10.1073/pnas.74.10.4624

Ding, J., Wang, K., Liu, W., She, Y., Sun, Q., Shi, J., Sun, H., Wang, D.-C., & Shao, F. (2016). Pore-forming activity and structural autoinhibition of the gasdermin family. *Nature*, *535*(7610), 111–116. https://doi.org/10.1038/nature18590

Dobin, A., Davis, C. A., Schlesinger, F., Drenkow, J., Zaleski, C., Jha, S., Batut, P., Chaisson, M., & Gingeras, T. R. (2013). STAR: ultrafast universal RNA-seq aligner. *Bioinformatics (Oxford, England)*, *29*(1), 15–21. https://doi.org/10.1093/bioinformatics/bts635

Dokka, S., Malanga, C. J., Shi, X., Chen, F., Castranova, V., & Rojanasakul, Y. (2000). Inhibition of endotoxin-induced lung inflammation by interleukin-10 gene transfer in mice. *American Journal of Physiology-Lung Cellular and Molecular Physiology*, *279*(5), L872–L877. https://doi.org/10.1152/ajplung.2000.279.5.L872

Dos Reis, E. C., Leal, V. N. C., Soares, J. L. da S., Fernandes, F. P., Souza de Lima, D., de Alencar, B. C., & Pontillo, A. (2019). Flagellin/NLRC4 Pathway Rescues NLRP3-Inflammasome Defect in Dendritic Cells From HIV-Infected Patients: Perspective for New Adjuvant in Immunocompromised Individuals. *Frontiers in Immunology*, *10*, 1291. https://doi.org/10.3389/fimmu.2019.01291

Dostert, C., Pétrilli, V., Van Bruggen, R., Steele, C., Mossman, B. T., & Tschopp, J. (2008). Innate Immune Activation Through Nalp3 Inflammasome Sensing of Asbestos and Silica. *Science*, *320*(5876), 674–677. https://doi.org/10.1126/science.1156995

Downs, K. P., Nguyen, H., Dorfleutner, A., & Stehlik, C. (2020). An overview of the non-canonical inflammasome. *Molecular Aspects of Medicine*, *76*, 100924. https://doi.org/10.1016/j.mam.2020.100924

Durinck, S., Moreau, Y., Kasprzyk, A., Davis, S., De Moor, B., Brazma, A., & Huber, W. (2005). BioMart and Bioconductor: a powerful link between biological databases and microarray data analysis. *Bioinformatics*, *21*(16), 3439–3440. https://doi.org/10.1093/bioinformatics/bti525

Durinck, S., Spellman, P. T., Birney, E., & Huber, W. (2009). Mapping identifiers for the integration of genomic datasets with the R/Bioconductor package biomaRt. *Nature Protocols*, *4*(8), 1184–1191. https://doi.org/10.1038/nprot.2009.97

Dutta, D., & Donaldson, J. G. (2012). Search for inhibitors of endocytosis. *Cellular Logistics*, *2*(4), 203–208. https://doi.org/10.4161/cl.23967

Eichholz, K., Bru, T., Tran, T. T. P., Fernandes, P., Welles, H., Mennechet, F. J. D., Manel, N., Alves, P., Perreau, M., & Kremer, E. J. (2016). Immune-Complexed Adenovirus Induce AIM2-Mediated Pyroptosis in Human Dendritic Cells. *PLoS Pathogens*, *12*(9), e1005871. https://doi.org/10.1371/journal.ppat.1005871

Elliott, J. M., Rouge, L., Wiesmann, C., & Scheer, J. M. (2009). Crystal Structure of Procaspase-1 Zymogen Domain Reveals Insight into Inflammatory Caspase Autoactivation. *Journal of Biological Chemistry*, *284*(10), 6546–6553. https://doi.org/10.1074/jbc.M806121200

Fernandes-Alnemri, T., Yu, J.-W., Datta, P., Wu, J., & Alnemri, E. S. (2009). AIM2 activates the inflammasome and cell death in response to cytoplasmic DNA. *Nature*, *458*(7237), 509–513. https://doi.org/10.1038/nature07710

Fine, P., Eames, K., & Heymann, D. L. (2011). "Herd Immunity": A Rough Guide. *Clinical Infectious Diseases*, *52*(7), 911–916. https://doi.org/10.1093/cid/cir007

Folegatti, P. M., Ewer, K. J., Aley, P. K., Angus, B., Becker, S., Belij-Rammerstorfer, S., Bellamy, D., Bibi, S., Bittaye, M., Clutterbuck, E. A., Dold, C., Faust, S. N., Finn, A., Flaxman, A. L., Hallis, B., Heath, P., Jenkin, D., Lazarus, R., Makinson, R., … Yau, Y. (2020). Safety and immunogenicity of the ChAdOx1 nCoV-19 vaccine against SARS-CoV-2: a preliminary report of a phase 1/2, single-blind, randomised controlled trial. *The Lancet*, *396*(10249), 467–478. https://doi.org/10.1016/S0140-6736(20)31604-4

Forster III, J., Nandi, D., & Kulkarni, A. (2022). mRNA-carrying lipid nanoparticles that induce lysosomal rupture activate NLRP3 inflammasome and reduce mRNA transfection efficiency. *Biomaterials Science*, *10*(19), 5566–5582. https://doi.org/10.1039/D2BM00883A

Franchi, L., & Núñez, G. (2008). The Nlrp3 inflammasome is critical for aluminium hydroxide-mediated IL-1beta secretion but dispensable for adjuvant activity. *European Journal of Immunology*, *38*(8), 2085–2089. https://doi.org/10.1002/eji.200838549

Gaidt, M. M., Ebert, T. S., Chauhan, D., Ramshorn, K., Pinci, F., Zuber, S., O'Duill, F., Schmid-Burgk, J. L., Hoss, F., Buhmann, R., Wittmann, G., Latz, E., Subklewe, M., & Hornung, V. (2017). The DNA Inflammasome in Human Myeloid Cells Is Initiated by a STING-Cell Death Program Upstream of NLRP3. *Cell*, *171*(5), 1110-1124.e18. https://doi.org/10.1016/j.cell.2017.09.039

Gaidt, M. M., Ebert, T. S., Chauhan, D., Schmidt, T., Schmid-Burgk, J. L., Rapino, F., Robertson, A. A. B., Cooper, M. A., Graf, T., & Hornung, V. (2016). Human Monocytes Engage an Alternative Inflammasome Pathway. *Immunity*, *44*(4), 833–846. https://doi.org/10.1016/j.immuni.2016.01.012

Garg, A. D., Leggatt, G. R., Land, W. G., Bianchi, M. E., Vénéreau, E., & Ceriotti, C. (2015). DAMPs from cell death to new life. *Article*, *6*, 1. https://doi.org/10.3389/fimmu.2015.00422

Garlanda, C., Dinarello, C. A., & Mantovani, A. (2013). The Interleukin-1 Family: Back to the Future. *Immunity*, *39*(6), 1003–1018. https://doi.org/10.1016/j.immuni.2013.11.010

Gery, I., Gershon, R. K., & Waksman, B. H. (1972). Potentiation of the T-lymphocyte response to mitogens. I. The responding cell. *The Journal of Experimental Medicine*, *136*(1), 128–142. https://doi.org/10.1084/jem.136.1.128

Gery, I., & Waksman, B. H. (1972). Potentiation of the T-lymphocyte response to mitogens. II. The cellular source of potentiating mediator(s). *The Journal of Experimental Medicine*, *136*(1), 143–155. https://doi.org/10.1084/jem.136.1.143

Gewirtz, A. T., Navas, T. A., Lyons, S., Godowski, P. J., & Madara, J. L. (2001). Cutting Edge: Bacterial Flagellin Activates Basolaterally Expressed TLR5 to Induce Epithelial Proinflammatory Gene Expression. *The Journal of Immunology*, *167*(4), 1882–1885. https://doi.org/10.4049/jimmunol.167.4.1882

Ghayur, T., Banerjee, S., Hugunin, M., Butler, D., Herzog, L., Carter, A., Quintal, L., Sekut, L., Talanian, R., Paskind, M., Wong, W., Kamen, R., Tracey, D., & Alien, H. (1997). Caspase-1 processes IFN-γ-inducing factor and regulates LPS-induced IFN- γ production. *Nature*, *386*(6625), 619–623. https://doi.org/10.1038/386619a0

Girardin, S. E., Boneca, I. G., Carneiro, L. A. M., Antignac, A., Jéhanno, M., Viala, J., Tedin, K., Taha, M.-K., Labigne, A., Zäthringer, U., Coyle, A. J., DiStefano, P. S., Bertin, J., Sansonetti, P. J., & Philpott, D. J. (2003). Nod1 Detects a Unique Muropeptide from Gram-Negative Bacterial Peptidoglycan. *Science*, *300*(5625), 1584–1587. https://doi.org/10.1126/science.1084677

Girardin, S. E., Boneca, I. G., Viala, J., Chamaillard, M., Labigne, A., Thomas, G., Philpott, D. J., & Sansonetti, P. J. (2003). Nod2 Is a General Sensor of Peptidoglycan through Muramyl Dipeptide (MDP) Detection. *Journal of Biological Chemistry*, *278*(11), 8869–8872. https://doi.org/10.1074/jbc.C200651200

Gong, Z., Pan, J., Shen, Q., Li, M., & Peng, Y. (2018). Mitochondrial dysfunction induces NLRP3 inflammasome activation during cerebral ischemia/reperfusion injury. *Journal of Neuroinflammation*, *15*(1), 242. https://doi.org/10.1186/s12974-018-1282-6

Guicciardi, M. E., & Gores, G. J. (2013). Complete lysosomal disruption: A route to necrosis, not to the inflammasome. *Cell Cycle*, *12*(13), 1995–1995. https://doi.org/10.4161/cc.25317

Halle, A., Hornung, V., Petzold, G. C., Stewart, C. R., Monks, B. G., Reinheckel, T., Fitzgerald, K. A., Latz, E., Moore, K. J., & Golenbock, D. T. (2008). The NALP3 inflammasome is involved in the innate immune response to amyloid-β. *Nature Immunology*, *9*(8), 857–865. https://doi.org/10.1038/ni.1636

Harrison, P. F., Pattison, A. D., Powell, D. R., & Beilharz, T. H. (2019). Topconfects: a package for confident effect sizes in differential expression analysis provides a more biologically useful ranked gene list. *Genome Biology*, *20*(1), 67. https://doi.org/10.1186/s13059-019-1674-7

Hawwari, I., Rossnagel, L., Rosero, N., Maasewerd, S., Vasconcelos, M. B., Jentzsch, M., Demczuk, A., Teichmann, L. L., Meffert, L., Bertheloot, D., Ribeiro, L. S., Kallabis, S., Meissner, F., Arditi, M., Atici, A. E., Noval Rivas, M., & Franklin, B. S. (2024). Platelet transcription factors license the pro-inflammatory cytokine response of human monocytes. *EMBO Molecular Medicine*, *16*(8), 1901–1929. https://doi.org/10.1038/s44321-024-00093-3

Hayashi, F., Smith, K. D., Ozinsky, A., Hawn, T. R., Yi, E. C., Goodlett, D. R., Eng, J. K., Akira, S., Underhill, D. M., & Aderem, A. (2001). The innate immune response to bacterial flagellin is mediated by Toll-like receptor 5. *Nature*, *410*(6832), 1099–1103. https://doi.org/10.1038/35074106

He, W., Wan, H., Hu, L., Chen, P., Wang, X., Huang, Z., Yang, Z.-H., Zhong, C.-Q., & Han, J. (2015). Gasdermin D is an executor of pyroptosis and required for interleukin-1β secretion. *Cell Research*, *25*(12), 1285–1298. https://doi.org/10.1038/cr.2015.139

He, Y., Zeng, M. Y., Yang, D., Motro, B., & Núñez, G. (2016). NEK7 is an essential mediator of NLRP3 activation downstream of potassium efflux. *Nature*, *530*(7590), 354–357. https://doi.org/10.1038/nature16959

Heid, M. E., Keyel, P. A., Kamga, C., Shiva, S., Watkins, S. C., & Salter, R. D. (2013). Mitochondrial Reactive Oxygen Species Induces NLRP3-Dependent Lysosomal

Damage and Inflammasome Activation. *The Journal of Immunology*, *191*(10), 5230–5238. https://doi.org/10.4049/jimmunol.1301490

Heil, F., Hemmi, H., Hochrein, H., Ampenberger, F., Kirschning, C., Akira, S., Lipford, G., Wagner, H., & Bauer, S. (2004). Species-Specific Recognition of Single-Stranded RNA via Toll-like Receptor 7 and 8. *Science*, *303*(5663), 1526–1529. https://doi.org/10.1126/science.1093620

Held, J., Esse, J., Tascilar, K., Steininger, P., Schober, K., Irrgang, P., Alsalameh, R., Tenbusch, M., Seggewies, C., & Bogdan, C. (2021). Reactogenicity Correlates Only Weakly with Humoral Immunogenicity after COVID-19 Vaccination with BNT162b2 mRNA (Comirnaty®). *Vaccines*, *9*(10), 1063. https://doi.org/10.3390/vaccines9101063

Hemmi, H., Takeuchi, O., Kawai, T., Kaisho, T., Sato, S., Sanjo, H., Matsumoto, M., Hoshino, K., Wagner, H., Takeda, K., & Akira, S. (2000). A Toll-like receptor recognizes bacterial DNA. *Nature*, *408*(6813), 740–745. https://doi.org/10.1038/35047123

Holm, C. K., Jensen, S. B., Jakobsen, M. R., Cheshenko, N., Horan, K. A., Moeller, H. B., Gonzalez-Dosal, R., Rasmussen, S. B., Christensen, M. H., Yarovinsky, T. O., Rixon, F. J., Herold, B. C., Fitzgerald, K. A., & Paludan, S. R. (2012). Virus-cell fusion as a trigger of innate immunity dependent on the adaptor STING. *Nature Immunology*, *13*(8), 737–743. https://doi.org/10.1038/ni.2350

Honda, K., & Taniguchi, T. (2006). IRFs: master regulators of signalling by Toll-like receptors and cytosolic pattern-recognition receptors. *Nature Reviews Immunology*, *6*(9), 644–658. https://doi.org/10.1038/nri1900

Hornung, V., Ablasser, A., Charrel-Dennis, M., Bauernfeind, F., Horvath, G., Caffrey, Daniel. R., Latz, E., & Fitzgerald, K. A. (2009). AIM2 recognizes cytosolic dsDNA and forms a caspase-1-activating inflammasome with ASC. *Nature*, *458*(7237), 514–518. https://doi.org/10.1038/nature07725

Hornung, V., Bauernfeind, F., Halle, A., Samstad, E. O., Kono, H., Rock, K. L., Fitzgerald, K. A., & Latz, E. (2008). Silica crystals and aluminum salts activate the NALP3 inflammasome through phagosomal destabilization. *Nature Immunology*, *9*(8), 847–856. https://doi.org/10.1038/ni.1631

Hornung, V., & Latz, E. (2010). Critical functions of priming and lysosomal damage for NLRP3 activation. *European Journal of Immunology*, *40*(3), 620–623. https://doi.org/10.1002/eji.200940185

Hou, X., Zaks, T., Langer, R., & Dong, Y. (2021). Lipid nanoparticles for mRNA delivery. *Nature Reviews Materials*, *6*(12), 1078–1094. https://doi.org/10.1038/s41578-021-00358-0

Hou, Y., Chen, M., Bian, Y., Hu, Y., Chuan, J., Zhong, L., Zhu, Y., & Tong, R. (2024). Insights into vaccines for elderly individuals: from the impacts of immunosenescence to delivery strategies. *Npj Vaccines*, *9*(1), 77. https://doi.org/10.1038/s41541-024-00874-4

Jackson, L. A., Anderson, E. J., Rouphael, N. G., Roberts, P. C., Makhene, M., Coler, R. N., McCullough, M. P., Chappell, J. D., Denison, M. R., Stevens, L. J., Pruijssers, A. J., McDermott, A., Flach, B., Doria-Rose, N. A., Corbett, K. S., Morabito, K. M., O'Dell, S., Schmidt, S. D., Swanson, P. A., … Beigel, J. H. (2020). An mRNA Vaccine against SARS-CoV-2 — Preliminary Report. *New England Journal of Medicine*, *383*(20), 1920–1931. https://doi.org/10.1056/NEJMoa2022483

Jakic, B., Kimpel, J., Olson, W., Labi, V., & Hermann-Kleiter, N. (2021). Bacterial Infection with Listeria monocytogenes in Mice and Subsequent Analysis of AntigenSpecific CD8 T Cell Responses. *BIO-PROTOCOL*, *11*(23). https://doi.org/10.21769/BioProtoc.4247

Janeway, C. A. (1989). Approaching the Asymptote? Evolution and Revolution in Immunology. *Cold Spring Harbor Symposia on Quantitative Biology*, *54*(0), 1–13. https://doi.org/10.1101/SQB.1989.054.01.003

Janeway, C. A., & Medzhitov, R. (2002). Innate Immune Recognition. *Annual Review of Immunology*, *20*(1), 197–216. https://doi.org/10.1146/annurev.immunol.20.083001.084359

Janeway CA Jr, T. P. W. M. et al. (2001). *Immunobiology: The Immune System in Health and Disease. 5th edition.* Garland Pub.

Jiang, M., Väisänen, E., Kolehmainen, P., Huttunen, M., Ylä-Herttuala, S., Meri, S., Österlund, P., & Julkunen, I. (2023). COVID-19 adenovirus vector vaccine induces higher interferon and pro-inflammatory responses than mRNA vaccines in human

PBMCs, macrophages and moDCs. *Vaccine*, *41*(26), 3813–3823. https://doi.org/10.1016/j.vaccine.2023.04.049

Jorda, A., Bergmann, F., Ristl, R., Radner, H., Sieghart, D., Aletaha, D., & Zeitlinger, M. (2023). Association between reactogenicity and immunogenicity after BNT162b2 booster vaccination: a secondary analysis of a prospective cohort study. *Clinical Microbiology and Infection*, *29*(9), 1188–1195. https://doi.org/10.1016/j.cmi.2023.05.028

Ju, Y., Lee, W. S., Pilkington, E. H., Kelly, H. G., Li, S., Selva, K. J., Wragg, K. M., Subbarao, K., Nguyen, T. H. O., Rowntree, L. C., Allen, L. F., Bond, K., Williamson, D. A., Truong, N. P., Plebanski, M., Kedzierska, K., Mahanty, S., Chung, A. W., Caruso, F., … Kent, S. J. (2022). Anti-PEG Antibodies Boosted in Humans by SARS-CoV-2 Lipid Nanoparticle mRNA Vaccine. *ACS Nano*, *16*(8), 11769–11780. https://doi.org/10.1021/acsnano.2c04543

Kamentsky, L., Jones, T. R., Fraser, A., Bray, M.-A., Logan, D. J., Madden, K. L., Ljosa, V., Rueden, C., Eliceiri, K. W., & Carpenter, A. E. (2011). Improved structure, function and compatibility for CellProfiler: modular high-throughput image analysis software. *Bioinformatics*, *27*(8), 1179–1180. https://doi.org/10.1093/bioinformatics/btr095

Kanneganti, T.-D., Özören, N., Body-Malapel, M., Amer, A., Park, J.-H., Franchi, L., Whitfield, J., Barchet, W., Colonna, M., Vandenabeele, P., Bertin, J., Coyle, A., Grant, E. P., Akira, S., & Núñez, G. (2006). Bacterial RNA and small antiviral compounds activate caspase-1 through cryopyrin/Nalp3. *Nature*, *440*(7081), 233–236. https://doi.org/10.1038/nature04517

Kato, H., Takeuchi, O., Sato, S., Yoneyama, M., Yamamoto, M., Matsui, K., Uematsu, S., Jung, A., Kawai, T., Ishii, K. J., Yamaguchi, O., Otsu, K., Tsujimura, T., Koh, C.-S., Reis e Sousa, C., Matsuura, Y., Fujita, T., & Akira, S. (2006). Differential roles of MDA5 and RIG-I helicases in the recognition of RNA viruses. *Nature*, *441*(7089), 101–105. https://doi.org/10.1038/nature04734

Kayagaki, N., Kornfeld, O. S., Lee, B. L., Stowe, I. B., O'Rourke, K., Li, Q., Sandoval, W., Yan, D., Kang, J., Xu, M., Zhang, J., Lee, W. P., McKenzie, B. S., Ulas, G., Payandeh, J., Roose-Girma, M., Modrusan, Z., Reja, R., Sagolla, M., … Dixit, V. M. (2021). NINJ1

mediates plasma membrane rupture during lytic cell death. *Nature*, *591*(7848), 131–136. https://doi.org/10.1038/s41586-021-03218-7

Kayagaki, N., Stowe, I. B., Lee, B. L., O'Rourke, K., Anderson, K., Warming, S., Cuellar, T., Haley, B., Roose-Girma, M., Phung, Q. T., Liu, P. S., Lill, J. R., Li, H., Wu, J., Kummerfeld, S., Zhang, J., Lee, W. P., Snipas, S. J., Salvesen, G. S., … Dixit, V. M. (2015). Caspase-11 cleaves gasdermin D for non-canonical inflammasome signalling. *Nature*, *526*(7575), 666–671. https://doi.org/10.1038/nature15541

Keech, C., Albert, G., Cho, I., Robertson, A., Reed, P., Neal, S., Plested, J. S., Zhu, M., Cloney-Clark, S., Zhou, H., Smith, G., Patel, N., Frieman, M. B., Haupt, R. E., Logue, J., McGrath, M., Weston, S., Piedra, P. A., Desai, C., … Glenn, G. M. (2020). Phase 1–2 Trial of a SARS-CoV-2 Recombinant Spike Protein Nanoparticle Vaccine. *New England Journal of Medicine*, *383*(24), 2320–2332. https://doi.org/10.1056/NEJMoa2026920

Kirschning, C. J., & Schumann, R. R. (2002). *TLR2: Cellular Sensor for Microbial and Endogenous Molecular Patterns* (pp. 121–144). https://doi.org/10.1007/978-3-642-59430-4_8

Kostura, M. J., Tocci, M. J., Limjuco, G., Chin, J., Cameron, P., Hillman, A. G., Chartrain, N. A., & Schmidt, J. A. (1989). Identification of a monocyte specific pre-interleukin 1 beta convertase activity. *Proceedings of the National Academy of Sciences*, *86*(14), 5227–5231. https://doi.org/10.1073/pnas.86.14.5227

Kumari, P., Russo, A. J., Shivcharan, S., & Rathinam, V. A. (2020). AIM2 in health and disease: Inflammasome and beyond. *Immunological Reviews*, *297*(1), 83–95. https://doi.org/10.1111/imr.12903

Kyriakidis, N. C., López-Cortés, A., González, E. V., Grimaldos, A. B., & Prado, E. O. (2021). SARS-CoV-2 vaccines strategies: a comprehensive review of phase 3 candidates. *Npj Vaccines*, *6*(1), 28. https://doi.org/10.1038/s41541-021-00292-w

Law, C. W., Chen, Y., Shi, W., & Smyth, G. K. (2014). voom: precision weights unlock linear model analysis tools for RNA-seq read counts. *Genome Biology*, *15*(2), R29. https://doi.org/10.1186/gb-2014-15-2-r29

Lee, Y., Jeong, M., Park, J., Jung, H., & Lee, H. (2023). Immunogenicity of lipid nanoparticles and its impact on the efficacy of mRNA vaccines and therapeutics. *Experimental & Molecular Medicine*, *55*(10), 2085–2096. https://doi.org/10.1038/s12276-023-01086-x

Lee, Y., Ng, M., Daniel, K., & Wayne, E. (2021). Rapid growth in the COVID-19 era. *MRS Bulletin*, *46*(9), 847–853. https://doi.org/10.1557/s43577-021-00185-2

Li, C., Lee, A., Grigoryan, L., Arunachalam, P. S., Scott, M. K. D., Trisal, M., Wimmers, F., Sanyal, M., Weidenbacher, P. A., Feng, Y., Adamska, J. Z., Valore, E., Wang, Y., Verma, R., Reis, N., Dunham, D., O'Hara, R., Park, H., Luo, W., … Pulendran, B. (2022). Mechanisms of innate and adaptive immunity to the Pfizer-BioNTech BNT162b2 vaccine. *Nature Immunology*, *23*(4), 543–555. https://doi.org/10.1038/s41590-022-01163-9

Li, H., Willingham, S. B., Ting, J. P.-Y., & Re, F. (2008). Cutting Edge: Inflammasome Activation by Alum and Alum's Adjuvant Effect Are Mediated by NLRP3. *The Journal of Immunology*, *181*(1), 17–21. https://doi.org/10.4049/jimmunol.181.1.17

Liang, F., Lindgren, G., Lin, A., Thompson, E. A., Ols, S., Röhss, J., John, S., Hassett, K., Yuzhakov, O., Bahl, K., Brito, L. A., Salter, H., Ciaramella, G., & Loré, K. (2017). Efficient Targeting and Activation of Antigen-Presenting Cells In Vivo after Modified mRNA Vaccine Administration in Rhesus Macaques. *Molecular Therapy*, *25*(12), 2635–2647. https://doi.org/10.1016/j.ymthe.2017.08.006

Lim, S. Y., Kim, J. Y., Park, S., Kwon, J.-S., Park, J. Y., Cha, H. H., Suh, M. H., Lee, H. J., Lim, J. S., Bae, S., Jung, J., Lee, N., Kim, K., Shum, D., Jee, Y., & Kim, S.-H. (2021). Correlation between Reactogenicity and Immunogenicity after the ChAdOx1 nCoV-19 and BNT162b2 mRNA Vaccination. *Immune Network*, *21*(6). https://doi.org/10.4110/in.2021.21.e41

Lin, R., & Porto, B. N. (2025). Pyroptosis in Respiratory Virus Infections: A Narrative Review of Mechanisms, Pathophysiology, and Potential Therapeutic Interventions. *Microorganisms*, *13*(9), 2109. https://doi.org/10.3390/microorganisms13092109

Liston, A., & Masters, S. L. (2017). Homeostasis-altering molecular processes as mechanisms of inflammasome activation. In *Nature Reviews Immunology* (Vol. 17, Issue 3, pp. 208–214). Nature Publishing Group. https://doi.org/10.1038/nri.2016.151

Lonez, C., Bessodes, M., Scherman, D., Vandenbranden, M., Escriou, V., & Ruysschaert, J.-M. (2014). Cationic lipid nanocarriers activate Toll-like receptor 2 and NLRP3 inflammasome pathways. *Nanomedicine: Nanotechnology, Biology and Medicine*, *10*(4), 775–782. https://doi.org/10.1016/j.nano.2013.12.003

Lu, A., Magupalli, V. G., Ruan, J., Yin, Q., Atianand, M. K., Vos, M. R., Schröder, G. F., Fitzgerald, K. A., Wu, H., & Egelman, E. H. (2014). Unified Polymerization Mechanism for the Assembly of ASC-Dependent Inflammasomes. *Cell*, *156*(6), 1193–1206. https://doi.org/10.1016/j.cell.2014.02.008

Luheshi, N. M., Giles, J. A., Lopez-Castejon, G., & Brough, D. (2012). Sphingosine regulates the NLRP3-inflammasome and IL-1 β release from macrophages. *European Journal of Immunology*, *42*(3), 716–725. https://doi.org/10.1002/eji.201142079

Macia, E., Ehrlich, M., Massol, R., Boucrot, E., Brunner, C., & Kirchhausen, T. (2006). Dynasore, a Cell-Permeable Inhibitor of Dynamin. *Developmental Cell*, *10*(6), 839–850. https://doi.org/10.1016/j.devcel.2006.04.002

Mangan, M. S. J., Olhava, E. J., Roush, W. R., Seidel, H. M., Glick, G. D., & Latz, E. (2018). Targeting the NLRP3 inflammasome in inflammatory diseases. In *Nature Reviews Drug Discovery* (Vol. 17, Issue 8, pp. 588–606). Nature Publishing Group. https://doi.org/10.1038/nrd.2018.97

Mantovani, A., & Netea, M. G. (2020). Trained Innate Immunity, Epigenetics, and Covid-19. *New England Journal of Medicine*, *383*(11), 1078–1080. https://doi.org/10.1056/NEJMcibr2011679

Marshall, J. S., Warrington, R., Watson, W., & Kim, H. L. (2018). An introduction to immunology and immunopathology. *Allergy, Asthma & Clinical Immunology*, *14*(S2), 49. https://doi.org/10.1186/s13223-018-0278-1

Martinon, F. (2010). Signaling by ROS drives inflammasome activation. *European Journal of Immunology*, *40*(3), 616–619. https://doi.org/10.1002/eji.200940168

Martinon, F., Burns, K., & Tschopp, J. (2002). The Inflammasome: A Molecular Platform Triggering Activation of Inflammatory Caspases and Processing of proIL-beta. *Molecular Cell*, *10*(2), 417–426. https://doi.org/10.1016/S1097-2765(02)00599-3

McCarthy, D. J., & Smyth, G. K. (2009). Testing significance relative to a fold-change threshold is a TREAT. *Bioinformatics*, *25*(6), 765–771. https://doi.org/10.1093/bioinformatics/btp053

McQuin, C., Goodman, A., Chernyshev, V., Kamentsky, L., Cimini, B. A., Karhohs, K. W., Doan, M., Ding, L., Rafelski, S. M., Thirstrup, D., Wiegraebe, W., Singh, S., Becker, T., Caicedo, J. C., & Carpenter, A. E. (2018). CellProfiler 3.0: Next-generation image processing for biology. *PLOS Biology*, *16*(7), e2005970. https://doi.org/10.1371/journal.pbio.2005970

Medzhitov, R. (2008). Origin and physiological roles of inflammation. *Nature*, *454*(7203), 428–435. https://doi.org/10.1038/nature07201

Miao, E. A., Alpuche-Aranda, C. M., Dors, M., Clark, A. E., Bader, M. W., Miller, S. I., & Aderem, A. (2006). Cytoplasmic flagellin activates caspase-1 and secretion of interleukin 1β via Ipaf. *Nature Immunology*, *7*(6), 569–575. https://doi.org/10.1038/ni1344

Ming, S., Thirumala, M., Kanneganti, D., Man, S. M., & Kanneganti, T.-D. (2015). *Regulation of inflammasome activation*.

Mishra, S. R., Mahapatra, K. K., Behera, B. P., Patra, S., Bhol, C. S., Panigrahi, D. P., Praharaj, P. P., Singh, A., Patil, S., Dhiman, R., & Bhutia, S. K. (2021). Mitochondrial dysfunction as a driver of NLRP3 inflammasome activation and its modulation through mitophagy for potential therapeutics. *The International Journal of Biochemistry & Cell Biology*, *136*, 106013. https://doi.org/10.1016/j.biocel.2021.106013

Mizel, S. B., & Ben-Zvi, A. (1980). Studies on the role of lymphocyte-activating factor (Interleukin 1) in antigen-induced lymph node lymphocyte proliferation. *Cellular Immunology*, *54*(2), 382–389. https://doi.org/10.1016/0008-8749(80)90218-X

Montaser, M., Lalmanach, G., & Mach, L. (2002). CA-074, But Not Its Methyl Ester CA-074Me, Is a Selective Inhibitor of Cathepsin B within Living Cells. *Biological Chemistry*, *383*(7–8). https://doi.org/10.1515/BC.2002.147

Mudge, J. M., Carbonell-Sala, S., Diekhans, M., Martinez, J. G., Hunt, T., Jungreis, I., Loveland, J. E., Arnan, C., Barnes, I., Bennett, R., Berry, A., Bignell, A., Cerdán-Vélez, D., Cochran, K., Cortés, L. T., Davidson, C., Donaldson, S., Dursun, C., Fatima, R., …

Frankish, A. (2025). GENCODE 2025: reference gene annotation for human and mouse. *Nucleic Acids Research*, *53*(D1), D966–D975. https://doi.org/10.1093/nar/gkae1078

Muñoz-Planillo, R., Kuffa, P., Martínez-Colón, G., Smith, B. L., Rajendiran, T. M., & Núñez, G. (2013). K+ Efflux Is the Common Trigger of NLRP3 Inflammasome Activation by Bacterial Toxins and Particulate Matter. *Immunity*, *38*(6), 1142–1153. https://doi.org/10.1016/j.immuni.2013.05.016

Ndeupen, S., Qin, Z., Jacobsen, S., Bouteau, A., Estanbouli, H., & Igyártó, B. Z. (2021). The mRNA-LNP platform's lipid nanoparticle component used in preclinical vaccine studies is highly inflammatory. *IScience*, *24*(12), 103479. https://doi.org/10.1016/j.isci.2021.103479

Obrig, T. G., Culp, W. J., McKeehan, W. L., & Hardesty, B. (1971). The mechanism by which cycloheximide and related glutarimide antibiotics inhibit peptide synthesis on reticulocyte ribosomes. *The Journal of Biological Chemistry*, *246*(1), 174–181.

Oh, P., Horner, T., Witkiewicz, H., & Schnitzer, J. E. (2012). Endothelin Induces Rapid, Dynamin-mediated Budding of Endothelial Caveolae Rich in ET-B. *Journal of Biological Chemistry*, *287*(21), 17353–17362. https://doi.org/10.1074/jbc.M111.338897

O'Hagan, D. T., & Fox, C. B. (2015). New generation adjuvants – From empiricism to rational design. *Vaccine*, *33*, B14–B20. https://doi.org/10.1016/j.vaccine.2015.01.088

Orlowski, G. M., Colbert, J. D., Sharma, S., Bogyo, M., Robertson, S. A., & Rock, K. L. (2015). Multiple Cathepsins Promote Pro–IL-1β Synthesis and NLRP3-Mediated IL-1β Activation. *The Journal of Immunology*, *195*(4), 1685–1697. https://doi.org/10.4049/jimmunol.1500509

Paknahad, M. H., Yancheshmeh, F. B., & Soleimani, A. (2023). Cardiovascular complications of COVID-19 vaccines: A review of case-report and case-series studies. *Heart & Lung*, *59*, 173–180. https://doi.org/10.1016/j.hrtlng.2023.02.003

Pétrilli, V., Papin, S., Dostert, C., Mayor, A., Martinon, F., & Tschopp, J. (2007). Activation of the NALP3 inflammasome is triggered by low intracellular potassium concentration. *Cell Death & Differentiation*, *14*(9), 1583–1589. https://doi.org/10.1038/sj.cdd.4402195

Pierre, V., Draica, F., Di Fusco, M., Yang, J., Nunez-Gonzalez, S., Kamar, J., Lopez, S., Moran, M. M., Nguyen, J., Alvarez, P., Cha-Silva, A., Gavaghan, M., Yehoshua, A.,

Stapleton, N., & Burnett, H. (2023). The impact of vaccination and outpatient treatment on the economic burden of Covid-19 in the United States omicron era: a systematic literature review. *Journal of Medical Economics*, *26*(1), 1519–1531. https://doi.org/10.1080/13696998.2023.2281882

Plotkin, S. (2014). History of vaccination. *Proceedings of the National Academy of Sciences*, *111*(34), 12283–12287. https://doi.org/10.1073/pnas.1400472111

Polack, F. P., Thomas, S. J., Kitchin, N., Absalon, J., Gurtman, A., Lockhart, S., Perez, J. L., Pérez Marc, G., Moreira, E. D., Zerbini, C., Bailey, R., Swanson, K. A., Roychoudhury, S., Koury, K., Li, P., Kalina, W. V., Cooper, D., Frenck, R. W., Hammitt, L. L., … Gruber, W. C. (2020). Safety and Efficacy of the BNT162b2 mRNA Covid-19 Vaccine. *New England Journal of Medicine*, *383*(27), 2603–2615. https://doi.org/10.1056/NEJMoa2034577

Poltorak, A., He, X., Smirnova, I., Liu, M.-Y., Huffel, C. Van, Du, X., Birdwell, D., Alejos, E., Silva, M., Galanos, C., Freudenberg, M., Ricciardi-Castagnoli, P., Layton, B., & Beutler, B. (1998). Defective LPS Signaling in C3H/HeJ and C57BL/10ScCr Mice: Mutations in *Tlr4* Gene. *Science*, *282*(5396), 2085–2088. https://doi.org/10.1126/science.282.5396.2085

Próchnicki, T., Vasconcelos, M. B., Robinson, K. S., Mangan, M. S. J., De Graaf, D., Shkarina, K., Lovotti, M., Standke, L., Kaiser, R., Stahl, R., Duthie, F. G., Rothe, M., Antonova, K., Jenster, L.-M., Lau, Z. H., Rösing, S., Mirza, N., Gottschild, C., Wachten, D., … Latz, E. (2023). Mitochondrial damage activates the NLRP10 inflammasome. *Nature Immunology*, *24*(4), 595–603. https://doi.org/10.1038/s41590-023-01451-y

Provine, N. M., Amini, A., Garner, L. C., Spencer, A. J., Dold, C., Hutchings, C., Silva Reyes, L., FitzPatrick, M. E. B., Chinnakannan, S., Oguti, B., Raymond, M., Ulaszewska, M., Troise, F., Sharpe, H., Morgan, S. B., Hinks, T. S. C., Lambe, T., Capone, S., Folgori, A., … Klenerman, P. (2021). MAIT cell activation augments adenovirus vector vaccine immunogenicity. *Science*, *371*(6528), 521–526. https://doi.org/10.1126/science.aax8819

Pulendran, B., S. Arunachalam, P., & O'Hagan, D. T. (2021). Emerging concepts in the science of vaccine adjuvants. *Nature Reviews Drug Discovery*, *20*(6), 454–475. https://doi.org/10.1038/s41573-021-00163-y

Qureshi, S. T., Larivière, L., Leveque, G., Clermont, S., Moore, K. J., Gros, P., & Malo, D. (1999). Endotoxin-tolerant Mice Have Mutations in Toll-like Receptor 4 (*Tlr4*). *The Journal of Experimental Medicine*, *189*(4), 615–625. https://doi.org/10.1084/jem.189.4.615

Rahman, T., Nagar, A., Duffy, E. B., Okuda, K., Silverman, N., & Harton, J. A. (2020). NLRP3 Sensing of Diverse Inflammatory Stimuli Requires Distinct Structural Features. *Frontiers in Immunology*, *11*. https://doi.org/10.3389/fimmu.2020.01828

Reed, S. G., Orr, M. T., & Fox, C. B. (2013). Key roles of adjuvants in modern vaccines. *Nature Medicine*, *19*(12), 1597–1608. https://doi.org/10.1038/nm.3409

Rehwinkel, J., & Gack, M. U. (2020). RIG-I-like receptors: their regulation and roles in RNA sensing. *Nature Reviews Immunology*, *20*(9), 537–551. https://doi.org/10.1038/s41577-020-0288-3

Richards, N., Schaner, P., Diaz, A., Stuckey, J., Shelden, E., Wadhwa, A., & Gumucio, D. L. (2001). Interaction between Pyrin and the Apoptotic Speck Protein (ASC) Modulates ASC-induced Apoptosis. *Journal of Biological Chemistry*, *276*(42), 39320–39329. https://doi.org/10.1074/jbc.M104730200

Ritchie, M. E., Phipson, B., Wu, D., Hu, Y., Law, C. W., Shi, W., & Smyth, G. K. (2015). limma powers differential expression analyses for RNA-sequencing and microarray studies. *Nucleic Acids Research*, *43*(7), e47–e47. https://doi.org/10.1093/nar/gkv007

Rizzo, G. P., Sanches, R. C., Chavero, C., Bianchi, D. S., Apuzzo, E., Herrera, S. E., Agazzi, M. L., Cortez, M. L., Marmisollé, W. A., Keitelman, I. A., Trevani, A. S., Oliveira, S. C., Azzaroni, O., Smaldini, P. L., & Docena, G. H. (2024). *Poly(allylamine)/tripolyphosphate nanocomplex coacervate as a NLRP3-dependent systemic adjuvant for vaccine development*. https://doi.org/10.1101/2024.07.01.601578

Robinson, M. D., McCarthy, D. J., & Smyth, G. K. (2010). edgeR: a Bioconductor package for differential expression analysis of digital gene expression data. *Bioinformatics*, *26*(1), 139–140. https://doi.org/10.1093/bioinformatics/btp616

Robinson, M. D., & Oshlack, A. (2010). A scaling normalization method for differential expression analysis of RNA-seq data. *Genome Biology*, *11*(3), R25. https://doi.org/10.1186/gb-2010-11-3-r25

Rodrigues, C. M. C., & Plotkin, S. A. (2020). Impact of Vaccines; Health, Economic and Social Perspectives. *Frontiers in Microbiology*, *11*. https://doi.org/10.3389/fmicb.2020.01526

Rodríguez-Alcázar, J. F., Ataide, M. A., Engels, G., Schmitt-Mabmunyo, C., Garbi, N., Kastenmüller, W., Latz, E., & Franklin, B. S. (2019). Charcot–Leyden Crystals Activate the NLRP3 Inflammasome and Cause IL-1β Inflammation in Human Macrophages. *The Journal of Immunology*, *202*(2), 550–558. https://doi.org/10.4049/jimmunol.1800107

Rosenblum, H. G., Gee, J., Liu, R., Marquez, P. L., Zhang, B., Strid, P., Abara, W. E., McNeil, M. M., Myers, T. R., Hause, A. M., Su, J. R., Markowitz, L. E., Shimabukuro, T. T., & Shay, D. K. (2022). Safety of mRNA vaccines administered during the initial 6 months of the US COVID-19 vaccination programme: an observational study of reports to the Vaccine Adverse Event Reporting System and v-safe. *The Lancet Infectious Diseases*, *22*(6), 802–812. https://doi.org/10.1016/S1473-3099(22)00054-8

Rühl, S., & Broz, P. (2015). Caspase-11 activates a canonical NLRP3 inflammasome by promoting K (+) efflux. *European Journal of Immunology*, *45*(10), 2927–2936. https://doi.org/10.1002/eji.201545772

Sáez-Peñataro, J., Calvo, G., Bascuas, J., Mosquera, M., Marcos, M., Egri, N., & Torres, F. (2024). Association between Reactogenicity and Immunogenicity in a Vaccinated Cohort with Two mRNA SARS-CoV-2 Vaccines at a High-Complexity Reference Hospital: A Post Hoc Analysis on Immunology Aspects of a Prospective Cohort Study. *Vaccines*, *12*(6), 665. https://doi.org/10.3390/vaccines12060665

Schaer, C. A., Laczko, E., Schoedon, G., Schaer, D. J., & Vallelian, F. (2013). Chloroquine Interference with Hemoglobin Endocytic Trafficking Suppresses Adaptive Heme and Iron Homeostasis in Macrophages: The Paradox of an Antimalarial Agent. *Oxidative Medicine and Cellular Longevity*, *2013*, 1–10. https://doi.org/10.1155/2013/870472

Schroeder, H. W., & Cavacini, L. (2010). Structure and function of immunoglobulins. *Journal of Allergy and Clinical Immunology*, *125*(2), S41–S52. https://doi.org/10.1016/j.jaci.2009.09.046

Seydoux, E., Liang, H., Dubois Cauwelaert, N., Archer, M., Rintala, N. D., Kramer, R., Carter, D., Fox, C. B., & Orr, M. T. (2018). Effective Combination Adjuvants Engage Both TLR and Inflammasome Pathways To Promote Potent Adaptive Immune Responses. *The Journal of Immunology*, *201*(1), 98–112. https://doi.org/10.4049/jimmunol.1701604

Shi, J., Zhao, Y., Wang, K., Shi, X., Wang, Y., Huang, H., Zhuang, Y., Cai, T., Wang, F., & Shao, F. (2015). Cleavage of GSDMD by inflammatory caspases determines pyroptotic cell death. *Nature*, *526*(7575), 660–665. https://doi.org/10.1038/nature15514

Shi, J., Zhao, Y., Wang, Y., Gao, W., Ding, J., Li, P., Hu, L., & Shao, F. (2014). Inflammatory caspases are innate immune receptors for intracellular LPS. *Nature*, *514*(7521), 187–192. https://doi.org/10.1038/nature13683

Shimada, K., Crother, T. R., Karlin, J., Dagvadorj, J., Chiba, N., Chen, S., Ramanujan, V. K., Wolf, A. J., Vergnes, L., Ojcius, D. M., Rentsendorj, A., Vargas, M., Guerrero, C., Wang, Y., Fitzgerald, K. A., Underhill, D. M., Town, T., & Arditi, M. (2012). Oxidized Mitochondrial DNA Activates the NLRP3 Inflammasome during Apoptosis. *Immunity*, *36*(3), 401–414. https://doi.org/10.1016/j.immuni.2012.01.009

Sparmann, A., & Vogel, J. (2023). RNA-based medicine: from molecular mechanisms to therapy. *The EMBO Journal*, *42*(21). https://doi.org/10.15252/embj.2023114760

Srinivasula, S. M., Poyet, J.-L., Razmara, M., Datta, P., Zhang, Z., & Alnemri, E. S. (2002). The PYRIN-CARD Protein ASC Is an Activating Adaptor for Caspase-1. *Journal of Biological Chemistry*, *277*(24), 21119–21122. https://doi.org/10.1074/jbc.C200179200

Stertman, L., Palm, A.-K. E., Zarnegar, B., Carow, B., Lunderius Andersson, C., Magnusson, S. E., Carnrot, C., Shinde, V., Smith, G., Glenn, G., Fries, L., & Lövgren Bengtsson, K. (2023). The Matrix-MTM adjuvant: A critical component of vaccines for the 21 st century. *Human Vaccines & Immunotherapeutics*, *19*(1). https://doi.org/10.1080/21645515.2023.2189885

Stitham, J., Rodriguez-Velez, A., Zhang, X., Jeong, S.-J., & Razani, B. (2020). Inflammasomes: a preclinical assessment of targeting in atherosclerosis. *Expert Opinion on Therapeutic Targets*, *24*(9), 825–844. https://doi.org/10.1080/14728222.2020.1795831

Sun, L., Wu, J., Du, F., Chen, X., & Chen, Z. J. (2013). Cyclic GMP-AMP Synthase Is a Cytosolic DNA Sensor That Activates the Type I Interferon Pathway. *Science*, *339*(6121), 786–791. https://doi.org/10.1126/science.1232458

Svensson, A., Patzi Churqui, M., Schlüter, K., Lind, L., & Eriksson, K. (2017). Maturation-dependent expression of AIM2 in human B-cells. *PLOS ONE*, *12*(8), e0183268. https://doi.org/10.1371/journal.pone.0183268

Szebeni, J., Storm, G., Ljubimova, J. Y., Castells, M., Phillips, E. J., Turjeman, K., Barenholz, Y., Crommelin, D. J. A., & Dobrovolskaia, M. A. (2022). Applying lessons learned from nanomedicines to understand rare hypersensitivity reactions to mRNA-based SARS-CoV-2 vaccines. *Nature Nanotechnology*, *17*(4), 337–346. https://doi.org/10.1038/s41565-022-01071-x

Tahtinen, S., Tong, A.-J., Himmels, P., Oh, J., Paler-Martinez, A., Kim, L., Wichner, S., Oei, Y., McCarron, M. J., Freund, E. C., Amir, Z. A., de la Cruz, C. C., Haley, B., Blanchette, C., Schartner, J. M., Ye, W., Yadav, M., Sahin, U., Delamarre, L., & Mellman, I. (2022). IL-1 and IL-1ra are key regulators of the inflammatory response to RNA vaccines. *Nature Immunology*, *23*(4), 532–542. https://doi.org/10.1038/s41590-022-01160-y

Tak, P. P., & Firestein, G. S. (2001). NF-κB: a key role in inflammatory diseases. *Journal of Clinical Investigation*, *107*(1), 7–11. https://doi.org/10.1172/JCI11830

Takeda, K., Takeuchi, O., & Akira, S. (2002). Recognition of lipopeptides by Toll-like receptors. *Journal of Endotoxin Research*, *8*(6), 459–463. https://doi.org/10.1179/096805102125001073

Takeuchi, O., & Akira, S. (2010). Pattern Recognition Receptors and Inflammation. In *Cell* (Vol. 140, Issue 6, pp. 805–820). Elsevier B.V. https://doi.org/10.1016/j.cell.2010.01.022

Takeuchi, O., Sato, S., Horiuchi, T., Hoshino, K., Takeda, K., Dong, Z., Modlin, R. L., & Akira, S. (2002). Cutting Edge: Role of Toll-Like Receptor 1 in Mediating Immune Response to Microbial Lipoproteins. *The Journal of Immunology*, *169*(1), 10–14. https://doi.org/10.4049/jimmunol.169.1.10

Tanaka, T., Legat, A., Adam, E., Steuve, J., Gatot, J., Vandenbranden, M., Ulianov, L., Lonez, C., Ruysschaert, J., Muraille, E., Tuynder, M., Goldman, M., & Jacquet, A. (2008). DiC14-amidine cationic liposomes stimulate myeloid dendritic cells through Toll-like

receptor 4. *European Journal of Immunology*, *38*(5), 1351–1357. https://doi.org/10.1002/eji.200737998

Tapia-Abellán, A., Angosto-Bazarra, D., Alarcón-Vila, C., Baños, M. C., Hafner-Bratkovič, I., Oliva, B., & Pelegrín, P. (2021). Sensing low intracellular potassium by NLRP3 results in a stable open structure that promotes inflammasome activation. *Science Advances*, *7*(38). https://doi.org/10.1126/sciadv.abf4468

The R Core Team. (2025). *R: A Language and Environment for Statistical Computing*. https://www.gnu.org/copyleft/gpl.html.

Usdan, L., Patel, S., Rodriguez, H., Xu, X., Lee, D.-Y., Finn, D., Wyper, H., Lowry, F. S., Mensa, F. J., Lu, C., Cooper, D., Koury, K., Anderson, A. S., Türeci, Ö., Şahin, U., Swanson, K. A., Gruber, W. C., Kitchin, N., Andrews, C., … Wadsworth, L. (2024). A Bivalent Omicron-BA.4/BA.5-Adapted BNT162b2 Booster in ≥12-Year-Olds. *Clinical Infectious Diseases*, *78*(5), 1194–1203. https://doi.org/10.1093/cid/ciad718

Veeranki, S., Duan, X., Panchanathan, R., Liu, H., & Choubey, D. (2011). IFI16 Protein Mediates the Anti-inflammatory Actions of the Type-I Interferons through Suppression of Activation of Caspase-1 by Inflammasomes. *PLoS ONE*, *6*(10), e27040. https://doi.org/10.1371/journal.pone.0027040

Verbeke, R., Hogan, M. J., Loré, K., & Pardi, N. (2022). Innate immune mechanisms of mRNA vaccines. *Immunity*, *55*(11), 1993–2005. https://doi.org/10.1016/j.immuni.2022.10.014

von Kleist, L., Stahlschmidt, W., Bulut, H., Gromova, K., Puchkov, D., Robertson, M. J., MacGregor, K. A., Tomilin, N., Pechstein, A., Chau, N., Chircop, M., Sakoff, J., von Kries, J. P., Saenger, W., Kräusslich, H.-G., Shupliakov, O., Robinson, P. J., McCluskey, A., & Haucke, V. (2011). Role of the Clathrin Terminal Domain in Regulating Coated Pit Dynamics Revealed by Small Molecule Inhibition. *Cell*, *146*(3), 471–484. https://doi.org/10.1016/j.cell.2011.06.025

Vyleta, M. L., Wong, J., & Magun, B. E. (2012). Suppression of Ribosomal Function Triggers Innate Immune Signaling through Activation of the NLRP3 Inflammasome. *PLoS ONE*, *7*(5), e36044. https://doi.org/10.1371/journal.pone.0036044

Walsh, E. E., Frenck, R. W., Falsey, A. R., Kitchin, N., Absalon, J., Gurtman, A., Lockhart, S., Neuzil, K., Mulligan, M. J., Bailey, R., Swanson, K. A., Li, P., Koury, K., Kalina, W.,

Cooper, D., Fontes-Garfias, C., Shi, P.-Y., Türeci, Ö., Tompkins, K. R., … Gruber, W. C. (2020). Safety and Immunogenicity of Two RNA-Based Covid-19 Vaccine Candidates. *New England Journal of Medicine*, *383*(25), 2439–2450. https://doi.org/10.1056/NEJMoa2027906

Wannamaker, W., Davies, R., Namchuk, M., Pollard, J., Ford, P., Ku, G., Decker, C., Charifson, P., Weber, P., Germann, U. A., Kuida, K., & Randle, J. C. R. (2007). (*S*)-1-((*S*)-2-{[1-(4-Amino-3-chloro-phenyl)-methanoyl]-amino}-3,3-dimethyl-butanoyl)-pyrrolidine-2-carboxylic acid ((2 *R* ,3 *S*)-2-ethoxy-5-oxo-tetrahydro-furan-3-yl)-amide (VX-765), an Orally Available Selective Interleukin (IL)-Converting Enzyme/Caspase-1 Inhibitor, Exhibits Potent Anti-Inflammatory Activities by Inhibiting the Release of IL-1β and IL-18. *Journal of Pharmacology and Experimental Therapeutics*, *321*(2), 509–516. https://doi.org/10.1124/jpet.106.111344

Watson, O. J., Barnsley, G., Toor, J., Hogan, A. B., Winskill, P., & Ghani, A. C. (2022). Global impact of the first year of COVID-19 vaccination: a mathematical modelling study. *The Lancet Infectious Diseases*, *22*(9), 1293–1302. https://doi.org/10.1016/S1473-3099(22)00320-6

Weismann, D., & Binder, C. J. (2012). The innate immune response to products of phospholipid peroxidation. *Biochimica et Biophysica Acta (BBA) - Biomembranes*, *1818*(10), 2465–2475. https://doi.org/10.1016/j.bbamem.2012.01.018

Yang, J.-X., Hsieh, K.-C., Chen, Y.-L., Lee, C.-K., Conti, M., Chuang, T.-H., Wu, C.-P., & Jin, S.-L. C. (2017). Phosphodiesterase 4B negatively regulates endotoxin-activated interleukin-1 receptor antagonist responses in macrophages. *Scientific Reports*, *7*(1), 46165. https://doi.org/10.1038/srep46165

Zanoni, I., Tan, Y., Di Gioia, M., Broggi, A., Ruan, J., Shi, J., Donado, C. A., Shao, F., Wu, H., Springstead, J. R., & Kagan, J. C. (2016). An endogenous caspase-11 ligand elicits interleukin-1 release from living dendritic cells. *Science*, *352*(6290), 1232–1236. https://doi.org/10.1126/science.aaf3036

Zarnegar, B., Carow, B., Eriksson, J., Spennare, E., Öhlund, P., Akpinar, E., Bringeland, E., Osterman, I. L., Lundqvist, L., Antti, J., Handin, N., Helgesson, P.-H., Bankefors, J., Lövgren Bengtsson, K., Sellin, M. E., Palm, A.-K. E., Stertman, L., & Lunderius

Andersson, C. (2025). Matrix-M adjuvant triggers inflammasome activation and enables antigen cross-presentation through induction of lysosomal membrane permeabilization. *Npj Vaccines*, *10*(1), 184. https://doi.org/10.1038/s41541-025-01243-5

Zhang, X., Goel, V., & Robbie, G. J. (2020). Pharmacokinetics of Patisiran, the First Approved RNA Interference Therapy in Patients With Hereditary Transthyretin-Mediated Amyloidosis. *The Journal of Clinical Pharmacology*, *60*(5), 573–585. https://doi.org/10.1002/jcph.1553

Zhao, T., Cai, Y., Jiang, Y., He, X., Wei, Y., Yu, Y., & Tian, X. (2023). Vaccine adjuvants: mechanisms and platforms. *Signal Transduction and Targeted Therapy*, *8*(1), 283. https://doi.org/10.1038/s41392-023-01557-7

Zhao, Y., Liang, B., Sheng, S., Wang, C., Jin, B., Zhang, X., Cheng, Y., Shen, C., & Zheng, F. (2024). AIM2 inflammasome regulated by the IFN-γ/JAK2/STAT1 pathway promotes activation and pyroptosis of monocytes in Coronary Artery Disease. *Immunity, Inflammation and Disease*, *12*(6). https://doi.org/10.1002/iid3.1317

Zhou, R., Yazdi, A. S., Menu, P., & Tschopp, J. (2011). A role for mitochondria in NLRP3 inflammasome activation. *Nature*, *469*(7329), 221–226. https://doi.org/10.1038/nature09663

10. Statement on own contribution

The work was carried out at the Institute of Innate Immunity under the supervision of Prof. Dr. med. Eicke Latz.

The study was conceptually designed by Prof. Dr. med. Eicke Latz (supervisor), Dr. Tomasz Próchniki (advisor), and myself, Matilde Bartolomei Vasconcelos (PhD student).

All RNA sequencing data was performed by the Next Generation Sequencing Core Facility of the Medical Faculty at the University of Bonn. The analyses related to RNA sequencing were performed by Dr. Jamie Gearing (PostDoc researcher from Eicke Latz's research group Immunobiology of Inflammation at the German Rheumatology Research Center, Berlin).

The mouse experiments were carried out by me with the support of Maximilian Rothe and Lukas Rossnagel (Institute of Innate Immunity).

The flow cytometry data was generated with the support of Lukas Rossnagel (Institute of Innate Immunity).

The multiplex cytokine measurements were performed with the support of Christabel Mennicken (Institute of Innate Immunity).

The HEK cells expressing NLRP3 and AIM2 were made by Yonas Tesfamariam (Institute of Innate Immunity).

The cell lines used in Figure 8 were made by or with the help of Anil Akbal, Rainer Stahl, and Fraser Duthie (Institute of Innate Immunity), and the Flow Cytometry Core Facility of the Medical Faculty at the University of Bonn.

The data used for the evaluation was generated and compiled independently.

The statistical evaluation was carried out by me independently.

In preparing this work, I used ChatGPT to help with literature finding. After using this tool, I reviewed and edited the relevant passages, and take full responsibility for the content of the published dissertation.

I hereby confirm that my thesis complies with the Statement by the Executive Committee of the Deutsche Forschungsgemeinschaft (DFG, German Research Foundation) on the Influence of Generative Models of Text and Image Creation on Science and the Humanities and on the DFG's Funding Activities.